From the Klinik für Anästhesiologie und Operative Intensivmedizin
(Academic Representative: Prof. Dr. med. Norbert Weiler)
at the University Medical Center Schleswig-Holstein, Campus Kiel
at Kiel University

Pathways of Helium Postconditioning induced Cardioprotection

Dissertation
to acquire the doctoral degree (Dr. med.)
at the Faculty of Medicine

at Kiel University

presented by

Moritz Flick

from **Pinneberg**

Kiel, **2017**

1st Reviewer: Prof. Dr. Martin Albrecht

2nd Reviewer: Prof. Dr. Thilo Wedel

Date of oral examination: 08.03.2018

Approved for printing, Kiel, 09.12.2017

Signed:

Prof. Dr. Johann Roider

(Chairperson of the Examination Committee)

Table of Contents

Table of Contents I
List of Figures and Tables III
List of Abbreviations IV
1. Introduction 1
1.1 Coronary Artery Disease 1
1.2 Myocardial Infarction 2
1.3 Reperfusion Injury 2
1.4 The Concept of Ischemic Conditioning 4
1.5 Pharmacological Conditioning 6
1.6 Helium Conditioning 7
1.7 Mechanisms Behind Cardioprotection: RISK and SAFE Pathways 8
1.8 The Role of Caveolins in Cardioprotection 9
1.9 Autophagy in Helium Postconditioning 11
1.10 Aims of the Study 13
2. Materials and Methods 14
2.1 Materials 14
2.1.1 Chemicals and Reagents 14
2.1.2 Antibodies 14
2.1.3 Oligonucleotides 15
2.1.4 Solutions 15
2.2 Methods 17
2.2.1 Ethics 17
2.2.2 Animal Model of Ischemia/Reperfusion 17
2.2.3 Preparation of Cytosolic-, Membrane- and Mitochondrial-Fractions from Ischemic AAR and Non-Ischemic NAAR Tissue 19
2.2.4 Bradford Protein Assay 20
2.2.5 Western Blot 20
2.2.6 Isolation of RNA and cDNA Preparation 21
2.2.7 Reverse Transcriptase Real Time PCR 21
2.2.8 Statistical Analyses 22

3. Results **23**
3.1 Main Findings 23
3.2 mRNA Expression Analyses of Caveolin-1 and Caveolin-3 23
3.3 Protein Analyses of Caveolin-1 and Caveolin-3 24
3.4 Phosphorylation of RISK Pathway Associated Proteins 28
3.5 Protein Analyses of Autophagy Associated Proteins 30
3.6 Protein Analyses of Caveolin-1 and Caveolin-3 after 5 and 30 Min of Helium Postconditioning 30
4. Discussion **31**
4.1 Helium Postconditioning and Cardioprotection 31
4.2 Helium Postconditioning and Caveolins 32
4.3 Helium Postconditioning and RISK Pathway Activation 34
4.4 Helium Postconditioning and Autophagy 36
4.5 Caveolins and Mitochondria 37
4.6 Limitations of the Study 38
4.7 Conclusion and Outlook 39
5. Abstract **40**
6. References **42**
7. Appendix **51**
7.1 Caveolin-1 and Caveolin-3 after 5 Min of Reperfusion or Helium Postconditioning 51
7.2 Caveolin-1 and Caveolin-3 after 30 Min of Reperfusion or Helium Postconditioning 52
7.3 Hemodynamics 53
7.4 Publication Flick et al., 2016 54
7.5 Publication Oei et al., 2015 62
8. Cooperation **72**
9. Acknowledgements **73**
10. Curriculum Vitae **74**

List of Figures

Figure 1: Potential Effects of Ischemia and Reperfusion. 4
Figure 2: Concept of Pre- and Postconditioning. 5
Figure 3: Caveolae and Caveolins. 10
Figure 4: Autolysosome Formation. 12
Figure 5: Scheme of Coronary Artery Occlusion. 17
Figure 6: Experimental Setting. 18
Figure 7: Schematic Overview of Tissue Processing. 19
Figure 8: Quantification of mRNA Expression of Caveolin-1 and Caveolin-3 in Sham, I/R15 and I/R+He15 Treated Animals. 24
Figure 9: Protein Levels of Caveolin-1 and Caveolin-3 in Membrane Fractions of Sham, I/R15 and I/R+He15 Treated Animals. 25
Figure 10: Protein Levels of Caveolin-1 and Caveolin-3 in Cytosolic and Mitochondrial Fractions of Sham, I/R15 and I/R+He15 Treated Animals. 26
Figure 11: Protein Levels of Caveolin-1 and Caveolin-3 in Serum of Sham, I/R15 and I/R+He15 Treated Animals. 27
Figure 12: Phosphorylation Levels of RISK Pathway Associated Proteins in Ischemic AAR Cardiac Tissue of Sham, I/R15 and I/R+He15 Treated Animals. 28
Figure 13: Phosphorylation Levels of RISK Pathway Associated Proteins in Non-Ischemic NAAR Cardiac Tissue of Sham, I/R15 and I/R+He15 Treated Animals. 29
Figure 14: Protein Levels of Bcl-1 in Mitochondrial Fractions of Sham, I/R15 and I/R+He15 Treated Animals. 30

List of Tables

Table 1: List of Antibodies. 14
Table 2: Overview of Primers. 15
Table 3: Main Findings. 23

List of Abbreviations

Unit-abbreviations are used according to the International System of Units.
Other abbreviations were used as follows:

AAR	area at risk
ACS	acute coronary syndrome
Act	actin
Akt	protein kinase B
ATP	adenosine triphosphate
ATPase	adenosine 5'-triphosphatase
Bcl-1	beclin-1
BPM	beats per minute
BSA	bovine serum albumin
Cav	caveolin
cDNA	complementary deoxyribonucleic acid
CSD	caveolin scaffolding domain
DNA	deoxyribonucleic acid
dT	deoxythymidine
dNTP	deoxynucleotide triphosphate
DTT	dithiothreitol
EDTA	ethylenediaminetetraacetic acid
eNOS	endothelial nitric oxide synthase
Erk	extracellular signal-regulated kinase
et al.	et alii
GAPDH	glyceraldehyde-3-phosphatedehydrogenase
GPCR	G-protein coupled receptor
GSK	glycogen synthase kinase
HePoc	helium postconditioning
I/R	ischemia/reperfusion injury
IC	ischemic conditioning
IPC	ischemic preconditioning
IPoc	ischemic postconditioning
JAK	Janus kinase

KO	knockout
LAD	left anterior descending artery
LC	1A/1B-light chain
LCA	left coronary artery
LDL	low-density-lipoprotein
MOPS	3-morpholinopropanesulfonic acid
mPTP	mitochondrial permeability transition pore
NAAR	not area at risk
NIH	national institutes of health
Nq	fluorescence threshold to determine the starting concentration
N0	starting concentration
PBS	phosphate buffer saline
PCR	polymerase chain reaction
pH	potential of hydrogen
PHB1	prohibitin-1
PI3K	phosphoinositide-3-kinase
RISK	reperfusion injury salvage kinase
PKC	protein kinase C
qRT-PCR	quantitative reverse transcriptase polymerase chain reaction
RCA	right coronary artery
RNA	ribonucleic acid
RNase	ribonuclease
ROS	reactive oxygen species
RyR	ryanodine receptor
SAFE	survivor activating factor enhancement
SDS	sodium dodecyl sulfate
SDS-PAGE	sodium dodecyl sulfate polyacrylamide gel electrophoresis
SEM	standard error of mean
SR	sarcoplasmic reticulum
STAT	signal transducer and activator of transcription
TNF	tumor necrosis factor
Vps	vacuolar protein-sorting

1. Introduction

1.1 Coronary Artery Disease

Coronary artery disease and subsequent myocardial infarction are major reasons of patient mortality (Kramarow et al., 2013, O'Gara et al., 2013). In 2014 chronic ischemic heart disease and acute myocardial infarction were the two leading causes of death in Germany according to the German Federal Statistical Office (Statistisches-Bundesamt-Deutschland, 2014).

Myocardial ischemia occurs, when blood flow in the coronary vessels is restricted and supply of oxygen as well as other nutrients to the myocardial tissue is inhibited. A common cause of partial or complete blockage of the coronary arteries is atherosclerosis, a multifactorial process, induced by damage to the endothelium. Cholesterol rich low-density-lipoprotein (LDL) particles infiltrate the intima layer, which causes macrophage cells to accumulate oxidized lipids by endocytosis. Subsequently the endothelium thickens (Chen et al., 2016). Cytokines enhance the fibrotic remodeling process by stimulating smooth muscle cell proliferation. Over time the medial layer of the vessel becomes atrophic and the elastic lamina may rupture (Gaze, 2013). Collagen forms a hard fibrous cap over the lesion, referred to as fibro-lipid plaque. This vascular remodeling with thickening of the intimal layer and the formation of fibro-lipid plaques is referred to as coronary artery disease (Badimon et al., 2012). As the lesion grows the lumen may be narrowed or detached. Thrombi or ruptured plaques may travel downstream and completely occlude arteries (Falk, 2006). If the blood flow is not re-established, myocardial ischemia occurs, cell death pathways are induced and eventually cardiomyocytes demise, a process called myocardial infarction (Hausenloy et al., 2013). During myocardial infarction patients may present with acute coronary syndrome undergoing strong chest pain and vegetative symptoms (Bruyninckx et al., 2008).

1.2 Myocardial Infarction

Tissue damage and type of cell death during myocardial infarction depend on the area supplied by the occluded vessel and the duration of occlusion (Hamacher-Brady et al., 2006, Matsumura et al., 1998). Severe ischemia stops oxygen supply and alters mitochondrial metabolism with consequent abrogation of its membrane potential. Additionally, adenosine triphosphate (ATP) levels decrease quickly causing failure of ATP dependent ion pumps, e.g. the Na^+-ATPase (Baines, 2009). Active Ca^{2+} efflux and reuptake into the sarcoplasmic reticulum (SR) are limited resulting in uncontrolled electrolyte shifts and Ca^{2+} overload (Yellon et al., 2007). The mitochondrial permeability transition pore (mPTP) is an emerging endpoint and its opening induced cell death (Baines, 2009).

When mitochondrial respiration halts, the pH decreases and anaerobic metabolism takes over causing production of acidic catabolites. Lower pH-values may have severe consequences under physiological conditions. During ischemia however, they might even be beneficial as they increase the threshold of mPTP opening (figure 1) (Griffiths et al., 1995). When reperfusion is restored the pH increases very quickly, which might be detrimental to surrounding tissue (Cohen et al., 2007). Furthermore these processes are accompanied by activation of intracellular proteases, e.g. calpain, which lead to damage of myofibrils and trigger destructive rigor contracture. As a consequence of cellular stress the mPTP opens and cell death becomes imminent (Padilla et al., 2003).

1.3 Reperfusion Injury

The detrimental effects of arterial occlusion are evident. In contrast, it has been discussed controversially, whether the phenomenon of reperfusion injury is a distinct process or just an enhancement of damage sustained during ischemia (Kloner, 1993, Jennings et al., 1960). In recent years, it has become widely accepted that significant damage occurs immediately after reperfusion is restored (Hausenloy et al., 2004b). Reperfusion injury can occur in different manners and patients may present arrhythmias and stunning while blood flow is re-established (Piper et al., 1998).

The current gold standard therapy, to alleviate the extent of damage from coronary artery occlusion, is the induction of reperfusion and re-oxygenation through pharmacological dissolution or dislodgement of the clot. Thus, making reperfusion injury an inevitable side effect (Yellon et al., 2007, Ovize et al., 2010).

As underlying mechanisms, Ca^{2+} alterations and mPTP opening gained focus as closely related key mediators of reperfusion induced-cell death (figure 1) (Ibáñez et al., 2015, Piper et al., 1998). During the reperfusion phase, intracellular Na^+ may also increase, as pH restoration is associated with Na^+ influx and impaired Na^+ pump function (Ruiz-Meana et al., 1999). Na^+ influx prompts additional intracellular Ca^{2+} increase through the Na^+/Ca^{2+}-exchanger (Marber et al., 1993). When ATP synthesis is restored, Ca^{2+} is pumped into the SR, which may result in fluctuations of Ca^{2+}. Ca^{2+} is released through the ryanodine receptor 2 channel (RyR2), if the cellular capacity is exceeded. These quick alterations in Ca^{2+} concentrations may lead to damaging hypercontracture, arrhythmias and mitochondrial Ca^{2+} overload (figure 1) (Ruiz-Meana et al., 2009).

Opening of the mPTP is an emerging point of several involved pathways and leads to subsequent cell death during ischemia and reperfusion. The mPTP is a non-specific channel located in the mitochondrial membrane (Heusch et al., 2010). Under physiological conditions, the mPTP remains mostly closed. Its opening occurs in response to the increased concentrations of Ca^{2+} and is catalyzed by an elevated pH during reperfusion. Other processes involved in mPTP opening are high concentrations of reactive oxygen species (ROS), inorganic phosphate and reduction of the inner membrane potential (Heusch et al., 2010). Consequent cell death is triggered by depolarization of the inner mitochondrial membrane potential as well as matrix swelling and eventually destruction of the membranes. Thus, the intermembrane space is liberated and proteins, such as cytochrome C, activate caspases and ultimately induce cell death (Kroemer et al., 2000, Kroemer et al., 2007).

Taken together, cardiac ischemia/reperfusion injury (I/R) is a major challenge in modern medicine. Not only ischemia is detrimental to the myocardium, but also

reperfusion injury can constitute to 50% of the final infarct size making its treatment a promising approach to reduce cardiac damage (Herzog et al., 1997).

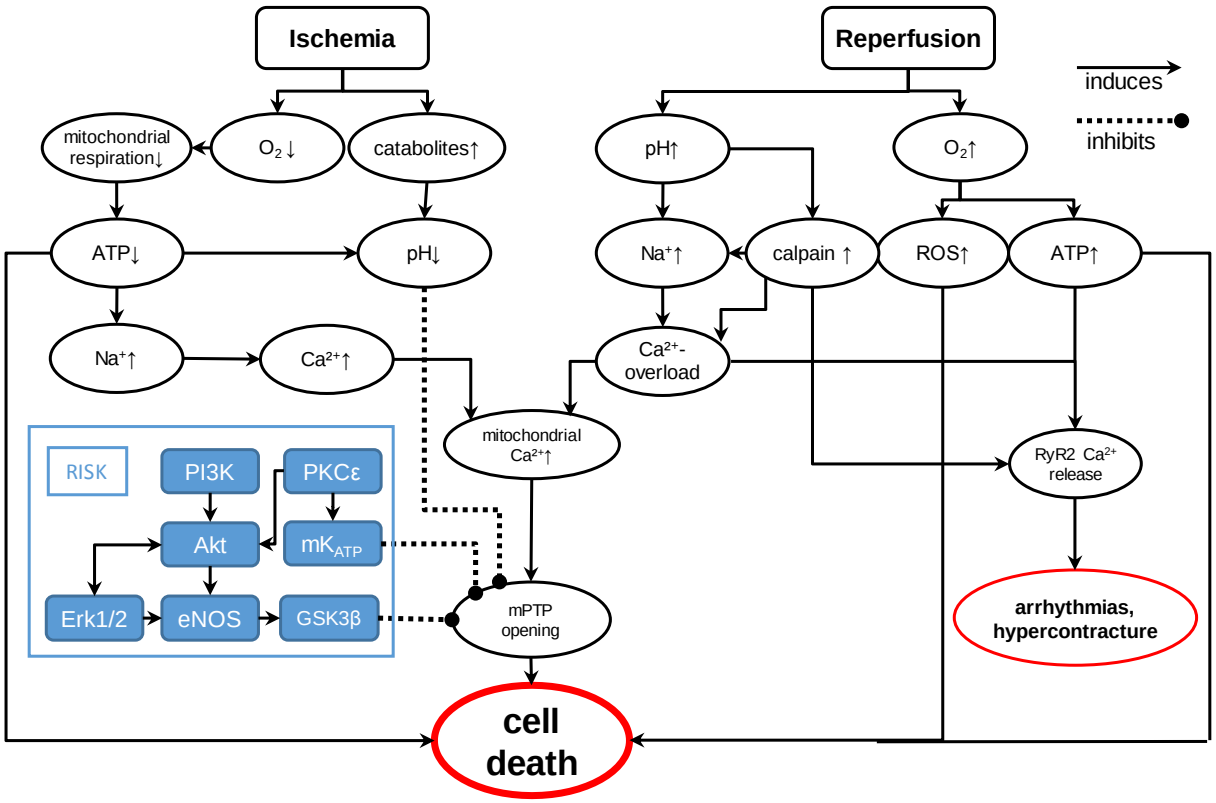

figure 1 ▲ Potential Effects of Ischemia and Reperfusion. RISK pathway (**blue**). Based on (Murphy et al., 2008)

1.4 The Concept of Ischemic Conditioning

In 1986 Murry et al. showed that brief cycles of non-lethal ischemia and reperfusion prior to prolonged myocardial infarction reduce the final infarct size (Murry et al., 1986). This concept, known as ischemic preconditioning (IPC, figure 2 A), has been successfully replicated in many studies making IPC a promising cardioprotective approach (Heusch, 2013). However, as ischemic events are hard to predict in non-experimental settings, it remains difficult to establish IPC in clinical practice. Hori et al. altered the strategy of IPC in 1991 and successfully used gradual restoration of blood flow in a dog model to reduce infarct damage (Hori et al., 1991). Cardioprotective effects similar to those of IPC were first reproduced by Zhao et al. using short repetitive cycles of IPoc (Zhao et al., 2003). Different studies confirmed these results (Kin et al., 2004, Yang et al., 2004). This new concept with additional

cycles of I/R after myocardial infarction, referred to as ischemic postconditioning (IPoc, figure 2 B), was developed to prevent reperfusion induced damage even after the ischemic event (Hausenloy et al., 2016).

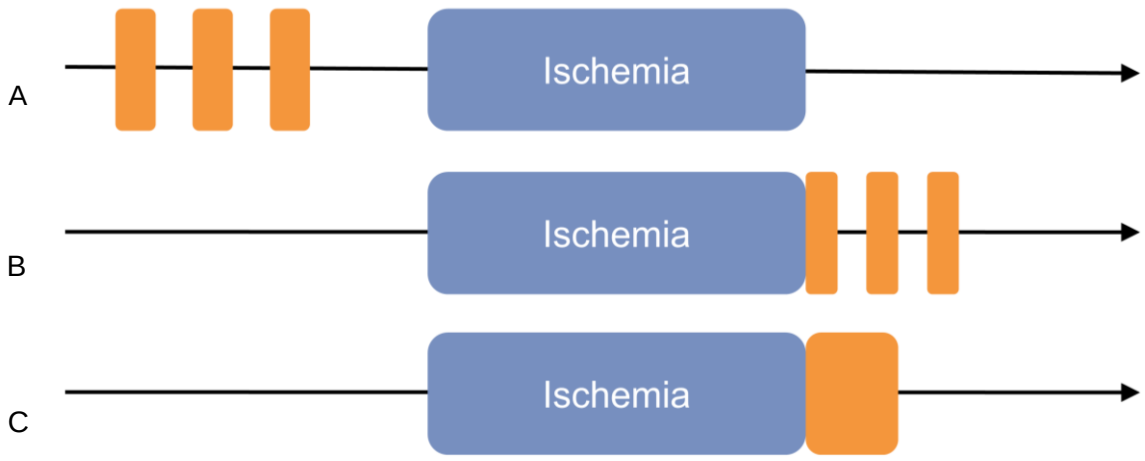

figure 2 ▲ Concept of Pre- and Postconditioning. Short intermittent, non-lethal cycles of cardioprotective stimuli (ischemia, anesthetics, pharmacological agents), preconditioning (**A**), prior to prolonged ischemia may reduce myocardial infarct size. Short periods of intervention after prolonged ischemia, postconditioning (**B**), may induce similar cardioprotection. Some stimuli may only be cardioprotective, when applied for a single cycle after prolonged ischemia, also referred to as postconditioning (**C**).

IPoc has been shown to protect against numerous aspects of I/R, including reduction of infarct size, interstitial and intracellular edema. It decreases Ca^{2+}-accumulation, ROS generation as well as the inflammatory response (Hausenloy et al., 2016).

As underlying mechanisms of cardioprotection Tsang et al. described involvement of the pro-survival reperfusion injury salvage kinase pathway (RISK, figure 1 and section 1.7) (Tsang et al., 2004). Later, the survivor activating factor enhancement pathway (SAFE) was identified to mediate cardioprotective effects of IPoc as well (section 1.7) (Hausenloy et al., 2011).

1.5 Pharmacological Conditioning

Cardioprotection may also be induced through certain pharmacological agents mimicking the effects of IPC and IPoc, referred to as pharmacological conditioning. Several substances have been investigated for their cardioprotective properties (Hausenloy et al., 2016). Applying these agents with an alike protocol as IPC and IPoc, with short application cycles before (pharmacological preconditioning) or after (pharmacological postconditioning) prolonged ischemia, results in reduced infarct size (Hausenloy et al., 2016). Some substances produce cardioprotection only when applied for a single cycle after prolonged ischemia (figure 2 C) (Sonne et al., 2008, Hausenloy et al., 2016).

Volatile anesthetics, e.g. sevoflurane (Toller et al., 1999) or isoflurane (Cason et al., 1997), are recognized to reduce infarct size after myocardial infarction in vitro and in vivo similar to ischemic conditioning (IC) (Mullenheim et al., 2002). However, these anesthetic gases may have unfavorable side effects on hemodynamics and cardiovascular parameters aside from causing anesthesia (Cason et al., 1997). The noble gas xenon gained focus as it has been shown to induce cardioprotection in the setting of pre- or postconditioning, while causing minimal cardiovascular changes (Preckel et al., 2000, Preckel et al., 2002, Weber et al., 2006).

Interestingly, the pathways underlying the cardioprotective effects in anesthetic conditioning are very similar to the ones induced in IC. Both, RISK and SAFE pathway, are known to be mediators involved in cardioprotection with the mPTP as an emerging end-point (section 1.7) (Hausenloy et al., 2016, Davidson et al., 2006).

A common challenge for all pharmacological conditioning strategies is their clinical translation, which remains difficult, as cardioprotective effects are often reduced or abolished in the existence of pathological conditions, e.g. diabetes, hypertension and/or several medications like P2Y12-inhibitors (Boengler et al., 2009, Ferdinandy et al., 2014).

1.6 Helium Conditioning

The noble gas helium is an odorless, colorless, inert, non-anesthetic gas. Helium is the sixth most occurring gas in the world and has a density that is approximately six times lower than atmospheric air (Oliver, 1984). The physical properties of helium reduce airway resistance and turbulences resulting in increased respiratory flow (Papamoschou, 1995). The first medical use of helium for respiratory diseases was described in 1936 by Barach et al. (Barach et al., 1936). Helium is mostly applied as a mixture of helium and oxygen, called heliox and is well established for medical use in pulmonary disease like asthma bronchial or chronic obstructive pulmonary disease (Valli et al., 2007). Studies investigating helium safety have shown no carcinogenic or toxic side effects (Harris et al., 2008). In fact, helium has been used in deep sea diving for decades and is used even in children with pulmonary diseases (Hess et al., 2006, Liet et al., 2015). Taken together, these characteristics make helium potentially an ideal medical agent.

In 2007 Pagel et al. first described cardioprotective effects of helium and several studies have replicated cardioprotective effects of helium preconditioning with short cycles of helium prior to prolonged ischemia (Huhn et al., 2012, Huhn et al., 2009a, Pagel et al., 2008a, Pagel et al., 2007). Helium postconditioning (HePoc), with helium ventilation during reperfusion, has also been shown to protect from myocardial I/R in different experimental studies (Huhn et al., 2009b, Oei et al., 2012). The underlying mechanisms of helium conditioning still need further research. However, it has been shown that helium preconditioning influences the RISK pathway kinases extracellular signal-regulated kinase 1/2 (Erk1/2), phosphatidylinositol 3-kinase (PI3K), protein kinase B (Akt) and glycogen synthase kinase-3β (GSK-3β) (Halestrap et al., 2007, Nishihara et al., 2007). Thus, it is anticipated that the mentioned molecules might play an important role in HePoc. Other involved signaling may include pro-survival autophagy as expression of autophagy related genes, beclin-1 (Bcl-1) and sequestosome-1, is upregulated during HePoc (Oei et al., 2015b).

1.7 Mechanisms Behind Cardioprotection: RISK and SAFE Pathways

At the time of discovery of the concept of IC, the pathways were unknown. First studies investigating cardioprotective effects of IC suggested washout of ischemic catabolites as well as restauration of ATP synthesis as important underlying effectors (Murry et al., 1986). 30 years later the understanding of signaling pathways behind IC induced cardioprotection has advanced, indicating a network of complex and diverse mechanisms to be responsible for cardioprotection.

One key target of ischemic and pharmacologic conditioning is the RISK pathway (Yellon et al., 1999, Hausenloy et al., 2004b). The RISK pathway is a pro-survival pathway consisting of several effector-kinases including PI3K, Akt, Erk1/2 and proteinkinase Cε (PKCε). Interestingly, these kinases are not arranged into separated pathways, but have to be understood as a communicating network of co-factors (figure 1) (Hausenloy et al., 2004a). Signaling through PI3K induces cardioprotection in I/R through its downstream effector serine-threonine kinase Akt (Tsang et al., 2004). Like Akt, the activation of Erk1/2 triggers a signal cascade that regulates cell proliferation and cell death (Yue et al., 2000). Erk1/2 has been shown to mediate different cell pathways (Dagda et al., 2008, Kassan et al., 2016). However, the exact mechanisms through which different conditioning strategies activate the RISK pathway kinases, are yet unclear. Explanations involve intermediary factors, e.g. adenosine or PKC. It is not known, whether these kinases emerge in a mutual pathway or use different end-effectors to mediate their pro-survival signals. However, several components of the RISK pathway converge on the mitochondria and a role for prevention of mPTP opening seems likely (figure 1) (Davidson et al., 2006).

The SAFE pathway is a simultaneously activated signal cascade, which has been closely related to the RISK pathway and cardioprotection (Goodman et al., 2008, Lecour, 2009). Lecour et al. first described the cardioprotective SAFE pathway, which involves the tumor necrosis factor α (TNFα), which in other settings may be detrimental (Lecour, 2009). Its activation occurs at the onset of reperfusion, but has also been reported for IC (Hausenloy et al., 2016). The SAFE pathway may produce cardioprotection independently from the RISK pathway through activation of the Janus kinase (JAK) and the signal transducer and activator of transcription 3

(STAT3) (Lecour et al., 2005). However, several interactions between RISK and SAFE pathway have been described (Somers et al., 2012).

As described previously, mPTP opening is a common consequence of ischemia (Weiss et al., 2003). Opening of the mPTP within the first min of reperfusion is caused by Ca^{2+} overload in the mitochondria, oxidative stress and ATP depletion. RISK and SAFE pathway activation through IC targets the mitochondria with mPTP acting as a converging point to attenuate cellular damage (Hausenloy et al., 2005, Hausenloy et al., 2006).

1.8 The Role of Caveolins in Cardioprotection

Caveolae are flask like invaginations of the plasma membrane, which have been described first in 1953 by George Palade using electron microscopy (Palade, 1953). Since then caveolae have been discovered in most cell types (Patel et al., 2008) with only few exceptions, e.g. erythrocytes, lymphocytes and neurons (Yousuke T. Horikawa, 2014). Caveolae are lipid enriched structures made of sphingolipids, cholesterol and fatty acids (Pike, 2006). They are key mediators of physiological cellular functions, including adrenergic receptor regulation, Ca^{2+}-homeostasis, endocytosis and surface signaling (Schilling et al., 2015). Interestingly, several of these mechanisms have also been shown to be involved in cellular responses to I/R and cardioprotection induced by IC (Yousuke T. Horikawa, 2014).

Caveolin (Cav) is the essential structural protein for the formation of caveolae (figure 3). Caveolins exist in three isoforms, Cav-1, Cav-2 and Cav-3. Cav-1 and Cav-2 are expressed by different cell types, including endothelial cells, fibroblasts and pneumocytes (Yousuke T. Horikawa, 2014). Cav-3 has been shown to be the predominant isoform muscle tissue (Song et al., 1996). Knockout (KO) models have been developed for each of the Cav-isoforms with different effects on the organisms and support the idea of tissue specificity. While Cav-1 KO mice show absolute deprivation of caveolar invaginations in several cell types (Drab et al., 2001, Razani et al., 2001), Cav-3 KO mice present with caveolae loss in skeletal as well as myocardial muscle cells (Hagiwara et al., 2000). In Cav-2 KO mice no changes of caveolae formation in the myocardium were reported, but lung parenchyma showed

pathological alterations (Razani et al., 2002). Many functions and signaling processes of caveolins are mediated through a scaffolding domain (CSD, figure 3) (Sargiacomo et al., 1995, Feron et al., 2006).

The CSD is a 20 amino acid long, hydrophobic region in the cytoplasmic amino terminal tail, which can communicate with signaling partners through hydrophobic interactions. Several proteins and pathways have been connected to the CSD and have been shown to interact with GPCRs (Head et al., 2005), eNOS, Erk1/2, or the PI3K/Akt signaling pathway (figure 3) (Ballard-Croft et al., 2006, Fecchi et al., 2006).

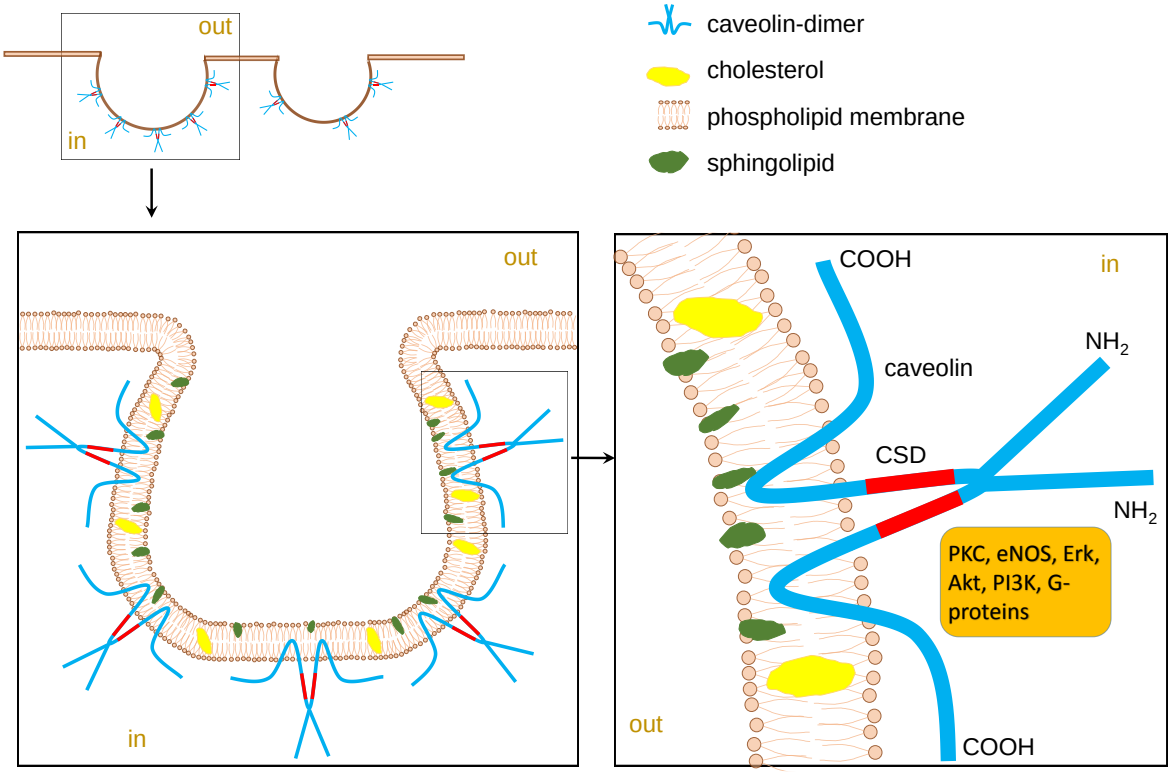

figure 3 ▲ Caveolae and Caveolins. Caveolae are small lipid and cholesterol enriched invaginations of the plasma membrane. Essential for caveolae formation are caveolins (**blue**), which exist in three isoforms Cav-1, Cav-2, Cav-3. Functioning caveolins form dimers and contain a scaffolding domain, CSD (**red**), which interacts with several signaling proteins (**orange box**). Based on (Ushio-Fukai et al., 2006)

Cav-1 and Cav-3 activation and signaling may be mediated by I/R (Ballard-Croft et al., 2006). Interestingly the infusion of the CSD of Cav-1 into hearts undergoing I/R resulted in improved endothelial function and cardiac function (Young et al., 2001). Additionally roles of Cav-1 and Cav-3 in cardioprotection have been shown through overexpression models of Cav-1 and Cav-3, which present innate resistance to

cardiac I/R (Schilling et al., 2015). Cav KO models however, prevent conditioning induced cardioprotection (Yousuke T. Horikawa, 2014).

As other conditioning strategies, e.g. IC, have been related to caveolins and CSD-mediated signaling, a role of caveolins in HePoc induced cardioprotection can be suspected (Schilling et al., 2015).

1.9 Autophagy in Helium Postconditioning

During myocardial infarction, different survival- and death-pathways influence the level and extent of tissue damage as well as clinical outcome. Autophagy, also referred to as type II cell death, is a highly regulated process of degradation and phagocytosis of cellular components (Thapalia et al., 2014). Autophagic signaling is induced by a class-III-PI3K complex involving Vps34 and Bcl-1. A phagophore is formed from membrane parts of the mitochondria, ER and/or Golgi apparatus as well as endosomes. The phagophore matures forming the autophagosome, which fuses with lysosomes sequestering lysosomal acids for target degradation building and autolysosome (figure 4) (Glick et al., 2010).

Therefore, autophagy can promote cell survival during cellular stress as digestion of cellular structures can provide energy from amino or fatty acids. It may target specific cell structures or proteins for digestion (Fink et al., 2005). However, the process can also be non-selective and dismantle essential cell components enhancing cellular damage (Glick et al., 2010). Consequently the over-activation of autophagy may result in cell death or lead to e.g. neurodegenerative, liver or cardiac disorders (Konstantinidis et al., 2012).

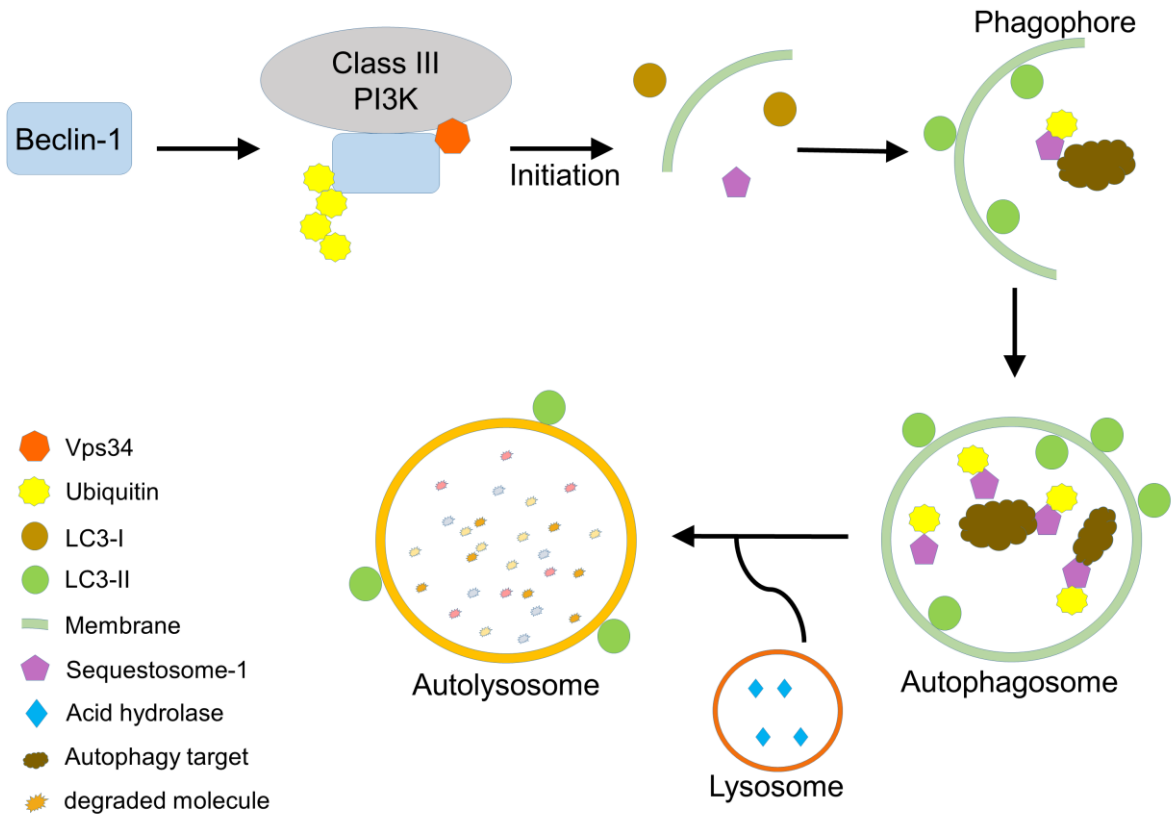

figure 4 ▲ Autolysosome Formation. Ubiquitinated Bcl-1 in the Class-III-PI3K complex initiates the assembly of a membrane-particles, which elongate and form the phagophore. Sequestosome-1 mediates LC3-I, which may be conjugated to LC3-II and is involved in recruitment of autophagosomal membranes. Sequestosome-1 regulates selective autophagy and identifies targets. Fusion with lysosomes results in autolysosome formation and induces degradation of the sequestered molecules. Based on (Sriram et al., 2011)

In long living cells, like cardiomyocytes, autophagy of mitochondria, mitophagy, is a continuous process helping to maintain cellular functioning (Gottlieb et al., 2009). Damaged mitochondria release cytochrome C, which triggers apoptosis, and have a significant role in ROS production. Therefore their removal may decrease oxidative damage and benefit cellular functioning (Kavazis et al., 2008). Additionally, the surviving highly functional mitochondria have a more efficient ATP synthesis and higher threshold for mPTP opening. During myocardial infarction, the most damaged mitochondria are selectively digested by mitophagy, referred to as mitochondrial quality control (Twig et al., 2008). Mitochondrial quality control during cellular stress may stimulate mitochondrial biogenesis and increase number of functioning mitochondria (Kavazis et al., 2008). Taken together, it can be assumed that autophagy and, especially, mitophagy are essential for cardioprotection (Huang et al., 2010) and several pharmacological conditioning protocols, including HePoc, present upregulated autophagy genes like Bcl-1 (Oei et al., 2015b, Wei et al., 2013).

1.10 Aims of the Study

HePoc is a safe treatment for myocardial I/R, which reduces infarct size and cardiac damage. Further insight on underlying mechanism is needed for clinical implementation. In this study, a HePoc rat model, which is, to some extent, resistant to cardiac I/R, was employed. Using western blot and quantitative reverse transcriptase polymerase chain reaction (qRT-PCR), myocardial caveolins as well as RISK pathway kinases and autophagy associated proteins were investigated as possible mediators of HePoc induced cardioprotection.

The main goals of the study were:

(I) To investigate changes of Cav-1 and Cav-3 protein expressions in different cellular fractions and blood (through serum analyses) after I/R as well as HePoc

(II) To evaluate different effects of HePoc on mRNA and protein expression on ischemic AAR and non-ischemic NAAR tissue

(III) To analyze whether activation of RISK pathway and autophagy related proteins is associated with HePoc

The results of the present work give new insight in the effects and underlying protective signaling of HePoc. Our findings may enable further advancement of HePoc research and aid the transfer of HePoc into the clinical setting.

2. Materials and Methods

2.1 Materials

2.1.1 Chemicals and Reagents

Chemicals and solutions were purchased from Merck (Amsterdam, the Netherlands), Carl Roth (Karlsruhe, Germany), Roche (Almere, the Netherlands) or Sigma-Aldrich (Zwijndrecht, the Netherlands), unless stated otherwise.

2.1.2 Antibodies

Antibody	Dilution	Species	Manufacturer
Actin	1:5000	rabbit	Cell Signaling Technology, Cambridge, UK
Cav-1	1:40000	mouse	BD Biosciences, Franklin Lakes, NJ, USA
Cav-3	1:20000	mouse	BD Biosciences
Bcl-1	1:1000	rabbit	Cell Signaling Technology
Sequestosome-1	1:2000	mouse	Abcam, Cambridge, UK
PHB1	1:5000	rabbit	Cell Signaling Technology
NaK-ATPase	1:10000	rabbit	Cell Signaling Technology
pAkt	1:500	rabbit	Cell Signaling Technology
Akt	1:2000	rabbit	Cell Signaling Technology
pErk1/2	1:2000	rabbit	Cell Signaling Technology
Erk1/2	1:2000	rabbit	Cell Signaling Technology
pPKCε	1:1000	rabbit	Milipore, Billerica, MA, USA
PKCε	1:2000	rabbit	Milipore
pPI3K	1:2000	rabbit	Cell Signaling Technology
PI3K	1:2000	rabbit	Cell Signaling Technology

Table 1 ▲ List of Antibodies.

2.1.3 Oligonucleotides

Gene	Direction	Sequence
Cav-1	forward	5’ CGT AGA CTC CGA GGG ACA TC 3’
	reverse	5’ CGT ACA CTT GCT TCT CAT TCA C 3’
Cav-3	forward	5’ CCA AGA ACA TCA ATG AGG ACA TTG TG 3’
	reverse	5’ GTG GCA GAA GGA GAT ACA G 3’
GAPDH	forward	5’ TGC CCC CAT GTT TGT GAT G 3’
	reverse	5’ GCT GAC AAT CTT GAG GGA GTT GT 3’

Table 2 ▲Overview of Primers.

2.1.4 Solutions

Greenberger Lysis Buffer: 8.77 g of sodium chloride together with 1.82 g tris (hydroxymethyl) aminomethane (Sigma 7-9®), 0.20 g of magnesium chloride, monohydrate, 0.11 g of calcium chloride and 5 ml 1% Triton were diluted in 400 ml Milli-Q water. The pH was adjusted to 7.4 with hydrochloric acid and afterwards the volume was filled up to 1 l total with Milli-Q water. 100 µl (100 mg/ml) of each protease inhibitor, Pepstatin A, Leupeptin and Aprotinine, were added shortly before use.

Lysis Stock Solution: 60.57 mg of Sigma 7-9®, 210.00 mg of sodium fluoride, 36.78 mg sodium orthovanadate and 76.08 mg triethylene glycol diamine tetraacetic acid were diluted in 100 ml Milli-Q water.

Tris-hydrochloride, 0.5 mol/l, pH 7.4: 15.8 g of tris-hydrochloride were dissolved in 150 ml Milli-Q water. The pH was corrected to 7.4 with sodium hydroxide. Milli-Q water was added to a total volume of 200 ml.

Inase Inhibitor Mix: Aprotinine 1 mg, Leupeptin 1 mg and Pepstatin A 1 mg were mixed with 10 ml tris-hydrochloride solution (0.5 mol/l, pH 7.4).

Okadaic Acid, 100 µmol/l: 50 µg of okadaic acid potassium salt (stored at -20°C) was diluted in 593 µl Milli-Q water. An end concentration of 100 µmol/l was obtained.

Lysis Buffer: 10 ml lysis stock solution was mixed with 200 µl Inase Inhibitor Mix, 7.7 mg dithiothreitol (DTT) and 100 µl okadaic acid (100 µmol/l).

5x Sample Buffer: 5x Sample Buffer contains 1.0 g sodium dodecyl sulfate (SDS), 25 mg bromophenol blue and 150 mg Sigma 7-9® in 4 ml Milli-Q water. Then 5 ml glycerol were added to the solution, which was next heated to 50°C. The pH was adjusted to 6.8 with hydrochloric acid before 1 ml mercaptoethanol was added.

10x 3-Morpholinopropanesulfonic Acid (MOPS) Running Buffer: 60.6 g Sigma7-9®, 104.6 g MOPS, 10 g SDS, 3 g ethylenediaminetetraacetic acid (EDTA) were dissolved in 1000 ml Milli-Q water.

1x MOPS Running Buffer: 50 ml 10x MOPS Running Buffer were added to 450 ml Milli-Q water.

10x Transfer Buffer: 30 g Sigma 7-9® and 144 g glycine were dissolved in Milli-Q water to a total volume of 1000 ml.

1x Transfer Buffer: 200 ml 10x Transfer Buffer were added to 1400 ml Milli-Q water. 400 ml methanol were added before the solution was stored at 4°C.

Tween PBS (TBS-T), pH 8: 6 g Sigma 7-9®, 22.2 g sodium chloride and 2 ml Tween 20® were dissolved in 2000 ml Milli-Q water. Before use, the pH was corrected to 8.0 with hydrochloric acid. The solution was stored at 4°C.

2.2 Methods

2.2.1 Ethics

Animal experiments were performed in accordance with the Guide for Care and Use of Laboratory Animals (NIH Publication No. 85-23, revised 1996) and approved by the Academic Medical Center's animal ethics committee (DAA102650).

2.2.2 Animal Model of Ischemia/Reperfusion

Male Wistar rats (354 to 426 g, age range of 12 to 16 weeks) were acclimatized for seven d with sequences of 12 h light and 12 h dark and access to food and water ad libitum. Animals were anesthetized by intraperitoneal S-ketamine (150 mg/kg)/diazepam (1.5 mg/kg) injection and surgical procedures were performed as described previously (Oei et al., 2012). All rats were ventilated mechanically and the carotid artery was canulated to register the mean arterial pressure (section 7.3) and draw blood samples. Animals were left untreated for 15 min before the start of the respective experimental protocol. The aortic pressure was measured using a fluid filled pressure catheter. The analog signal was digitalized with an analogue-to-digital converter (Powerlab/8SP, ADInstruments Pty Ltd, Castle Hill, Australia) and recorded with Chart 5.0 for Windows (ADInstruments Pty Ltd, Castle Hill, Australia).

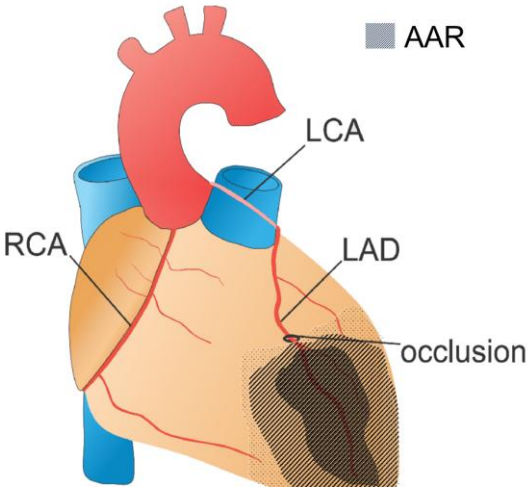

figure 5 ▲ Scheme of Coronary Artery Occlusion. LCA = left coronary artery, LAD = left anterior descending artery, RCA = right coronary artery, AAR = (ischemic) area at risk.

The left anterior descending coronary artery (LAD) branching out of the left coronary artery (LCA) was encircled with a single puncture 5-0 Prolene suture (Ethicon Johnson&Johnson, Amersfoort, the Netherlands) through the myocardium. Regional ischemia was induced by tightening of the suture, which was re-opened in order to begin reperfusion (figure 5). In animals subjected to I/R only, the ischemic period was followed by 5, 15 or 30 min of reperfusion, respectively

(I/R5, 15, 30) (figure 6). The treatment groups were ventilated with heliox (70% helium and 30% oxygen, Linde Gas Benelux, Dieren, the Netherlands) at 24 min of ischemia ensuring sufficient helium concentrations in the lungs at the onset of reperfusion. HePoc was performed for 5, 15 or 30 min of reperfusion (I/R+He5, 15, 30) (figure 6). The Sham group received surgical treatment without undergoing I/R or HePoc. Tissue was obtained from the ischemic area at risk (AAR) and the non-ischemic, not area at risk (NAAR). AAR and NAAR were separated and ground in a pre-cooled mortar (Oei et al., 2015b). The AAR was determined histologically on the basis of the pathological demarcation zone at low power view (10x magnification), extending from the suture to the apex of the heart (figure 5) (Oei et al., 2015b). AAR as well as the NAAR tissue was snap frozen in liquid nitrogen and stored at -80°C until further processing.

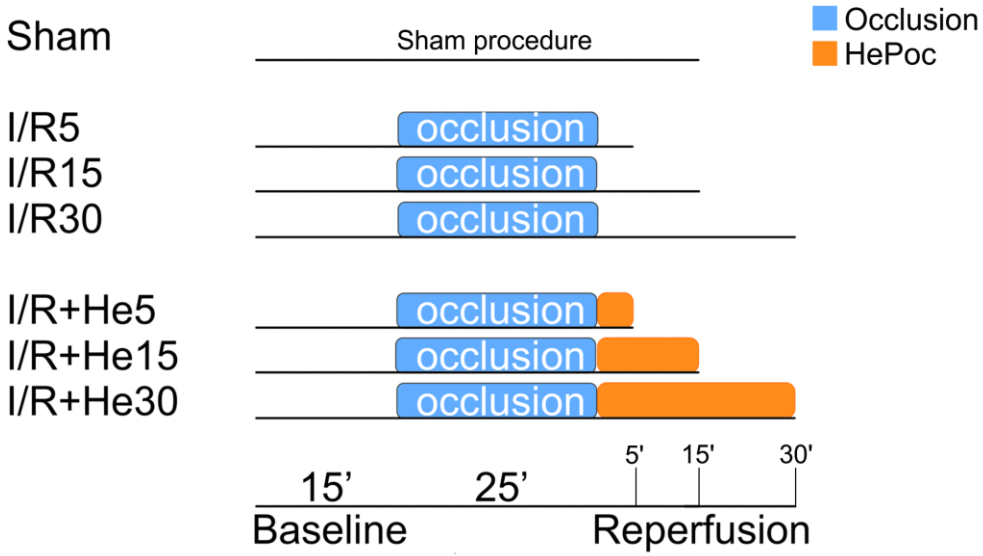

figure 6 ▲ Experimental Setting. After 15 min of baseline-stabilization the LAD was ligated to commence ischemia in the left ventricle (figure 5). The study groups underwent 15 min of reperfusion and 15 min of reperfusion with helium ventilation. The Sham operated group did not undergo ischemia. The experiments were performed with 5 and 30 min periods, respectively. However, these results are only shown in the appendix as groups showed no significant differences (section 7.1 and 7.2). The results and discussion section will focus on the 15 min intervention groups only. (Flick et al., 2016)

2.2.3 Preparation of Cytosolic-, Membrane- and Mitochondrial- Fractions from Ischemic AAR and Non-Ischemic NAAR Tissue

For fraction separation, lysis buffer, inase-inhibitor mix, DTT and okadaic acid, according to section 2.1.4, were added. The samples were mixed with a homogenizer (Ultra-Turrax T8, IKA) and 50 µl of the respective sample were pipetted into new vials containing 450 µl of Tripur for RNA analyses. The remaining homogenate was centrifuged at 1000 g, 4°C for 10 min, the supernatant subsequently at 10000 g, 4°C for 15 min. The resulting supernatant was pipetted into new vials, while the remaining pellet was re-suspended with lysis buffer (1%Triton X-100) to be used as the mitochondrial fraction. Samples were centrifuged again at 5000 g, 4°C for 15 min and the supernatant was used as the cytosolic fraction. The pellet was mixed with lysis buffer, vortexed and after 60 min of incubation on ice centrifuged at 5000 g, 4°C for 15 min. The supernatant was obtained as the membrane fraction (figure 7). All fractions were stored at -80°C.

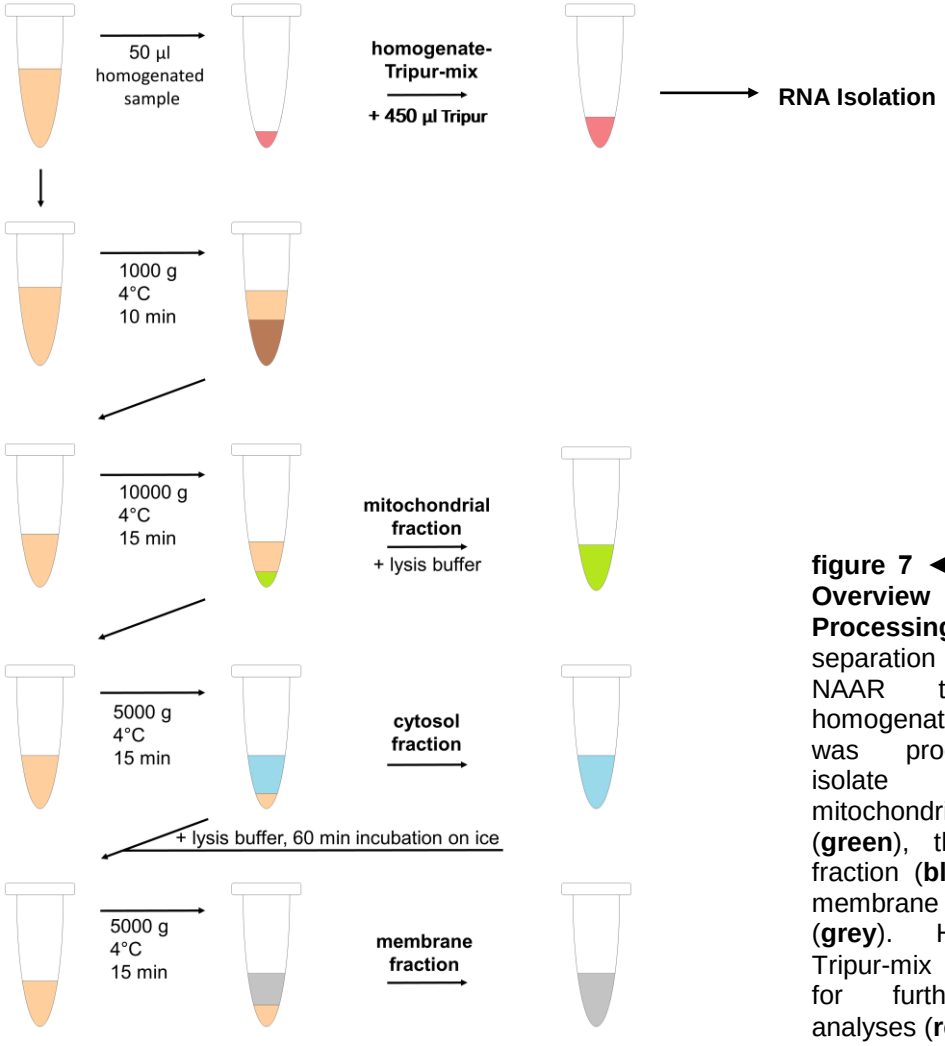

figure 7 ◄ Schematic Overview of Tissue Processing. After separation of AAR and NAAR the tissue homogenate (**beige**) was processed to isolate the mitochondrial fraction (**green**), the cytosolic fraction (**blue**) and the membrane fraction (**grey**). Homogenate-Tripur-mix was stored for further mRNA analyses (**red**).

2.2.4 Bradford Protein Assay

Bradford Protein Assays (Bio-Rad, Hercules, CA, USA) were performed in duplicates on standard 96-well plates. For the bovine serum albumin (BSA) standard curve 10 µl of each pre-diluted BSA standard solutions was pipetted in duplicate. 10 µl of sample was pipetted into each well. Afterwards 140 µl/well of Bradford reagent were added and mixed on a microplate mixer. Concentrations of each sample were calculated by reading the absorbance at 595 nm with a microplate reader.

2.2.5 Western Blot

Protein concentrations were measured as described in section 2.2.4 and diluted to align concentrations. Equal amounts of protein were mixed with SDS-PAGE sample buffer (SDS, Bromophenol Blue, TrisBase, Glycerol and Mercaptoethanol), the samples were vortexed and heated to 95°C for 5 min. Samples were separated by SDS-PAGE using Criterion™ XT precast gels (Bio-Rad, Hercules, CA, USA) and transferred onto a Immobilin-FL Membrane (Millipore, Billerica, MA, USA). The membrane was washed in Odyssey® Blocking Buffer (LI-COR, Lincoln, NE, USA) for 60 min and incubated with target antibodies overnight (table 1). After washing the membrane for 3x5 min in cold, fresh TBS-T, the blot was incubated for 60 min with IRDye800 CW or IRDye680 CW conjugated mouse- or rabbit-antibody (1:5000, LI-COR, Lincoln, NE, USA). The membranes were washed again for 3x5 min and scanned using Odyssey ® Infrared Scanning Software v2.1 (LI-COR, Lincoln, NE, USA), which was later used for quantification of the blots. Results were presented as ratio of the target protein over a fraction-specific reference protein: cytosolic fraction, actin; membrane fraction, tubulin; mitochondrial fraction prohibitin-1 (PHB1) (for Cav-1, Cav-3 and RISK pathway proteins) or NaK-ATPase (for Bcl-1 and sequestosome-1). RISK pathway proteins were analyzed as ratio of phosphorylated:total protein. Duplicate western blots were performed for all experiments.

2.2.6 Isolation of RNA and cDNA Preparation

A total of 450 µl tissue-homogenate-Tripur mix was diluted 1:10 with 1-Bromo-3-chloropropane (Sigma-Aldrich, Zwijndrecht, the Netherlands) and shaken vigorously for 15 sec. After 10 min of incubation at room temperature, the samples were centrifuged at 12000 g, 4°C for 15 min. The upper layer containing RNA was pipetted into clean vials and precipitated by adding 250 µl isopropanol followed by another 10 min incubation period. RNA was centrifuged at 12000 g, 4°C for 8 min resulting in RNA pellets and supernatants, which were removed to dissolve the RNA pellet in 1ml 75% ethanol. The samples were centrifuged at 12000 g, 4°C for 5 min and after this ethanol was removed and RNA was dissolved in 20 µl of Milli-Q water. RNA was heated at 60°C for 5 min, followed by a short centrifugation, vortexing and another heating at 60°C for 5 min. RNA concentrations were determined by UV-vis absorbance spectroscopy (NanoDrop, Thermo Scientific, Rockford, IL, USA). RNA yields typically ranged from 0.16 to 1.08 µg/µl. cDNA was synthesized using the First Strand cDNA Synthesis Kit for qRT-PCR (Roche, Almere, the Netherlands). Amplicons were diluted to 1 µg RNA/10 µl Milli-Q. 1 µl oligo-(dT)-primer (50 µmol/l) was added before samples were heated for 10 min at 65°C. cDNA-mix was added containing 4 µl 5x RT-buffer, 2 µl dNTP-mix, 0.5 µl RNase inhibitor (40 U/µl), 0.5 µl RT (20 U/µl) and 2 µl Milli-Q water. The samples were heated at 55°C for 30 min and then heated at 85°C for 5 min. The cDNA samples were diluted with 60 µl Milli-Q water and stored at -80°C.

2.2.7 Reverse Transcriptase Real Time PCR

cDNA samples were diluted 1:5 in Milli-Q water before adding 5 µl Sybr Green I MasterMix (Roche, Almere, the Netherlands) and 0.5 µl of sense- and anti-sense-primer for Cav-1, Cav-3, or glyceraldehyde-3-phosphatedehydrogenase (GAPDH) as reference gene (table 2) (all Invitrogen, Breda, the Netherlands). qRT-PCR was performed in the LightCycler480 (Roche, Almere, the Netherlands) with following conditions: Pre-incubation heating to 95°C for 10 min, followed by 45 cycles of amplification (95°C for 15 sec, 56°C for 10 sec, 72°C for 15 sec) and a melting curve analysis. Amplicons that showed amplification of nonspecific products were excluded from analyses. Subsequently for each amplicon its baseline was determined and

corrected using LinRegPCR software (AMC Heart Failure Research Center, Amsterdam, the Netherlands) according to Ruijter and colleagues (Ruijter et al., 2009). Each amplicon was corrected for baseline fluorescence. Amplicons that did not reach Nq before cycle 45 were considered undetectable. The individual PCR efficiencies were calculated and amplicons with an efficiency <1.80 or >2.00 were excluded from further analyses. The mean efficiency of each target gene was used to calculate the starting concentration (N0) per amplicon. All samples were normalized to the N0 of the reference gene GAPDH. Differences in expression of the gene of interest in the experimental groups (I/R15 vs. I/R+He15) and Sham were calculated.

2.2.8 Statistical Analyses

Kruskal-Wallis tests with Dunn's post hoc analyses were performed to determine differences of protein levels and mRNA-expression between the groups. GraphPad Prism 5 (GraphPad Software, La Jolla, CA, USA) was used to perform tests. Statistical significance was assumed if $P<0.05$. Variables are expressed as mean ± standard error of the mean (SEM).

3. Results

3.1 Main Findings

	Target	Location	I/R+He15 vs. I/R15	P-Value	Figure
mRNA	*Cav-1*	AAR whole tissue	↑	P<0.05	*8 A*
protein	*Cav-1*	AAR Membrane	↑	P<0.01	*9 A*
	Cav-3	AAR Membrane	↑	P<0.05	*9 B*
		Serum	↑	P<0.05	*11 B*
	Akt	AAR Cytosol	↑	P<0.05	*12 A*
		NAAR Cytosol	↑	P<0.05	*13 A*
	Erk1	AAR Cytosol	↑	P<0.05	*12 C*
		NAAR Cytosol	↓	P<0.001	13 C
	Erk2	AAR Cytosol	↑	P<0.05	*12 B*
		NAAR Cytosol	↓	P<0.001	*13 B*
	Bcl-1	AAR Mitochondria	↑	P<0.05	*14 A*
		NAAR Mitochondria	↑	P<0.05	*14 B*

↑ *significant increase*
↓ *significant decrease*

Table 3 ▲ Main Findings.

3.2 mRNA Expression Analyses of Caveolin-1 and Caveolin-3

To measure mRNA expression of Cav-1 and Cav-3, qRT-PCR was performed with mRNA isolated from whole tissue (figure 7). In the ischemic tissue of the I/R15 group, both Cav-1 and Cav-3 showed significantly reduced mRNA expression [AAR: Cav-1, I/R15 (4.49±0.37) P<0.05 vs. Sham (6.81±0.91); figure 8 A; Cav-3, I/R15 (3.82±0.18) P<0.01 vs. Sham (5.06±0.29); figure 8 B]. The HePoc group presented increased

expression of Cav-1 in comparison to I/R, but no differences vs. Sham [AAR: Cav-1, I/R+He15 (5.65±0.25) P<0.05 vs. I/R15 (4.49±0.37); figure 8 A]. Cav-3 expression was also reduced after HePoc compared to Sham, but showed no differences vs I/R [AAR: Cav-3, I/R+He15 (3.54±0.21) P<0.001 vs. Sham (5.06±0.29); figure 8 B]. In the NAAR, Cav-1 and Cav-3 mRNA expression were lower after HePoc in comparison to Sham [NAAR: Cav-1, I/R+He15 (0.66±0.11) P<0.05 vs. Sham (1.58±0.34); figure 8 A; Cav-3, I/R+He15 (4.70±0.31) P<0.01 vs. Sham (6.70±0.38); figure 8 B]. No differences were found comparing mRNA expression of Cav-1 and Cav-3 between I/R15 and I/R+He15 in NAAR tissue.

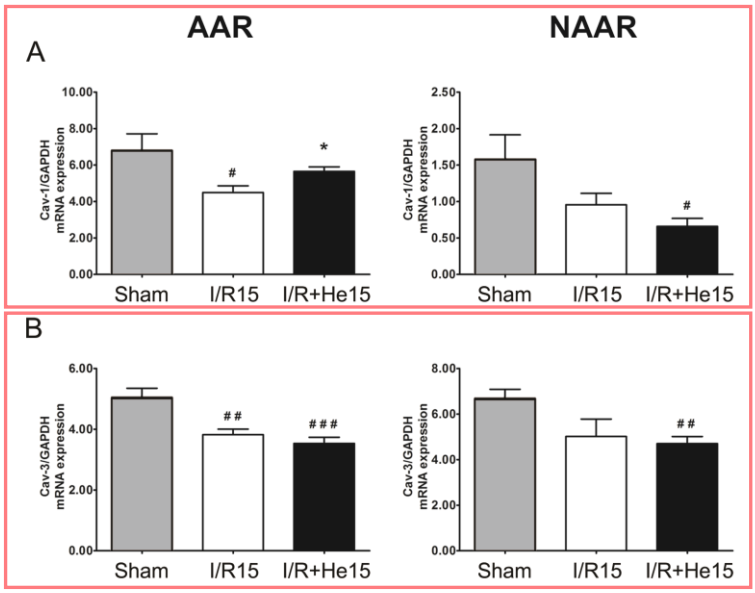

figure 8 ▲ Quantification of mRNA Expression of Caveolin-1 and Caveolin-3 in Sham, I/R15 and I/R+He15 Treated Animals. mRNA expression of Cav-1 (**A**) and Cav-3 (**B**) was measured in AAR and NAAR tissue (red) using GAPDH as reference gene. mRNA levels are displayed as ratio of Cav-1 or Cav-3:GAPDH. Results show the mean ± SEM. A pound sign indicates differences vs. Sham (#=P<0.05, ##=P<0.01 ###=P<0.001), whereas the asterisk indicates differences vs. I/R15 (*=P<0.05). n=8 in each group. (Flick et al., 2016)

3.3 Protein Analyses of Caveolin-1 and Caveolin-3

For protein analyses using western blot, the tissue was separated into cellular fractions as described in section 2.2.3 (figure 7).

HePoc significantly increased accumulation of Cav-1 and Cav-3 in the membrane fraction of ischemic cardiac tissue, AAR, compared to Sham and I/R15 [AAR: Cav-1, I/R+He15 (45.53±8.38) P<0.01 vs. Sham (17.38±4.31); P<0.01 vs. I/R15

(20.43±4.44); figure 9 A; Cav-3, I/R+He15 (12.62±2.35) P<0.05 vs. Sham (5.99±1.21); P<0.05 vs. I/R15 (6.52±1.13); figure 9 B]. In the NAAR tissue protein expression of caveolins in the membrane fraction did not show differences between groups (figure 9 A and B). In the cytosolic and mitochondrial fraction no differences of protein levels of Cav-1 and Cav-3 were detected in AAR or NAAR tissue (figure 10).

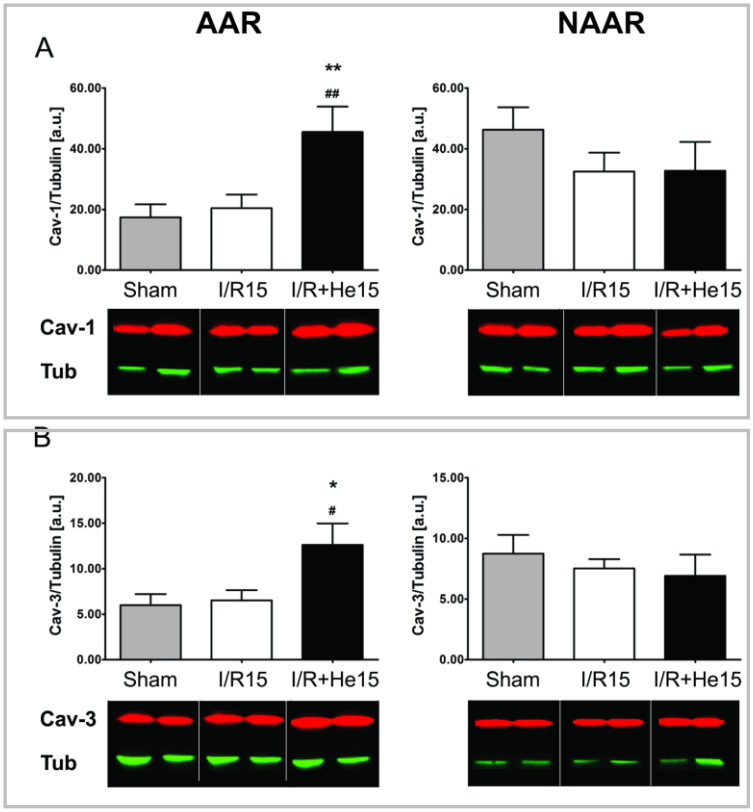

figure 9 ▲ Protein Levels of Caveolin-1 and Caveolin-3 in Membrane Fractions of Sham, I/R15 and I/R+He15 Treated Animals. Data are shown as ratios of Cav-1:tubulin (**A**) and Cav-3:tubulin (**B**) in AAR and NAAR membrane fractions (grey). Columns display the mean ± SEM. A pound sign indicates differences compared to Sham (#=P<0.05, ##=P<0.01), whereas the asterisk indicates differences compared to I/R15 (*=P<0.05, **=P<0.01). Bands display a representative example of western blot analyses. Sham: n=6, I/R15 and I/R+He15: n=7. (Flick et al., 2016)

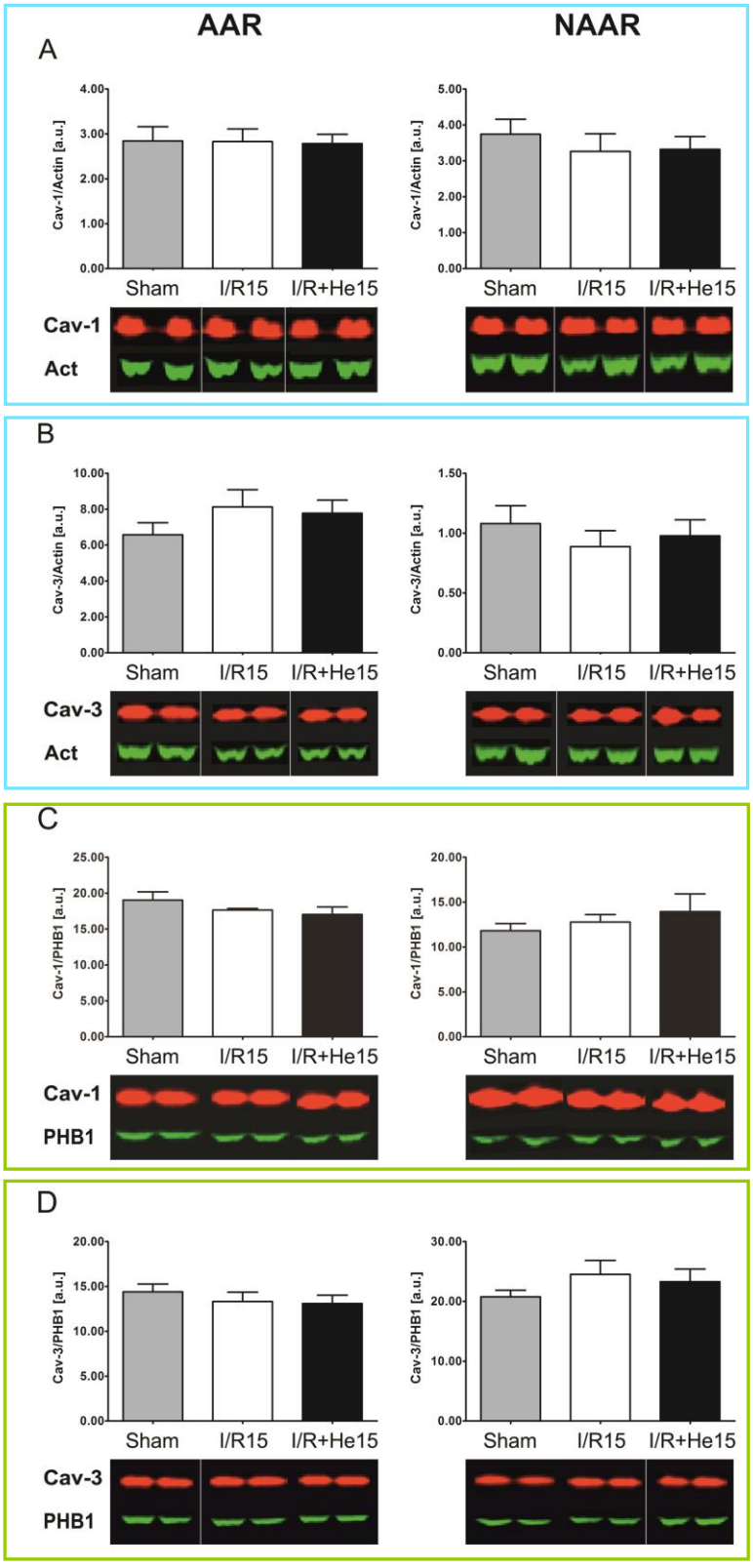

figure 10 ▲ Protein Levels of Caveolin-1 and Caveolin-3 in Cytosolic and Mitochondrial Fractions of Sham, I/R15 and I/R+He15 Treated Animals. Values are displayed as ratio of Cav-1 or Cav-3 and control protein actin (Act) in cytosol (**A**+**B**, blue) or prohibitin-1 (PHB1) for mitochondria (**C**+**D**, green). Columns display the mean ± SEM. Bands display a representative example of western blot analyses. n=7 in each group. (Flick et al., 2016)

Serum analyses did not present any differences of Cav-1 levels (figure 11 A), whereas serum from I/R+He15 group revealed increased amounts of Cav-3 [Serum: Cav-3, I/R+He15 (8.23±0.48) P<0.05 vs. I/R15 (6.79±0.41); figure 11 B].

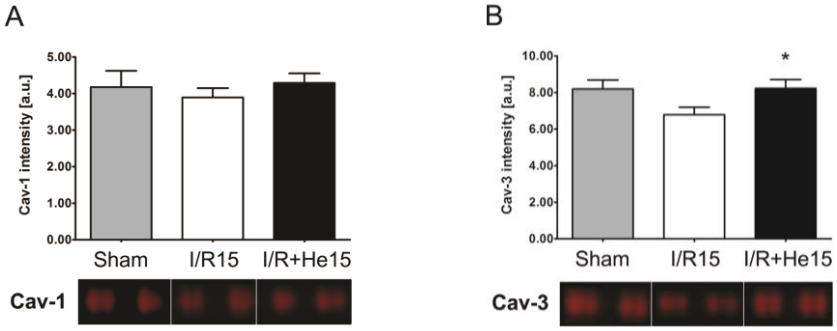

figure 11 ▲ Protein Levels of Caveolin-1 and Caveolin-3 in Serum of Sham, I/R15 and I/R+He15 Treated Animals. Data are shown as relative values of Cav-1 (**A**) and Cav-3 (**B**) in serum. Columns display the mean ± SEM. An asterisk indicates differences compared to I/R (*=P<0.05). Bands display a representative example of western blot analyses. Sham: n=4, I/R15 n=7, I/R+He15: n=7. (Flick et al., 2016)

3.4 Phosphorylation of RISK Pathway Associated Proteins

Western blot analyses of RISK pathway associated proteins showed increased phosphorylation levels of Akt in the ischemic tissue [AAR: I/R+He15 (6.50±0.68) P<0.05 vs. Sham (4.51±0.49); P<0.05; vs. I/R15 (4.38±0.33); figure 12 A]. Increased amounts of pAkt were also detected in non-ischemic NAAR tissue after HePoc [NAAR: I/R+He15 (6.51±0.70) P<0.05 vs. I/R15 (4.35±0.30); figure 13 A]. Erk1 and Erk2 showed increased activation after I/R compared to Sham [AAR: Erk1, I/R15 (12.37±1.54) P<0.01 vs. Sham (5.63±0.62); figure 12 B; Erk2, I/R (1.85±0.31) P<0.05 vs. Sham (1.22±0.08); figure 12 C]. HePoc treated animals showed even higher phosphorylation levels of both Erk1 and Erk2 in the ischemic tissue compared with I/R15 [AAR: Erk1, I/R+He15 (14.57±0.93), P<0.05 vs. I/R15 (12.37±1.54); figure 12 B; Erk2, I/R+He15 (2.68±0.18) P<0.05 vs. I/R15 (1.85±0.31); figure 12 C].

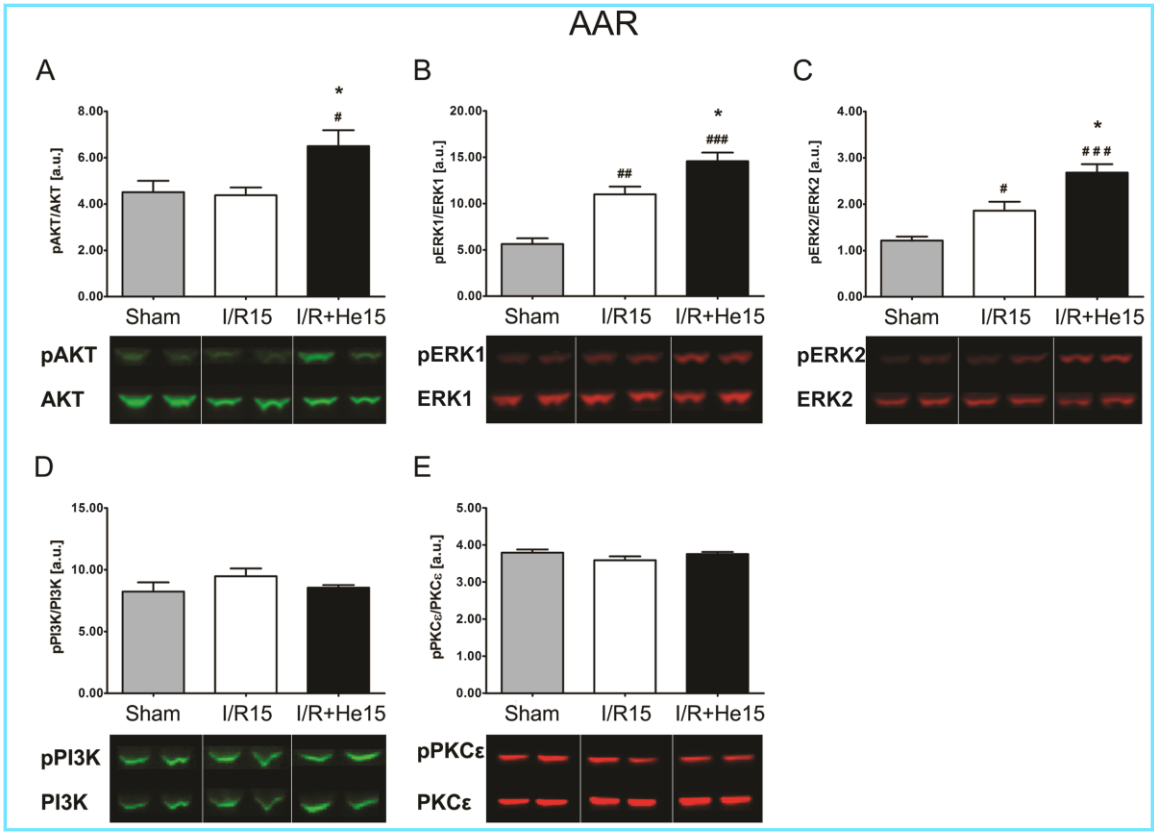

figure 12 ▲ Phosphorylation Levels of RISK Pathway Associated Proteins in Ischemic AAR Cardiac Tissue of Sham, I/R15 and I/R+He15 Treated Animals. Data are shown as ratios of phosphorylated protein:total protein in the AAR cytosolic fraction (blue). Columns display the mean ± SEM. A pound sign indicates differences compared to Sham (#=P<0.05, ##=P<0.01, ###=P<0.001), whereas the asterisk indicates differences compared to I/R15 (*=P<0.05). Bands display a representative example of western blot analyses. n=7 in each group. (Flick et al., 2016)

NAAR tissue analyses revealed, that Erk1 and Erk2 phosphorylation was reduced vs. Sham in both I/R15 and I/R+He15 [NAAR: Erk1, I/R15 (2.23±0.30); I/R+He15 (2.17±0.21) both P<0.001 vs. Sham (5.62±1.21); figure 13 B; Erk2, I/R15 (4.51±0.32); I/R+He15 (5.03±0.42) both P<0.001 vs. Sham (12.25±1.08); figure 13 C]. Phosphorylation levels of PI3K and PKCε showed no differences in any of the treatment groups (figure 12 D, 13 D, 12 E and 13 E).

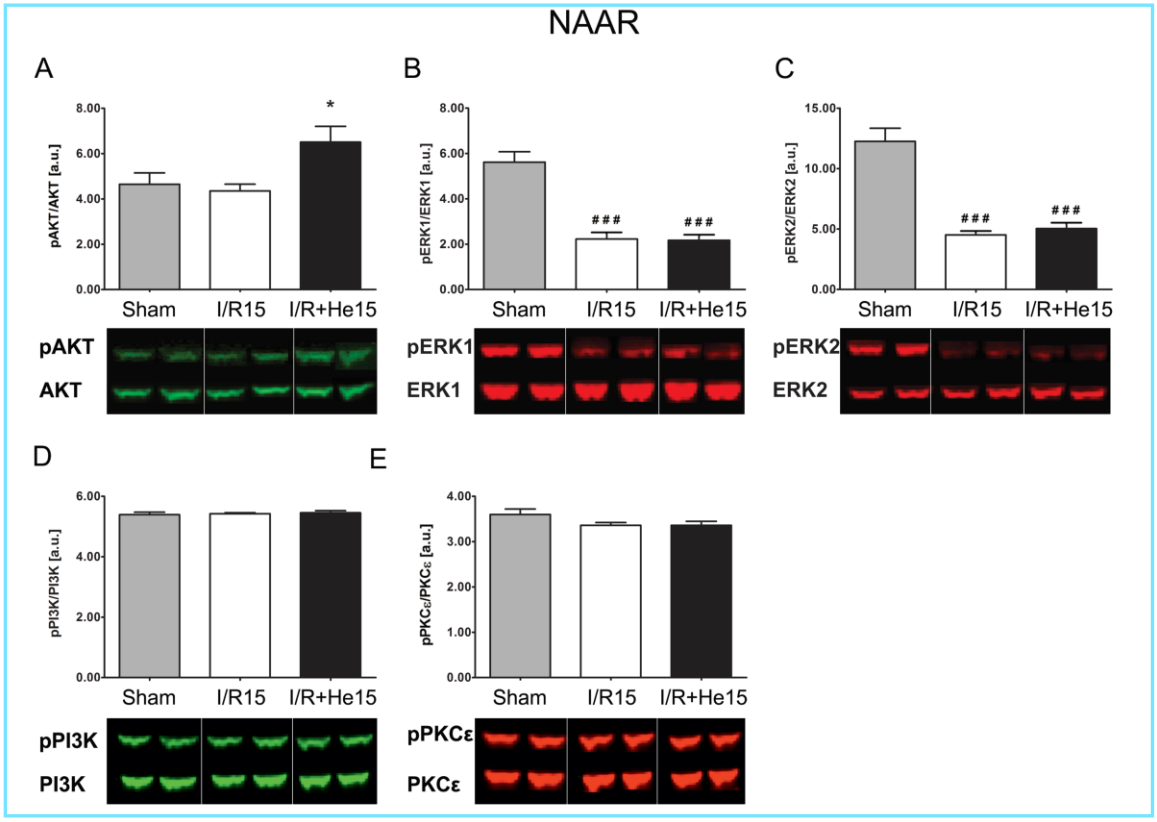

figure 13 ▲ Phosphorylation Levels of RISK Pathway Associated Proteins in Non-Ischemic NAAR Cardiac Tissue of Sham, I/R15 and I/R+He15 Treated Animals. Data are shown as ratios of phosphorylated protein:total protein in the NAAR cytosolic fraction (blue). Columns show the mean ± SEM. A pound sign indicates differences compared to Sham (###=P<0.001) whereas the asterisk indicates differences compared to I/R15 (*=P<0.05). Bands display a representative example of western blot analyses. n=7 in each group. (Flick et al., 2016)

3.5 Protein Analyses of Autophagy Associated Proteins

Our analyses of sequestosome-1 showed no differences between Sham, I/R and HePoc in any of the investigated cell fractions in AAR or NAAR (not shown). Bcl-1 levels in I/R15 group were significantly lower than Sham in both AAR and NAAR tissue [AAR: Bcl-1 I/R15 (1.99±0.14) P<0.05 vs. Sham (3.32±0.49); figure 14 A; NAAR: Bcl-1 I/R15 (2.70±0.12) P<0.05 vs. Sham (4.44±0.48); figure 14 B] However, Bcl-1 showed a significant increase after 15 min of HePoc in the mitochondrial fraction, similar results were found in both AAR and NAAR tissue [AAR: Bcl-1, I/R+He15 (2.62±0.17) P<0.05 vs. I/R15 (1.99±0.14); figure 14 A; NAAR: Bcl-1, I/R+He15 (3.77±0.17) P<0.05 vs. I/R15 (2.70±0.12); figure 14 B]. In the cytosolic and membrane fractions no significant differences were detected (not shown).

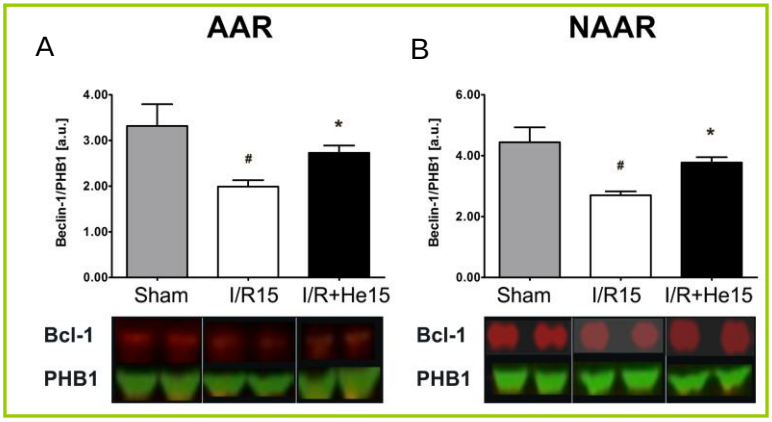

figure 14 ▲ Protein Levels of Bcl-1 in Mitochondrial Fractions of Sham, I/R15 and I/R+He15 Treated Animals. Values are displayed as ratio of Bcl-1 and control protein Prohibitin-1 (PHB1). Figures show results in AAR (**A**) and NAAR (**B**) tissue. Columns display the mean ± SEM. A pound sign indicates differences compared to Sham (#=P<0.05), whereas the asterisk indicates differences compared to I/R15 (*=P<0.05). Bands display an example of western blot analyses. n=7 for each group. Based on (Oei et al., 2015b)

3.6 Protein Analyses of Caveolin-1 and Caveolin-3 after 5 and 30 Min of HePoc

The results of western blot analyses of Cav-1 and Cav-3 in different cell compartments after 5 and 30 min of HePoc are not further described in the results section. No significant differences between the groups were found. The results are shown in the appendix (section 7.1 and 7.2).

4. Discussion

4.1 Helium Postconditioning and Cardioprotection

The cardioprotective effects of helium have been replicated in different animals and models (Huhn et al., 2009b, Pagel et al., 2007, Pagel et al., 2008b). For this thesis we used tissue from a HePoc rat model, which was previously investigated for myocardial damage with best outcome after 15 min of HePoc (Oei et al., 2015b). The tissue was obtained immediately after performing I/R or HePoc. It is widely accepted that damaging effects of reperfusion injury occur within the first min. Therefore cardioprotective signaling induced by HePoc has to take effect with the onset of reperfusion to reduce damage (Kin et al., 2004).

In line with the previous analyses of tissue profiles and infarct size (Oei et al., 2015b) our results indicate that duration of HePoc is of great importance. Too short, 5 min, or too long, 30 min, duration of HePoc showed no significant changes in protein expression in the different cellular fractions (section 7.1 and 7.2). Another HePoc rat model by Oei et al. showed similar results supporting the idea that duration of HePoc is of high importance (Oei et al., 2015a). Cardioprotection was also abolished in a rat model, where prolonged helium inhalation commenced with the onset of ischemia and continued for three hours of reperfusion (Hale et al., 2013). Other studies investigating liver protection and hepatic I/R came to a similar conclusion and showed no beneficial effect after elongated HePoc (Fukuda et al., 2007). In most studies no harmful side effects of helium ventilation were reported. Only a single study reports detrimental effects of helium conditioning in oxygen deprived human kidney cells after three hours of helium inhalation (Rizvi et al., 2010).

However, further research will be necessary to determine the ideal duration of postconditioning, in order to transfer the findings of our study to human models (Oei et al., 2015a).

4.2 Helium Postconditioning and Caveolins

Caveolins are important transmitters of pathways involved in cardioprotection and their repression in KO models reveals complete inhibition of advantageous effects in several settings (Yousuke T. Horikawa, 2014, Patel et al., 2007, Horikawa et al., 2008). While the exact involvement of caveolins in cardioprotection is yet unknown, more recent studies revealed an important role in transmembrane signaling (Fridolfsson et al., 2014).

In our setting we cannot confirm previous reports of caveolin reduction after I/R (Chaudhary et al., 2013), with no difference of Cav-1 and Cav-3 protein levels compared to Sham in any fraction of ischemic AAR tissue. However, our results show insignificant reduction of caveolin in the NAAR membrane and cytosolic fraction after both I/R and HePoc. As we understand, caveolins function mostly within membrane formations. Our analyses of the AAR membrane fraction revealed a significant increase of both, Cav-1 and Cav-3 after 15 min of HePoc. These results oppose recent results from Weber et al., who applied 30 min of helium ventilation in a mouse model. In their model Cav-1 analyses of whole cell protein levels presented significantly lower Cav-1 compared to the control group (Weber et al., 2013). Differences in used models, with longer helium ventilation and later tissue extraction, have to be taken in consideration, when comparing these results. Our findings of increased Cav-1 and Cav-3 in AAR membrane may indicate involvement of membrane-associated and therefore functioning, caveolins in HePoc-induced myocardial protection. Caveolins function as regulators for cellular processes. They are involved in metabolism and support compartmentalization of receptors and other proteins within the plasma membrane through their CSD (Ostrom, 2002, Patel et al., 2008). Interaction with and localization to caveolins of cardioprotective RISK pathway kinases, e.g. Erk1/2, PI3K and Akt, have been shown in several studies (Shack et al., 2003, Woodman et al., 2002, Smythe et al., 2006). A study by Ballard-Croft et al. even suggests that separate pathways can be activated specifically, when located to caveolar formations (Ballard-Croft et al., 2006). Underlining the importance of caveolins, the infusion of the CSD of Cav-1 into hearts undergoing I/R reduced cardiac damage (Young et al., 2001). However the exact role and purpose of caveolins within the membrane still need to be investigated.

In our study the analyses of mRNA expression showed a significant increase of Cav-1 after HePoc compared to I/R in AAR tissue. The mRNA levels of Cav-1 in HePoc group reached values similar to Sham animals. However, due to our model design, no conclusion, whether levels were decreased after I/R and re-elevated by HePoc or remained the same during the whole protocol, can be made. Cav-3 expression on the other hand was significantly reduced in comparison to Sham in both, AAR and NAAR, with no difference to the I/R only group.

Other studies with Cav-1 and Cav-3 KO models for I/R and conditioning protocols showed loss of cardioprotective effects in both designs (Patel et al., 2007, Tsutsumi et al., 2010a, Tsutsumi et al., 2010b). Overexpression of Cav-3 resulted in increased activation of respective pathways and even induced endogenous cardioprotection in a study conducted by Tsutsumi et al. (Tsutsumi et al., 2008). In addition, Cav-3 KO mice lack formation of caveolae and may present with cardiac hypertrophy and cardiomyopathy (Kikuchi et al., 2005). As mentioned earlier, the overexpression of Cav-3 lead to a significant increase of caveolae formation, improved cardiac function and innate cardioprotection against I/R (Tsutsumi et al., 2008, Horikawa et al., 2011). Overexpression of Cav-1 may result in inhibition of Erk1/2 signaling and vice versa, the activation of Erk1/2 has been shown to downregulate Cav-1 mRNA (Engelman et al., 1998). Our results show a different tendency with increased Erk1/2 activation and simultaneous mRNA upregulation of Cav-1 in AAR tissue. Interestingly Erk1/2 phosphorylation was significantly lower in NAAR tissue of our model supporting the thesis of negative correlation. However, in NAAR tissue Cav-1 mRNA showed a tendency of reduced expression after I/R and HePoc. This was previously reported in an I/R rat model by Ballard-Croft et al. (Ballard-Croft et al., 2006). Our findings of reduced Cav-3 mRNA expression in AAR tissue differ from the findings in same study, where Cav-3 expression was not altered by I/R (Ballard-Croft et al., 2006).

Our results indicate that HePoc not only induces changes of protein level, but also in mRNA expression. However, these changes are unlikely transferred into a protein response within the short time period for tissue extraction chosen in our current model. Nonetheless, they might indicate that I/R and HePoc induce long-term cellular responses. Even though the immediate effects of mRNA regulation are marginal, the

modulation of Cav-expression could benefit long term outcome and cardiac remodeling (Arslan et al., 2013).

Besides the effects on mRNA level, we found not only increased Cav-1 and Cav-3 in the membrane, but also higher levels of Cav-3 in the serum of HePoc groups. Interestingly, the previously mentioned model, in which Cav-1 was depleted from the tissue, showed higher Cav-1 and Cav-3 levels in the serum as well (Weber et al., 2013).

Serum caveolin has been researched in different medical fields and discussed controversially. Increased serum levels have been found in various cancers including prostate (Sugie et al., 2013), colorectal (Erdemli et al., 2016) or lung cancer (Han et al., 2014). Data suggest that serum caveolin might be linked to pro-angiogenic and pro-survival mechanisms in tumors (Tahir et al., 2008). Protective characteristics in physiological states have been reported for prevention of right heart hypertrophy and subsequent pulmonary hypertension (Jasmin et al., 2006). In contrast lower Cav-1 levels have been related to cerebral microbleeds. In the same study protective effects of circulating caveolins during acute cerebral bleeding are proposed supporting the idea of beneficial characteristics of caveolins in the serum (Zhang et al., 2016). Furthermore heart specific serum Cav-3 likely plays an important role in cardiac pathologies. Feiner et al. have reported significant decrease of Cav-3 in heart failure. Nonetheless the functioning of caveolins in the serum will need further investigation and the exact mechanism are yet unclear (Feiner et al., 2011). Together the current data points towards interactions between serum caveolins and specific tissue or organs.

4.3 Helium Postconditioning and RISK Pathway Activation

Recent studies have shown that mPTP signaling is transmitted through the CSD, an important binding site of caveolins (Fridolfsson et al., 2014). The CSD acts as a binding partner for many mediators and end-effectors involved in conditioning induced cardioprotection. One group of these known binding partners is RISK pathway associated kinases. These include the investigated kinases PI3K, Akt, PKCε and Erk1/2. PKCε and PI3K are known upstream mediators of Erk1/2 and Akt, which, when activated, cause inhibition of mPTP opening. Activation of these kinases has

been described for ischemic as well as pharmacological conditioning including anesthetic gases. Our findings of increased phosphorylation of Erk1/2 and Akt are in line with current opinion of these kinases as key players for cardioprotection. The analyses of Erk1/2 in the NAAR tissue, however, showed a significant decrease of Erk1/2 phosphorylation after I/R and HePoc. The implication of decreased Erk1/2 activity after I/R and HePoc cannot be resolved completely, however Erk1/2 decrease may lead to Cav-1 upregulation (Kavazis et al., 2008). Beneficial effects of Akt and Erk1/2 activation are not limited to cardiac tissue. Also activation of these kinases has been investigated as important factor in other organ-protection, e.g. neuroprotection, liver protection (Liu et al., 2016, Zhang et al., 2014). However, our results contradict previous (Huhn et al., 2009b), where 15 min of HePoc showed no effect on Erk1/2 and Akt phosphorylation in a similar model. In this study tissue was obtained 120 min after the onset of reperfusion. As phosphorylation may be processed quickly and cardioprotection occurs within the first min effects might not be visible after a longer time period.

Our findings in the AAR tissue support the idea of Erk1/2 as a substantial component of HePoc induced cardioprotection. Pagel et al. discovered a strong dependency of cardioprotection on Erk1/2 as beneficial effects were abolished, when Erk1/2-blockers were applied in a rabbit model. Interestingly the same model showed no infarct size reduction, when the upstream PI3K was blocked (Pagel et al., 2007). Our results reveal no increase in PI3K activation, but Akt, another downstream kinase of PI3K, showed significantly higher phosphorylation after HePoc compared to Sham and I/R only. Akt and Erk1/2 pathways have been identified as activators of eNOS, GSK-3β and inhibit Ca^{2+}-induced opening of the mPTP. Our results indicate that the downstream kinases might be activated through other processes. Several studies have also detected higher phosphorylation of PKCε in xenon- as well as helium-conditioning. Our model did not show alteration of PKCε phosphorylation in I/R or HePoc animals. Together these studies imply variation of signaling pathways between HePoc in different animal species as well as other conditioning procedures. Nevertheless it seems likely that similar end-effectors are involved.

4.4 Helium Postconditioning and Autophagy

Previously published experiments from this animal model showed significant upregulation of genes associated with autophagy and reduction of apoptosis associated genes (Oei et al., 2015b). Our analyses, investigating effects of HePoc on proteins Bcl-1 and sequestosome-1, which are well established in autophagy (Klionsky et al., 2012), indicate increased activation of autophagy after HePoc. The HePoc group showed a significant increase of Bcl-1 in the mitochondrial fraction of both AAR and NAAR tissue. Together, this suggests a shift of Bcl-1 towards the membrane, which might indicate induction of autophagy as it is substantial for phagophore-formation during I/R (Matsui et al., 2007). Even though research indicates that I/R itself induces autophagy, different pharmacological conditioning agents have been shown to augment autophagy induction (Wei et al., 2016, Huang et al., 2010). Our results contradict other in vitro models, which reported significant increases and upregulation of Bcl-1 after I/R (Matsui et al., 2007). In vitro models using Bcl-1 heterozygous KO mice showed reduction of autophagosome formation. In contrary to previous studies, these animals developed smaller infarct sizes compared to wild-type animals (Matsui et al., 2007). Nevertheless, research of I/R in different organs strengthens the hypothesis that autophagy is protective during I/R (Zhang et al., 2015, Yang et al., 2015, Thapalia et al., 2016). Hence, the increased Bcl-1 in mitochondrial fraction after HePoc may play an important role for cardioprotective effects.

The mRNA expression of another autophagy protein, sequestosome-1, was significantly upregulated in our model, as previously described (Oei et al., 2015b). However, our protein analyses of sequestosome-1 showed no significant difference of protein levels after HePoc compared to I/R only. Seqestosome-1 is involved in later processes of autophagy, consequently changes of sequestosome-1 may only be visible after a longer period of time.

A recent in vitro study by Kassan et al. indicates a link between autophagy and caveolins. Cav-3 KO cells showed decreased expression of autophagy markers, whereas overexpression Cav-3 resulted in protection against I/R and preserved mitochondrial function (Kassan et al., 2016).

Erk1/2 is a cardioprotective effector kinase, which also has been discussed in autophagy (Zhu et al., 2007). A study investigating Parkinson's disease provides evidence that Erk2 is an essential modulator of autophagy, including mitophagy (Dagda et al., 2008). Interestingly, in our model Erk1/2 showed higher activation in AAR tissue of HePoc groups. Erk1/2 may be involved in other signaling than described in section 4.3 and might be involved in pro-survival autophagy. However, our current setting gives no further insight on specific function or localization of Erk1/2, which might be an interesting aspect of further studies. Taken together our results may indicate increased autophagy initiation after HePoc.

4.5 Caveolins and Mitochondria

Within the cell, caveolins are not only important for cellular membrane associated processes, such as endocytosis or cellular signaling, but also have been identified to play key roles within the cell, e.g. mitochondrial functioning (Fridolfsson et al., 2012). Maintaining mitochondrial homeostasis during cellular stress in highly metabolic tissue, like myocardial muscle tissue, is crucial for cell survival. Fridolfsson et al. discovered that membrane-bound caveolin translocation from the plasma membrane to the mitochondria averts mitochondrial dysfunction and induces caveolin-dependent protective effects during cellular stress (Fridolfsson et al., 2012). Mitochondrial dysfunction may induce metabolic misbalance and eventually cause cell death. Several pathways leading to cell death emerge in the opening of the mPTP, which is especially eligible during cellular stress, like I/R (Hausenloy et al., 2003). As Pagel et al. showed in a rabbit model, mPTP opening is a key component of helium preconditioning induced cardioprotection as beneficial effects are eradicated, when atractyloside, a mPTP opener, is applied simultaneously (Pagel et al., 2007). Our protein analyses of the mitochondrial fraction showed no difference of Cav-1 or Cav-3 levels between groups. Nonetheless increased levels of Cav-1 and Cav-3 in the membrane fraction as well as the serum caveolins may be a sign of increased caveolin trafficking, which could potentially be involved in maintenance of mitochondrial functioning. However, it is unlikely to see significant changes in protein amounts after such short period, making it more likely that the differences in the fractions are caused by translocation or other processes.

4.6 Limitations of the Study

Due to the design of our study, with tissue extraction directly after the end of HePoc, we are able to investigate instant effects of HePoc. Some processes might only be activated and therefore measurable during reperfusion or at the end of HePoc intervention.

In some cases, the heart might undergo short periods of ischemia during the performed surgical procedures. This might mimic IPC and therefore conflict with our HePoc protocol. However, the procedures were executed likewise in the different groups, including the Sham control group. Therefore, possible effects should be equal and out-cancel each other.

Healthy young animals were employed in this study. Animal models with pathologies, e.g. diabetes or hypertension, which mimic the typical clinical patient, fail to show cardioprotection after HePoc (Huhn et al., 2009b). Most patients suffering from I/R present with several of these pathologies hindering the clinical translation.

Using the described study design, a connection between HePoc and effects on caveolins, RISK pathway and autophagy can only be described as correlation. Even though a causality seems likely, our model cannot prove dependency of cardioprotective effects on the described pathways. Further experiments, e.g. blocking experiments, will be necessary to investigate causality between HePoc and the described targets.

4.7 Conclusion and Outlook

The presented HePoc rat model enables us to explore the signaling pathways underlying the cardioprotective effects of helium.

Our results support the hypothesis of a complex signaling network involved in HePoc induced cardioprotection. We conclude, that membrane-associated caveolins are important mediators of cardioprotective signaling and that RISK pathway kinases Akt and Erk1/2 as well as an activation of autophagy may also be essential for HePoc induced cardioprotection. Further experiments, including blocking experiments, are necessary to inhibit specific targets and to distinguish between correlation and causality of activated pathways.

5. Abstract

Background: Short cycles of ventilation with anesthetic gases, such as isoflurane or xenon, prior to or after prolonged cardiac ischemia, called anesthetic pre- or postconditioning, are known to reduce cardiac damage. The underlying cellular mechanisms include the reperfusion injury salvage (RISK) pathway and recent studies also indicated recruitment of molecular signaling via caveolin (Cav) modulation. Postconditioning with the noble gas helium (HePoc) mimics cardioprotective effects. In the present study using a rat model, we investigated whether (1) HePoc alters protein or mRNA expression of Cav-1 and -3 and (2) activation of RISK pathway and (3) autophagy associated proteins.

Materials and Methods: In a previous study our animal model was analyzed showing significantly lower histological damage and reduced infarct size after 15 min of HePoc (Oei et al., 2015b). Here, heliox ventilation (70% He, 30% O_2) was applied after 25 min of ischemia and tissue from ischemic area at risk (AAR), non-ischemic not area at risk (NAAR), and serum was obtained. Cell fractions (cytosolic, mitochondrial, membrane) of Sham, I/R, I/R+He treated animals were separated and investigated for changes of Cav-1 and Cav-3 protein levels and mRNA expression (total tissue). Phosphorylation levels were measured to determine RISK pathway activation (Erk1/2, PI3K, PKCε and Akt). Protein levels of autophagy proteins Bcl-1 and sequestosome-1 were also measured.

Results: HePoc lead to an increase of Cav-1 mRNA expression compared to I/R only and additionally elevated levels of Cav-1 ($P<0.01$) and Cav-3 ($P<0.05$) in the membrane fraction of ischemic myocardium (AAR). RISK pathway kinase Akt was activated more in AAR and NAAR tissue of the HePoc group (both $P<0.05$). Erk1/2 phosphorylation was higher in AAR ($P<0.05$) after HePoc. However in NAAR tissue of I/R and HePoc treated animals, pErk1/2 was lower compared to Sham (both $P<0.001$). PKCε and PI3K showed no significant changes in phosphorylation. Furthermore Bcl-1 was significantly elevated in the mitochondrial fraction after HePoc in AAR ($P<0.05$) as well as NAAR ($P<0.05$), while sequestosome-1 levels showed no difference between groups.

Conclusion: We propose that HePoc activates a network of signaling cascades, which in turn induce cardioprotection. Respective mediators may include caveolins, RISK pathway kinases and proteins involved in autophagy.

6. References

ARSLAN, F., LAI, R. C., SMEETS, M. B., AKEROYD, L., CHOO, A., AGUOR, E. N., TIMMERS, L., VAN RIJEN, H. V., DOEVENDANS, P. A., PASTERKAMP, G., et al. 2013. Mesenchymal stem cell-derived exosomes increase ATP levels, decrease oxidative stress and activate PI3K/Akt pathway to enhance myocardial viability and prevent adverse remodeling after myocardial ischemia/reperfusion injury. *Stem Cell Res,* 10**,** 301-312.

BADIMON, L., PADRO, T. & VILAHUR, G. 2012. Atherosclerosis, platelets and thrombosis in acute ischaemic heart disease. *Eur Heart J Acute Cardiovasc Care,* 1**,** 60-74.

BAINES, C. P. 2009. The mitochondrial permeability transition pore and ischemia-reperfusion injury. *Basic Res Cardiol,* 104**,** 181-188.

BALLARD-CROFT, C., LOCKLAR, A. C., KRISTO, G. & LASLEY, R. D. 2006. Regional myocardial ischemia-induced activation of MAPKs is associated with subcellular redistribution of caveolin and cholesterol. *Am J Physiol Heart Circ Physiol,* 291**,** H658-667.

BARACH, A. L. & ECKMAN, M. 1936. The effects of inhalation of helium mixed with oxygen on the mechanics of respiration. *J Clin Invest,* 15**,** 47-61.

BOENGLER, K., SCHULZ, R. & HEUSCH, G. 2009. Loss of cardioprotection with ageing. *Cardiovasc Res,* 83**,** 247-261.

BRUYNINCKX, R., AERTGEERTS, B., BRUYNINCKX, P. & BUNTINX, F. 2008. Signs and symptoms in diagnosing acute myocardial infarction and acute coronary syndrome: a diagnostic meta-analysis. *Br J Gen Pract,* 58**,** 105-111.

CASON, B. A., GAMPERL, A. K., SLOCUM, R. E. & HICKEY, R. F. 1997. Anesthetic-induced preconditioning: previous administration of isoflurane decreases myocardial infarct size in rabbits. *Anesthesiology,* 87**,** 1182-1190.

CHAUDHARY, K. R., CHO, W. J., YANG, F., SAMOKHVALOV, V., EL-SIKHRY, H. E., DANIEL, E. E. & SEUBERT, J. M. 2013. Effect of ischemia reperfusion injury and epoxyeicosatrienoic acids on caveolin expression in mouse myocardium. *J Cardiovasc Pharmacol,* 61**,** 258-263.

CHEN, C., WEI, J., ALBADRI, A., ZARRINI, P. & BAIREY MERZ, C. N. 2016. Coronary microvascular dysfunction- epidemiology, pathogenesis, prognosis, diagnosis, risk factors and therapy. *Circ J,* 81**,** 3-11.

COHEN, M. V., YANG, X. M. & DOWNEY, J. M. 2007. The pH hypothesis of postconditioning: staccato reperfusion reintroduces oxygen and perpetuates myocardial acidosis. *Circulation,* 115**,** 1895-1903.

DAGDA, R. K., ZHU, J., KULICH, S. M. & CHU, C. T. 2008. Mitochondrially localized Erk2 regulates mitophagy and autophagic cell stress: implications for Parkinson's disease. *Autophagy,* 4**,** 770-82.

DAVIDSON, S. M., HAUSENLOY, D., DUCHEN, M. R. & YELLON, D. M. 2006. Signalling via the reperfusion injury signalling kinase (RISK) pathway links closure of the mitochondrial permeability transition pore to cardioprotection. *Int J Biochem Cell Biol,* 38**,** 414-419.

DRAB, M., VERKADE, P., ELGER, M., KASPER, M., LOHN, M., LAUTERBACH, B., MENNE, J., LINDSCHAU, C., MENDE, F., LUFT, F. C., et al. 2001. Loss of caveolae, vascular dysfunction, and pulmonary defects in caveolin-1 gene-disrupted mice. *Science,* 293**,** 2449-2452.

ENGELMAN, J. A., CHU, C., LIN, A., JO, H., IKEZU, T., OKAMOTO, T., KOHTZ, D. S. & LISANTI, M. P. 1998. Caveolin-mediated regulation of signaling along the p42/44 MAP kinase cascade in vivo. A role for the caveolin-scaffolding domain. *FEBS Lett,* 428**,** 205-211.

ERDEMLI, H. K., KOCABAS, R., SALIS, O., SEN, F., AKYOL, S., ESKIN, F., AKYOL, O., BEDIR, A. & SAHIN, A. F. 2016. Is serum caveolin-1 a useful biomarker for progression in patients with colorectal cancer? *Clin Lab,* 62**,** 401-408.

FALK, E. 2006. Pathogenesis of atherosclerosis. *J Am Coll Cardiol,* 47**,** C7-C12.

FECCHI, K., VOLONTE, D., HEZEL, M. P., SCHMECK, K. & GALBIATI, F. 2006. Spatial and temporal regulation of GLUT4 translocation by flotillin-1 and caveolin-3 in skeletal muscle cells. *FASEB J,* 20**,** 705-707.

FEINER, E. C., CHUNG, P., JASMIN, J. F., ZHANG, J., WHITAKER-MENEZES, D., MYERS, V., SONG, J., FELDMAN, E. W., FUNAKOSHI, H., DEGEORGE, B. R., JR., et al. 2011. Left ventricular dysfunction in murine models of heart failure and in failing human heart is associated with a selective decrease in the expression of caveolin-3. *J Card Fail,* 17**,** 253-263.

FERDINANDY, P., HAUSENLOY, D. J., HEUSCH, G., BAXTER, G. F. & SCHULZ, R. 2014. Interaction of risk factors, comorbidities, and comedications with ischemia/reperfusion injury and cardioprotection by preconditioning, postconditioning, and remote conditioning. *Pharmacol Rev,* 66**,** 1142-1174.

FERON, O. & BALLIGAND, J. L. 2006. Caveolins and the regulation of endothelial nitric oxide synthase in the heart. *Cardiovasc Res,* 69**,** 788-797.

FINK, S. L. & COOKSON, B. T. 2005. Apoptosis, pyroptosis, and necrosis: mechanistic description of dead and dying eukaryotic cells. *Infect Immun,* 73**,** 1907-1916.

FLICK, M., ALBRECHT, M., OEI, G. T., STEENSTRA, R., KERINDONGO, R. P., ZUURBIER, C. J., PATEL, H. H., HOLLMANN, M. W., PRECKEL, B. & WEBER, N. C. 2016. Helium postconditioning regulates expression of caveolin-1 and -3 and induces RISK pathway activation after ischaemia/reperfusion in cardiac tissue of rats. *Eur J Pharmacol,* 791**,** 718-725.

FRIDOLFSSON, H. N., KAWARAGUCHI, Y., ALI, S. S., PANNEERSELVAM, M., NIESMAN, I. R., FINLEY, J. C., KELLERHALS, S. E., MIGITA, M. Y., OKADA, H., MORENO, A. L., et al. 2012. Mitochondria-localized caveolin in adaptation to cellular stress and injury. *FASEB J,* 26**,** 4637-4649.

FRIDOLFSSON, H. N., ROTH, D. M., INSEL, P. A. & PATEL, H. H. 2014. Regulation of intracellular signaling and function by caveolin. *FASEB J,* 28**,** 3823-3831.

FUKUDA, K., ASOH, S., ISHIKAWA, M., YAMAMOTO, Y., OHSAWA, I. & OHTA, S. 2007. Inhalation of hydrogen gas suppresses hepatic injury caused by ischemia/reperfusion through reducing oxidative stress. *Biochem Biophys Res Commun,* 361**,** 670-674.

GAZE, D. C. 2013. Introduction to ischemic heart disease. *In:* GAZE, D. C. (ed.) *Ischemic Heart Disease.* Rijeka: InTech.

GLICK, D., BARTH, S. & MACLEOD, K. F. 2010. Autophagy: cellular and molecular mechanisms. *J Pathol,* 221**,** 3-12.

GOODMAN, M. D., KOCH, S. E., FULLER-BICER, G. A. & BUTLER, K. L. 2008. Regulating RISK: a role for JAK-STAT signaling in postconditioning? *Am J Physiol Heart Circ Physiol,* 295**,** H1649-1656.

GOTTLIEB, R. A., FINLEY, K. D. & MENTZER, R. M., JR. 2009. Cardioprotection requires taking out the trash. *Basic Res Cardiol,* 104**,** 169-180.

GRIFFITHS, E. J. & HALESTRAP, A. P. 1995. Mitochondrial non-specific pores remain closed during cardiac ischaemia, but open upon reperfusion. *Biochem J,* 307**,** 93-98.

HAGIWARA, Y., SASAOKA, T., ARAISHI, K., IMAMURA, M., YORIFUJI, H., NONAKA, I., OZAWA, E. & KIKUCHI, T. 2000. Caveolin-3 deficiency causes muscle degeneration in mice. *Hum Mol Genet,* 9**,** 3047-3054.

HALE, S. L., VANDERIPE, D. R. & KLONER, R. A. 2013. Continuous heliox breathing and the extent of anatomic zone of noreflow and necrosis following ischemia/reperfusion in the rabbit heart. *Open Cardiovasc Med J,* 8**,** 1-5.

HALESTRAP, A. P., CLARKE, S. J. & KHALIULIN, I. 2007. The role of mitochondria in protection of the heart by preconditioning. *Biochim Biophys Acta,* 1767**,** 1007-1031.

HAMACHER-BRADY, A., BRADY, N. R. & GOTTLIEB, R. A. 2006. The interplay between pro-death and pro-survival signaling pathways in myocardial ischemia/reperfusion injury: apoptosis meets autophagy. *Cardiovasc Drugs Ther,* 20**,** 445-462.

HAN, F., ZHANG, J., SHAO, J. & YI, X. 2014. Caveolin-1 promotes an invasive phenotype and predicts poor prognosis in large cell lung carcinoma. *Pathol Res Pract,* 210**,** 514-520.

HARRIS, P. D. & BARNES, R. 2008. The uses of helium and xenon in current clinical practice. *Anaesthesia,* 63**,** 284-293.

HAUSENLOY, D. J., BARRABES, J. A., BOTKER, H. E., DAVIDSON, S. M., DI LISA, F., DOWNEY, J., ENGSTROM, T., FERDINANDY, P., CARBRERA-FUENTES, H. A., HEUSCH, G., et al. 2016. Ischaemic conditioning and targeting reperfusion injury: a 30 year voyage of discovery. *Basic Res Cardiol,* 111**,** 70.

HAUSENLOY, D. J., DUCHEN, M. R. & YELLON, D. M. 2003. Inhibiting mitochondrial permeability transition pore opening at reperfusion protects against ischaemia-reperfusion injury. *Cardiovasc Res,* 60**,** 617-625.

HAUSENLOY, D. J., LECOUR, S. & YELLON, D. M. 2011. Reperfusion injury salvage kinase and survivor activating factor enhancement prosurvival signaling pathways in ischemic postconditioning: two sides of the same coin. *Antioxid Redox Signal,* 14**,** 893-907.

HAUSENLOY, D. J., MOCANU, M. M. & YELLON, D. M. 2004a. Cross-talk between the survival kinases during early reperfusion: its contribution to ischemic preconditioning. *Cardiovasc Res,* 63**,** 305-312.

HAUSENLOY, D. J., TSANG, A. & YELLON, D. M. 2005. The reperfusion injury salvage kinase pathway: a common target for both ischemic preconditioning and postconditioning. *Trends Cardiovasc Med,* 15**,** 69-75.

HAUSENLOY, D. J. & YELLON, D. M. 2004b. New directions for protecting the heart against ischaemia-reperfusion injury: targeting the reperfusion injury salvage kinase (RISK) pathway. *Cardiovasc Res,* 61**,** 448-460.

HAUSENLOY, D. J. & YELLON, D. M. 2006. Survival kinases in ischemic preconditioning and postconditioning. *Cardiovasc Res,* 70**,** 240-253.

HAUSENLOY, D. J. & YELLON, D. M. 2013. Myocardial ischemia-reperfusion injury: a neglected therapeutic target. *J Clin Invest,* 123**,** 92-100.

HEAD, B. P., PATEL, H. H., ROTH, D. M., LAI, N. C., NIESMAN, I. R., FARQUHAR, M. G. & INSEL, P. A. 2005. G-protein-coupled receptor signaling components localize in both sarcolemmal and intracellular caveolin-3-associated microdomains in adult cardiac myocytes. *J Biol Chem,* 280**,** 31036-31044.

HERZOG, W. R., VOGEL, R. A., SCHLOSSBERG, M. L., EDENBAUM, L. R., SCOTT, H. J. & SEREBRUANY, V. L. 1997. Short-term low dose intracoronary diltiazem administered at the onset of reperfusion reduces myocardial infarct size. *Int J Cardiol,* 59**,** 21-27.

HESS, D. R., FINK, J. B., VENKATARAMAN, S. T., KIM, I. K., MYERS, T. R. & TANO, B. D. 2006. The history and physics of heliox. *Respir Care,* 51**,** 608-612.

HEUSCH, G. 2013. Cardioprotection: chances and challenges of its translation to the clinic. *Lancet,* 381**,** 166-175.

HEUSCH, G., BOENGLER, K. & SCHULZ, R. 2010. Inhibition of mitochondrial permeability transition pore opening: the holy grail of cardioprotection. *Basic Res Cardiol,* 105**,** 151-154.

HORI, M., KITAKAZE, M., SATO, H., TAKASHIMA, S., IWAKURA, K., INOUE, M., KITABATAKE, A. & KAMADA, T. 1991. Staged reperfusion attenuates myocardial stunning in dogs. Role of transient acidosis during early reperfusion. *Circulation,* 84**,** 2135-2145.

HORIKAWA, Y. T., PANNEERSELVAM, M., KAWARAGUCHI, Y., TSUTSUMI, Y. M., ALI, S. S., BALIJEPALLI, R. C., MURRAY, F., HEAD, B. P., NIESMAN, I. R., RIEG, T., et al. 2011. Cardiac-specific overexpression of caveolin-3 attenuates cardiac hypertrophy

and increases natriuretic peptide expression and signaling. *J Am Coll Cardiol,* 57**,** 2273-2283.

HORIKAWA, Y. T., PATEL, H. H., TSUTSUMI, Y. M., JENNINGS, M. M., KIDD, M. W., HAGIWARA, Y., ISHIKAWA, Y., INSEL, P. A. & ROTH, D. M. 2008. Caveolin-3 expression and caveolae are required for isoflurane-induced cardiac protection from hypoxia and ischemia/reperfusion injury. *J Mol Cell Cardiol,* 44**,** 123-130.

HUANG, C., YITZHAKI, S., PERRY, C. N., LIU, W., GIRICZ, Z., MENTZER, R. M., JR. & GOTTLIEB, R. A. 2010. Autophagy induced by ischemic preconditioning is essential for cardioprotection. *J Cardiovasc Transl Res,* 3**,** 365-373.

HUHN, R., HEINEN, A., WEBER, N. C., HIEBER, S., HOLLMANN, M. W., SCHLACK, W. & PRECKEL, B. 2009a. Helium-induced late preconditioning in the rat heart in vivo. *Br J Anaesth,* 102**,** 614-619.

HUHN, R., HEINEN, A., WEBER, N. C., KERINDONGO, R. P., OEI, G. T., HOLLMANN, M. W., SCHLACK, W. & PRECKEL, B. 2009b. Helium-induced early preconditioning and postconditioning are abolished in obese Zucker rats in vivo. *J Pharmacol Exp Ther,* 329**,** 600-607.

HUHN, R., WEBER, N. C., PRECKEL, B., SCHLACK, W., BAUER, I., HOLLMANN, M. W. & HEINEN, A. 2012. Age-related loss of cardiac preconditioning: impact of protein kinase A. *Exp Gerontol,* 47**,** 116-121.

IBÁÑEZ, B., HEUSCH, G., OVIZE, M. & VAN DE WERF, F. 2015. Evolving therapies for myocardial ischemia/reperfusion injury. *J Am Coll Cardiol,* 65**,** 1454-1471.

JASMIN, J. F., MERCIER, I., DUPUIS, J., TANOWITZ, H. B. & LISANTI, M. P. 2006. Short-term administration of a cell-permeable caveolin-1 peptide prevents the development of monocrotaline-induced pulmonary hypertension and right ventricular hypertrophy. *Circulation,* 114**,** 912-920.

JENNINGS, R. B., SOMMERS, H. M., SMYTH, G. A., FLACK, H. A. & LINN, H. 1960. Myocardial necrosis induced by temporary occlusion of a coronary artery in the dog. *Arch Pathol,* 70**,** 68-78.

KASSAN, A., PHAM, U., NGUYEN, Q., REICHELT, M. E., CHO, E., PATEL, P. M., ROTH, D. M., HEAD, B. P. & PATEL, H. H. 2016. Caveolin-3 plays a critical role in autophagy after ischemia-reperfusion. *Am J Physiol Cell Physiol,* 311**,** C854-C865.

KAVAZIS, A. N., MCCLUNG, J. M., HOOD, D. A. & POWERS, S. K. 2008. Exercise induces a cardiac mitochondrial phenotype that resists apoptotic stimuli. *Am J Physiol Heart Circ Physiol,* 294**,** H928-935.

KIKUCHI, T., OKA, N., KOGA, A., MIYAZAKI, H., OHMURA, H. & IMAIZUMI, T. 2005. Behavior of caveolae and caveolin-3 during the development of myocyte hypertrophy. *J Cardiovasc Pharmacol,* 45**,** 204-210.

KIN, H., ZHAO, Z. Q., SUN, H. Y., WANG, N. P., CORVERA, J. S., HALKOS, M. E., KERENDI, F., GUYTON, R. A. & VINTEN-JOHANSEN, J. 2004. Postconditioning attenuates myocardial ischemia-reperfusion injury by inhibiting events in the early minutes of reperfusion. *Cardiovasc Res,* 62**,** 74-85.

KLIONSKY, D. J., ABDALLA, F. C., ABELIOVICH, H., ABRAHAM, R. T., ACEVEDO-AROZENA, A., ADELI, K., AGHOLME, L., AGNELLO, M., AGOSTINIS, P., AGUIRRE-GHISO, J. A., et al. 2012. Guidelines for the use and interpretation of assays for monitoring autophagy. *Autophagy,* 8**,** 445-544.

KLONER, R. A. 1993. Does reperfusion injury exist in humans? *J Am Coll Cardiol,* 21**,** 537-545.

KONSTANTINIDIS, K., WHELAN, R. S. & KITSIS, R. N. 2012. Mechanisms of cell death in heart disease. *Arterioscler Thromb Vasc Biol,* 32**,** 1552-1562.

KRAMAROW, E., LUBITZ, J. & FRANCIS, R., JR. 2013. Trends in the coronary heart disease risk profile of middle-aged adults. *Ann Epidemiol,* 23**,** 31-34.

KROEMER, G., GALLUZZI, L. & BRENNER, C. 2007. Mitochondrial membrane permeabilization in cell death. *Physiol Rev,* 87**,** 99-163.

KROEMER, G. & REED, J. C. 2000. Mitochondrial control of cell death. *Nat Med,* 6**,** 513-519.

LECOUR, S. 2009. Activation of the protective survivor activating factor enhancement (SAFE) pathway against reperfusion injury: Does it go beyond the RISK pathway? *J Mol Cell Cardiol,* 47**,** 32-40.

LECOUR, S., SULEMAN, N., DEUCHAR, G. A., SOMERS, S., LACERDA, L., HUISAMEN, B. & OPIE, L. H. 2005. Pharmacological preconditioning with tumor necrosis factor-α activates signal transducer and activator of transcription-3 at reperfusion without involving classic prosurvival kinases (Akt and extracellular signal–regulated kinase). *Circulation,* 112**,** 3911-3918.

LIET, J. M., DUCRUET, T., GUPTA, V. & CAMBONIE, G. 2015. Heliox inhalation therapy for bronchiolitis in infants. *Cochrane Database Syst Rev***,** CD006915.

LIU, S., YANG, Y., JIN, M., HOU, S., DONG, X., LU, J. & CHENG, W. 2016. Xenon-delayed postconditioning attenuates spinal cord ischemia/reperfusion injury through activation AKT and Erk signaling pathways in rats. *J Neurol Sci,* 368**,** 277-284.

MARBER, M. S., LATCHMAN, D. S., WALKER, J. M. & YELLON, D. M. 1993. Cardiac stress protein elevation 24 hours after brief ischemia or heat stress is associated with resistance to myocardial infarction. *Circulation,* 88**,** 1264-1272.

MATSUI, Y., TAKAGI, H., QU, X., ABDELLATIF, M., SAKODA, H., ASANO, T., LEVINE, B. & SADOSHIMA, J. 2007. Distinct roles of autophagy in the heart during ischemia and reperfusion: roles of AMP-activated protein kinase and Beclin 1 in mediating autophagy. *Circ Res,* 100**,** 914-922.

MATSUMURA, K., JEREMY, R. W., SCHAPER, J. & BECKER, L. C. 1998. Progression of myocardial necrosis during reperfusion of ischemic myocardium. *Circulation,* 97**,** 795-804.

MULLENHEIM, J., EBEL, D., FRASSDORF, J., PRECKEL, B., THAMER, V. & SCHLACK, W. 2002. Isoflurane preconditions myocardium against infarction via release of free radicals. *Anesthesiology,* 96**,** 934-940.

MURPHY, E. & STEENBERGEN, C. 2008. Mechanisms underlying acute protection from cardiac ischemia-reperfusion injury. *Physiol Rev,* 88**,** 581-609.

MURRY, C. E., JENNINGS, R. B. & REIMER, K. A. 1986. Preconditioning with ischemia: a delay of lethal cell injury in ischemic myocardium. *Circulation,* 74**,** 1124-1136.

NISHIHARA, M., MIURA, T., MIKI, T., TANNO, M., YANO, T., NAITOH, K., OHORI, K., HOTTA, H., TERASHIMA, Y. & SHIMAMOTO, K. 2007. Modulation of the mitochondrial permeability transition pore complex in GSK-3β-mediated myocardial protection. *J Mol Cell Cardiol,* 43**,** 564-570.

O'GARA, P. T., KUSHNER, F. G., ASCHEIM, D. D., CASEY, D. E., JR., CHUNG, M. K., DE LEMOS, J. A., ETTINGER, S. M., FANG, J. C., FESMIRE, F. M., FRANKLIN, B. A., et al. 2013. 2013 ACCF/AHA guideline for the management of ST-elevation myocardial infarction: executive summary: a report of the American College of Cardiology Foundation/American Heart Association Task Force on Practice Guidelines. *J Am Coll Cardiol,* 61**,** 485-510.

OEI, G. T., ASLAMI, H., KERINDONGO, R. P., STEENSTRA, R. J., BEURSKENS, C. J., TUIP-DE BOER, A. M., JUFFERMANS, N. P., HOLLMANN, M. W., PRECKEL, B. & WEBER, N. C. 2015a. Prolonged helium postconditioning protocols during early reperfusion do not induce cardioprotection in the rat heart in vivo: role of inflammatory cytokines. *J Immunol Res,* 2015**,** 216798.

OEI, G. T., HEGER, M., VAN GOLEN, R. F., ALLES, L. K., FLICK, M., VAN DER WAL, A. C., VAN GULIK, T. M., HOLLMANN, M. W., PRECKEL, B. & WEBER, N. C. 2015b. Reduction of cardiac cell death after helium postconditioning in rats: transcriptional analysis of cell death and survival pathways. *Mol Med,* 20**,** 516-526.

OEI, G. T., HUHN, R., HEINEN, A., HOLLMANN, M. W., SCHLACK, W. S., PRECKEL, B. & WEBER, N. C. 2012. Helium-induced cardioprotection of healthy and hypertensive rat myocardium in vivo. *Eur J Pharmacol,* 684**,** 125-131.

OLIVER, B. M. B., J.G.; FARRAR, H. IV 1984. Helium concentration in the Earth's lower atmosphere. *Geochim Cosmochim Acta,* 48**,** 1759-1767.

OSTROM, R. S. 2002. New determinants of receptor-effector coupling: trafficking and compartmentation in membrane microdomains. *Mol Pharmacol,* 61**,** 473-476.

OVIZE, M., BAXTER, G. F., DI LISA, F., FERDINANDY, P., GARCIA-DORADO, D., HAUSENLOY, D. J., HEUSCH, G., VINTEN-JOHANSEN, J., YELLON, D. M., SCHULZ, R., et al. 2010. Postconditioning and protection from reperfusion injury: where do we stand? Position paper from the Working Group of Cellular Biology of the Heart of the European Society of Cardiology. *Cardiovasc Res,* 87**,** 406-423.

PADILLA, F., GARCIA-DORADO, D., RODRIGUEZ-SINOVAS, A., RUIZ-MEANA, M., INSERTE, J. & SOLER-SOLER, J. 2003. Protection afforded by ischemic preconditioning is not mediated by effects on cell-to-cell electrical coupling during myocardial ischemia-reperfusion. *Am J Physiol Heart Circ Physiol,* 285**,** H1909-1916.

PAGEL, P. S., KROLIKOWSKI, J. G., PRATT, P. F., JR., SHIM, Y. H., AMOUR, J., WARLTIER, D. C. & WEIHRAUCH, D. 2008a. The mechanism of helium-induced preconditioning: a direct role for nitric oxide in rabbits. *Anesth Analg,* 107**,** 762-768.

PAGEL, P. S., KROLIKOWSKI, J. G., PRATT, P. F., JR., SHIM, Y. H., AMOUR, J., WARLTIER, D. C. & WEIHRAUCH, D. 2008b. Reactive oxygen species and mitochondrial adenosine triphosphate-regulated potassium channels mediate helium-induced preconditioning against myocardial infarction in vivo. *J Cardiothorac Vasc Anesth,* 22**,** 554-559.

PAGEL, P. S., KROLIKOWSKI, J. G., SHIM, Y. H., VENKATAPURAM, S., KERSTEN, J. R., WEIHRAUCH, D., WARLTIER, D. C. & PRATT, P. F., JR. 2007. Noble gases without anesthetic properties protect myocardium against infarction by activating prosurvival signaling kinases and inhibiting mitochondrial permeability transition in vivo. *Anesth Analg,* 105**,** 562-569.

PALADE, G. E. 1953. Fine structure of blood capillaries. *J Appl Phys,* 24**,** 1424–1436.

PAPAMOSCHOU, D. 1995. Theoretical validation of the respiratory benefits of helium-oxygen mixtures. *Respir Physiol,* 99**,** 183-190.

PATEL, H. H., MURRAY, F. & INSEL, P. A. 2008. Caveolae as organizers of pharmacologically relevant signal transduction molecules. *Annu Rev Pharmacol Toxicol,* 48**,** 359-391.

PATEL, H. H., TSUTSUMI, Y. M., HEAD, B. P., NIESMAN, I. R., JENNINGS, M., HORIKAWA, Y., HUANG, D., MORENO, A. L., PATEL, P. M., INSEL, P. A., et al. 2007. Mechanisms of cardiac protection from ischemia/reperfusion injury: a role for caveolae and caveolin-1. *FASEB J,* 21**,** 1565-1574.

PIKE, L. J. 2006. Rafts defined: a report on the keystone symposium on lipid rafts and cell function. *J Lipid Res,* 47**,** 1597-1598.

PIPER, H. M., GARCIA-DORADO, D. & OVIZE, M. 1998. A fresh look at reperfusion injury. *Cardiovasc Res,* 38**,** 291-300.

PRECKEL, B., MULLENHEIM, J., MOLOSCHAVIJ, A., THAMER, V. & SCHLACK, W. 2000. Xenon administration during early reperfusion reduces infarct size after regional ischemia in the rabbit heart in vivo. *Anesth Analg,* 91**,** 1327-1332.

PRECKEL, B., SCHLACK, W., HEIBEL, T. & RUTTEN, H. 2002. Xenon produces minimal haemodynamic effects in rabbits with chronically compromised left ventricular function. *Br J Anaesth,* 88**,** 264-269.

RAZANI, B., ENGELMAN, J. A., WANG, X. B., SCHUBERT, W., ZHANG, X. L., MARKS, C. B., MACALUSO, F., RUSSELL, R. G., LI, M., PESTELL, R. G., et al. 2001. Caveolin-1 null mice are viable but show evidence of hyperproliferative and vascular abnormalities. *J Biol Chem,* 276**,** 38121-38138.

RAZANI, B., WANG, X. B., ENGELMAN, J. A., BATTISTA, M., LAGAUD, G., ZHANG, X. L., KNEITZ, B., HOU, H., JR., CHRIST, G. J., EDELMANN, W., et al. 2002. Caveolin-2-deficient mice show evidence of severe pulmonary dysfunction without disruption of caveolae. *Mol Cell Biol,* 22**,** 2329-2344.

RIZVI, M., JAWAD, N., LI, Y., VIZCAYCHIPI, M. P., MAZE, M. & MA, D. 2010. Effect of noble gases on oxygen and glucose deprived injury in human tubular kidney cells. *Exp Biol Med (Maywood),* 235**,** 886-891.

RUIJTER, J. M., RAMAKERS, C., HOOGAARS, W. M., KARLEN, Y., BAKKER, O., VAN DEN HOFF, M. J. & MOORMAN, A. F. 2009. Amplification efficiency: linking baseline and bias in the analysis of quantitative PCR data. *Nucleic Acids Res,* 37**,** e45.

RUIZ-MEANA, M., ABELLÁN, A., MIRÓ-CASAS, E., AGULLÓ, E. & GARCIA-DORADO, D. 2009. Role of sarcoplasmic reticulum in mitochondrial permeability transition and cardiomyocyte death during reperfusion. *Am J Physiol Heart Circ Physiol,* 297**,** H1281-H1289.

RUIZ-MEANA, M., GARCIA-DORADO, D., HOFSTAETTER, B., PIPER, H. M. & SOLER-SOLER, J. 1999. Propagation of cardiomyocyte hypercontracture by passage of Na^+ through gap junctions. *Circ Res,* 85**,** 280-287.

SARGIACOMO, M., SCHERER, P. E., TANG, Z., KUBLER, E., SONG, K. S., SANDERS, M. C. & LISANTI, M. P. 1995. Oligomeric structure of caveolin: implications for caveolae membrane organization. *Proc Natl Acad Sci U S A,* 92**,** 9407-9411.

SCHILLING, J. M., ROTH, D. M. & PATEL, H. H. 2015. Caveolins in cardioprotection - translatability and mechanisms. *Br J Pharmacol,* 172**,** 2114-2125.

SHACK, S., WANG, X. T., KOKKONEN, G. C., GOROSPE, M., LONGO, D. L. & HOLBROOK, N. J. 2003. Caveolin-induced activation of the phosphatidylinositol 3-kinase/Akt pathway increases arsenite cytotoxicity. *Mol Cell Biol,* 23**,** 2407-2414.

SMYTHE, G. M. & RANDO, T. A. 2006. Altered caveolin-3 expression disrupts PI(3) kinase signaling leading to death of cultured muscle cells. *Exp Cell Res,* 312**,** 2816-2825.

SOMERS, S. J., FRIAS, M., LACERDA, L., OPIE, L. H. & LECOUR, S. 2012. Interplay between SAFE and RISK pathways in sphingosine-1-phosphate–induced cardioprotection. *Cardiovasc Drugs Ther,* 26**,** 227-237.

SONG, K. S., SCHERER, P. E., TANG, Z., OKAMOTO, T., LI, S., CHAFEL, M., CHU, C., KOHTZ, D. S. & LISANTI, M. P. 1996. Expression of caveolin-3 in skeletal, cardiac, and smooth muscle cells. Caveolin-3 is a component of the sarcolemma and co-fractionates with dystrophin and dystrophin-associated glycoproteins. *J Biol Chem,* 271**,** 15160-15165.

SONNE, D. P., ENGSTROM, T. & TREIMAN, M. 2008. Protective effects of GLP-1 analogues exendin-4 and GLP-1(9-36) amide against ischemia-reperfusion injury in rat heart. *Regul Pept,* 146**,** 243-249.

SRIRAM, S. M., HAN, D. H. & KIM, S. T. 2011. Partners in crime: ubiquitin-mediated degradation and autophagy. *Sci Signal,* 4**,** jc4.

STATISTISCHES-BUNDESAMT-DEUTSCHLAND 2014. Todesursachen - Anzahl der Gestorbenen nach Kapiteln der ICD-10.

SUGIE, S., MUKAI, S., TSUKINO, H., TODA, Y., YAMAUCHI, T., NISHIKATA, I., KURODA, Y., MORISHITA, K. & KAMOTO, T. 2013. Increased plasma caveolin-1 levels are associated with progression of prostate cancer among Japanese men. *Anticancer Res,* 33**,** 1893-1897.

TAHIR, S. A., YANG, G., GOLTSOV, A. A., WATANABE, M., TABATA, K., ADDAI, J., FATTAH EL, M. A., KADMON, D. & THOMPSON, T. C. 2008. Tumor cell-secreted caveolin-1 has proangiogenic activities in prostate cancer. *Cancer Res,* 68**,** 731-739.

THAPALIA, B. A., ZHOU, Z. & LIN, X. 2014. Autophagy, a process within reperfusion injury: an update. *Int J Clin Exp Pathol,* 7**,** 8322-8341.

THAPALIA, B. A., ZHOU, Z. & LIN, X. 2016. Sauchinone augments cardiomyocyte viability by enhancing autophagy proteins -PI3K, Erk1/2, AMPK and Beclin-1 during early ischemia-reperfusion injury in vitro. *Am J Transl Res,* 8**,** 3251-3265.

TOLLER, W. G., KERSTEN, J. R., PAGEL, P. S., HETTRICK, D. A. & WARLTIER, D. C. 1999. Sevoflurane reduces myocardial infarct size and decreases the time threshold for ischemic preconditioning in dogs. *Anesthesiology,* 91**,** 1437-1446.

TSANG, A., HAUSENLOY, D. J., MOCANU, M. M. & YELLON, D. M. 2004. Postconditioning: a form of "modified reperfusion" protects the myocardium by activating the phosphatidylinositol 3-kinase-Akt pathway. *Circ Res,* 95**,** 230-232.

TSUTSUMI, Y. M., HORIKAWA, Y. T., JENNINGS, M. M., KIDD, M. W., NIESMAN, I. R., YOKOYAMA, U., HEAD, B. P., HAGIWARA, Y., ISHIKAWA, Y., MIYANOHARA, A., et

al. 2008. Cardiac-specific overexpression of caveolin-3 induces endogenous cardiac protection by mimicking ischemic preconditioning. *Circulation,* 118**,** 1979-1988.
TSUTSUMI, Y. M., KAWARAGUCHI, Y., HORIKAWA, Y. T., NIESMAN, I. R., KIDD, M. W., CHIN-LEE, B., HEAD, B. P., PATEL, P. M., ROTH, D. M. & PATEL, H. H. 2010a. Role of caveolin-3 and glucose transporter-4 in isoflurane-induced delayed cardiac protection. *Anesthesiology,* 112**,** 1136-1145.
TSUTSUMI, Y. M., KAWARAGUCHI, Y., NIESMAN, I. R., PATEL, H. H. & ROTH, D. M. 2010b. Opioid-induced preconditioning is dependent on caveolin-3 expression. *Anesth Analg,* 111**,** 1117-1121.
TWIG, G., ELORZA, A., MOLINA, A. J., MOHAMED, H., WIKSTROM, J. D., WALZER, G., STILES, L., HAIGH, S. E., KATZ, S., LAS, G., et al. 2008. Fission and selective fusion govern mitochondrial segregation and elimination by autophagy. *EMBO J,* 27**,** 433-446.
USHIO-FUKAI, M. & ALEXANDER, R. W. 2006. Caveolin-dependent Angiotensin II type 1 receptor signaling in vascular smooth muscle. *Hypertension,* 48**,** 797-803.
VALLI, G., PAOLETTI, P., SAVI, D., MARTOLINI, D. & PALANGE, P. 2007. Clinical use of heliox in asthma and COPD. *Monaldi Arch Chest Dis,* 67**,** 159-164.
WEBER, N. C., SCHILLING, J. M., FINLEY, J. C., IRVINE, M., KELLERHALS, S. E., NIESMAN, I. R., ROTH, D. M., PRECKEL, B., HOLLMANN, M. W. & PATEL, H. H. 2013. Helium inhalation induces caveolin secretion to blood. *The FASEB Journal,* 27**,** 1089.3.
WEBER, N. C., TOMA, O., DAMLA, H., WOLTER, J. I., SCHLACK, W. & PRECKEL, B. 2006. Upstream signaling of protein kinase C-epsilon in xenon-induced pharmacological preconditioning. Implication of mitochondrial adenosine triphosphate dependent potassium channels and phosphatidylinositol-dependent kinase-1. *Eur J Pharmacol,* 539**,** 1-9.
WEI, C., GAO, J., LI, M., LI, H., WANG, Y., LI, H. & XU, C. 2016. Dopamine D2 receptors contribute to cardioprotection of ischemic post-conditioning via activating autophagy in isolated rat hearts. *Int J Cardiol,* 203**,** 837-839.
WEI, C., LI, H., HAN, L., ZHANG, L. & YANG, X. 2013. Activation of autophagy in ischemic postconditioning contributes to cardioprotective effects against ischemia/reperfusion injury in rat hearts. *J Cardiovasc Pharmacol,* 61**,** 416-422.
WEISS, J. N., KORGE, P., HONDA, H. M. & PING, P. 2003. Role of the mitochondrial permeability transition in myocardial disease. *Circ Res,* 93**,** 292-301.
WOODMAN, S. E., PARK, D. S., COHEN, A. W., CHEUNG, M. W., CHANDRA, M., SHIRANI, J., TANG, B., JELICKS, L. A., KITSIS, R. N., CHRIST, G. J., et al. 2002. Caveolin-3 knock-out mice develop a progressive cardiomyopathy and show hyperactivation of the p42/44 MAPK cascade. *J Biol Chem,* 277**,** 38988-38997.
YANG, J., WANG, Y., SUI, M., LIU, F., FU, Z. & WANG, Q. X. 2015. Tri-iodothyronine preconditioning protects against liver ischemia reperfusion injury through the regulation of autophagy by the MEK/Erk/mTORC1 axis. *Biochem Biophys Res Commun,* 467**,** 704-710.
YANG, X. M., PROCTOR, J. B., CUI, L., KRIEG, T., DOWNEY, J. M. & COHEN, M. V. 2004. Multiple, brief coronary occlusions during early reperfusion protect rabbit hearts by targeting cell signaling pathways. *J Am Coll Cardiol,* 44**,** 1103-1110.
YELLON, D. M. & BAXTER, G. F. 1999. Reperfusion injury revisited: is there a role for growth factor signaling in limiting lethal reperfusion injury? *Trends Cardiovasc Med,* 9**,** 245-249.
YELLON, D. M. & HAUSENLOY, D. J. 2007. Myocardial reperfusion injury. *N Engl J Med,* 357**,** 1121-1135.
YOUNG, L. H., IKEDA, Y. & LEFER, A. M. 2001. Caveolin-1 peptide exerts cardioprotective effects in myocardial ischemia-reperfusion via nitric oxide mechanism. *Am J Physiol Heart Circ Physiol,* 280**,** H2489-2495.
YOUSUKE T. HORIKAWA, M. D., PH.D.,, YASUO M. TSUTSUMI, M.D., PH.D., HEMAL H. PATEL, PH.D. AND DAVID M. ROTH, PH.D., M.D. 2014. Signaling epicenters: The

role of caveolae and caveolins in volatile anesthetic induced cardiac protection. *Curr Pharm Des,* 20**,** 5681-5689.

YUE, T. L., WANG, C., GU, J. L., MA, X. L., KUMAR, S., LEE, J. C., FEUERSTEIN, G. Z., THOMAS, H., MALEEFF, B. & OHLSTEIN, E. H. 2000. Inhibition of extracellular signal-regulated kinase enhances Ischemia/Reoxygenation-induced apoptosis in cultured cardiac myocytes and exaggerates reperfusion injury in isolated perfused heart. *Circ Res,* 86**,** 692-699.

ZHANG, D., LI, C., ZHOU, J., SONG, Y., FANG, X., OU, J., LI, J. & BAI, C. 2015. Autophagy protects against ischemia/reperfusion-induced lung injury through alleviating blood-air barrier damage. *J Heart Lung Transplant,* 34**,** 746-755.

ZHANG, J., ZHU, W., XIAO, L., CAO, Q., ZHANG, H., WANG, H., YE, Z., HAO, Y., DAI, Q., SUN, W., et al. 2016. Lower serum caveolin-1 Is associated with cerebral microbleeds in patients with acute ischemic stroke. *Oxid Med Cell Longev,* 2016**,** 9026787.

ZHANG, R., ZHANG, L., MANAENKO, A., YE, Z., LIU, W. & SUN, X. 2014. Helium preconditioning protects mouse liver against ischemia and reperfusion injury through the PI3K/Akt pathway. *J Hepatol,* 61**,** 1048-1055.

ZHAO, Z. Q., CORVERA, J. S., HALKOS, M. E., KERENDI, F., WANG, N. P., GUYTON, R. A. & VINTEN-JOHANSEN, J. 2003. Inhibition of myocardial injury by ischemic postconditioning during reperfusion: comparison with ischemic preconditioning. *Am J Physiol Heart Circ Physiol,* 285**,** H579-H588.

ZHU, J. H., HORBINSKI, C., GUO, F., WATKINS, S., UCHIYAMA, Y. & CHU, C. T. 2007. Regulation of autophagy by extracellular signal-regulated protein kinases during 1-methyl-4-phenylpyridinium-induced cell death. *Am J Pathol,* 170**,** 75-86.

7. Appendix

7.1 Caveolin-1 and Caveolin-3 after 5 Min of Reperfusion or Helium Postconditioning

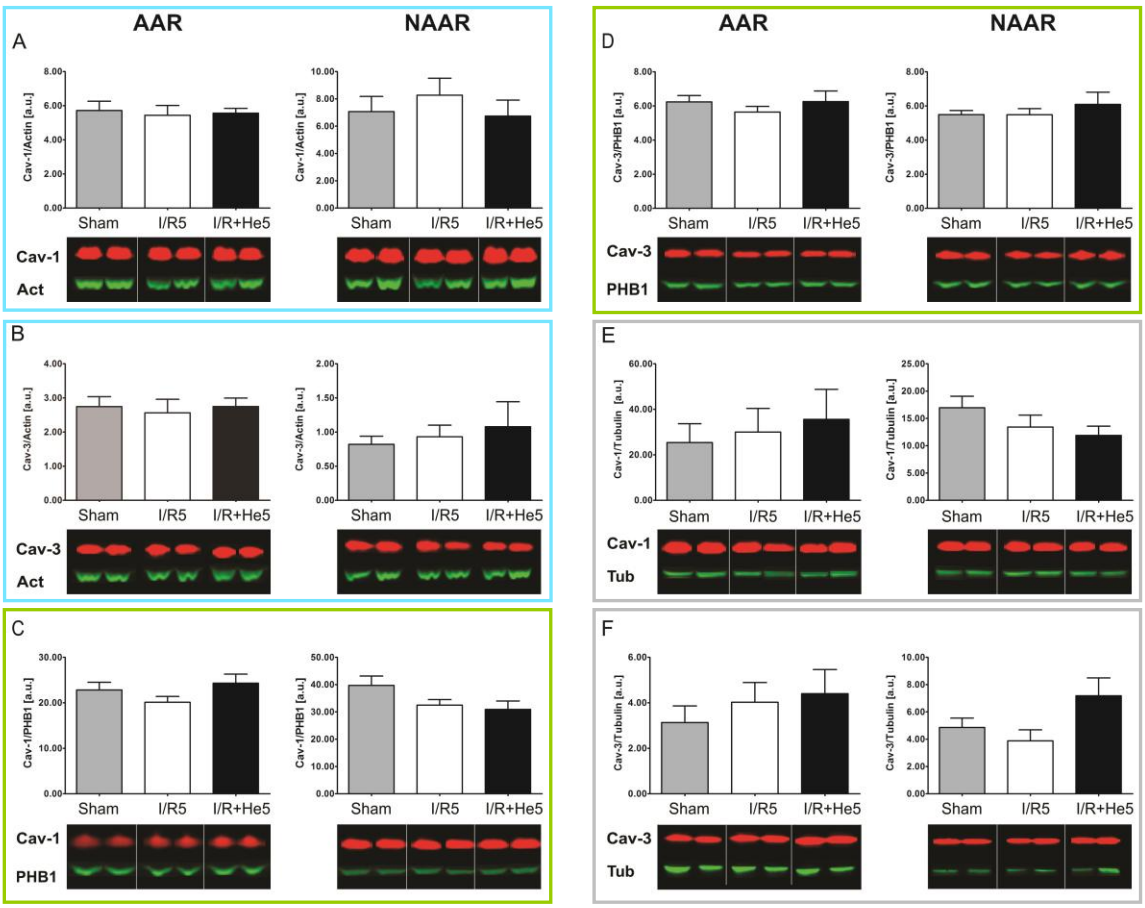

supplementary figure 1 ▲ Protein Levels of Caveolin-1 and Caveolin-3 in Sham, after 5 Min of I/R or I/R+HePoc in Cytosolic, Membrane and Mitochondrial Fractions of AAR and NAAR Tissue. Ratios are calculated as Cav-1:actin (cytosol **A**), Cav-1:PHB1 (mitochondria, **C**), Cav-1:tubulin (membrane, **E**) and Cav-3:actin (cytosol, **B**), Cav-3:PHB1 (mitochondria, **D**), Cav-3:tubulin (membrane, **F**). Columns display the mean ± SEM. AAR Membrane I/R+He5: n =6, other groups n=7 (Flick et al., 2016)

7.2 Caveolin-1 and Caveolin-3 after 30 Min of Reperfusion or Helium Postconditioning

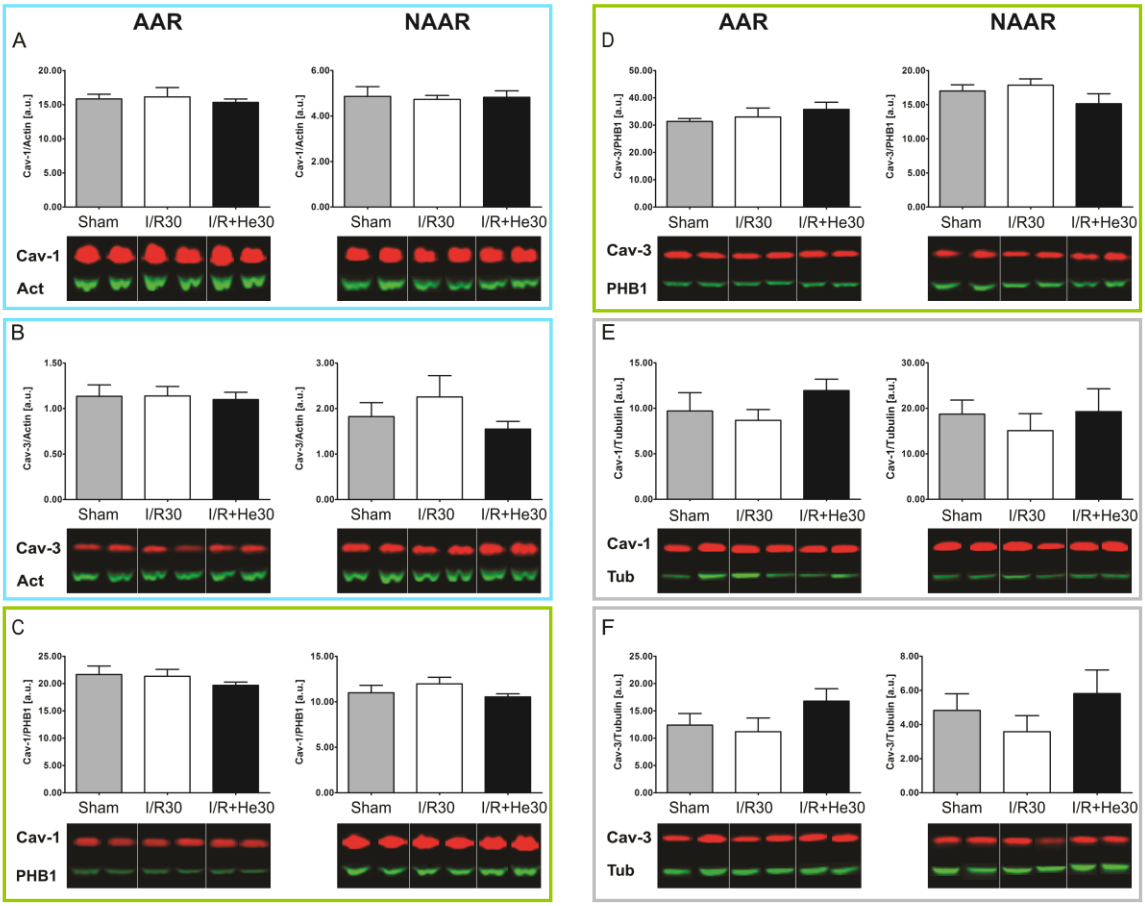

supplementary figure 2 ▲ Protein Levels of Caveolin-1 and Caveolin-3 in Sham, after 30 Min of I/R or I/R+HePoc in Cytosolic, Membrane and Mitochondrial Fractions of AAR and NAAR Tissue. Ratios are calculated as Cav-1:actin (cytosol **A**), Cav-1:PHB1 (mitochondria, **C**), Cav-1:tubulin (membrane, **E**) and Cav-3:actin (cytosol, **B**), Cav-3:PHB1 (mitochondria, **D**), Cav-3:tubulin (membrane, **F**). Columns display the mean ± SEM. NAAR Membrane I/R+He30: n =6, other groups n=7 (Flick et al., 2016)

7.3 Hemodynamics

Group	Baseline	24 Min of Ischemia	5 Min of Reperfusion	15 min of Reperfusion	30 min of Reperfusion
			mean arterial pressure (mmHg)		
Sham	111 ± 13	113 ± 22	113 ± 21	98 ± 20	-
I/R5	90 ± 33	95 ± 19	73 ± 20	-	-
I/R15	95 ± 24	93 ± 20	83 ± 21	62 ± 8	-
I/R30	96 ± 29	91 ± 28	80 ± 24	79 ± 21	60 ± 15
I/R+He5	102 ± 20	108 ± 23	78 ± 21	-	-
I/R+He15	102 ± 20	108 ± 17	96 ± 14	75 ± 11	-
I/R+He30	97 ± 25	100 ± 24	95 ± 18	91 ± 23	69 ± 15
			mean heart rate (BPM)		
Sham	372 ± 20	373 ± 20	363 ± 24	352 ± 32	-
I/R5	338 ± 29	354 ± 29	330 ± 18	-	-
I/R15	320 ± 60	340 ± 50	326 ± 46	306 ± 44	-
I/R30	329 ± 62	359 ± 39	342 ± 38	346 ± 41	320 ± 39
I/R+He5	360 ± 36	366 ± 16	344 ± 35	-	-
I/R+He15	338 ± 35	365 ± 36	350 ± 37	324 ± 34	-
I/R+He30	343 ± 57	366 ± 36	347 ± 47	359 ± 40	328 ± 51

supplementary table 1 ▲ Hemodynamics. Hemodynamics were measured after 15 min of baseline stabilization, 24 min of ischemia and after 5, 15 and 30 min of reperfusion. As analyzed by Oei et al., no statistical differences between the groups were found. Data are shown as mean ± standard deviation. (Oei et al., 2015b)

7.4 **Moritz Flick**, Martin Albrecht, Gezina T.M.L. Oei, Renske Steenstra, Raphaela P. Kerindongo, Coert J. Zuurbier, Hemal H. Patel, Markus W. Hollmann, Benedikt Preckel, Nina C. Weber; *Helium postconditioning regulates expression of caveolin-1 and -3 and induces RISK pathway activation after ischemia/reperfusion in cardiac tissue of rats.* Eur J Pharmacol. 2016 Nov 15; 791:718-725. doi:10.1016/j.ejphar.2016.10.012.

European Journal of Pharmacology 791 (2016) 718–725

Contents lists available at ScienceDirect

European Journal of Pharmacology

journal homepage: www.elsevier.com/locate/ejphar

Cardiovascular pharmacology

Helium postconditioning regulates expression of caveolin-1 and -3 and induces RISK pathway activation after ischaemia/reperfusion in cardiac tissue of rats

Moritz Flick[a,b,1], Martin Albrecht[b,1], Gezina T.M.L. Oei[a], Renske Steenstra[a], Raphaela P. Kerindongo[a], Coert J. Zuurbier[a], Hemal H. Patel[c], Markus W. Hollmann[a], Benedikt Preckel[a], Nina C. Weber[a,*]

[a] *Department of Anaesthesiology, Laboratory of Experimental Intensive Care and Anaesthesiology (L.E.I.C.A.), Academic Medical Centre (AMC), Meibergdreef 9, 1100 DD Amsterdam, The Netherlands*
[b] *Department of Anaesthesiology and Intensive Care Medicine, University Hospital Schleswig-Holstein, Campus Kiel, Arnold-Heller-Straße 3, 24105 Kiel, Germany*
[c] *Veterans Affairs San Diego Healthcare System and Department of Anaesthesiology, University of California, San Diego, 9500 Gilman Drive, 92093 La Jolla, California, USA*

ARTICLE INFO

Keywords:
Cardiac postconditioning
Helium
Caveolin
RISK pathway
Ischaemia reperfusion
Noble gases

ABSTRACT

Caveolae, lipid enriched invaginations of the plasma membrane, are epicentres of cellular signal transduction. The structural proteins of caveolae, caveolins, regulate effector pathways in anaesthetic-induced cardioprotection, including the RISK pathway. Helium (He) postconditioning (HePoc) is known to mimic anaesthetic conditioning and to prevent damage from myocardial infarction. We hypothesize that HePoc regulates caveolin-1 and caveolin-3 (Cav-1 and Cav-3) expression in the rat heart and activates the RISK pathway.

Male Wistar rats (n=8, each group) were subjected to 25 min of cardiac ischaemia followed by reperfusion (I/R) for 5, 15 or 30 min (I/R 5/15/30). The HePoc groups underwent I/R with 70% helium ventilation during reperfusion (IR+He 5/15/30 min). Sham animals received surgical treatment without I/R. After each protocol blood and hearts were retrieved. Tissue was obtained from the area-at-risk (AAR) and non-area-at-risk (NAAR) and processed for western blot analyses and reverse-transcription-real-time-polymerase-chain-reaction (RT-qPCR).

Protein analyses revealed increased amounts of Cav-1 and Cav-3 in the membrane of I/R+He15 (AAR: Cav-1, $P < 0.05$; Cav-3, $P < 0.05$; both vs. I/R15). In serum, Cav-3 was found to be elevated in I/R+He15 ($P < 0.05$ vs. I/R15). RT-qPCR showed increased expression of Cav-1 in IR+He15 in AAR tissue ($P < 0.05$ vs. I/R15). Phosphorylation of RISK pathway proteins pERK1/2 (AAR: $P < 0.05$ vs. I/R15) and pAKT (AAR: $P < 0.05$; NAAR $P < 0.05$; both vs. I/R15) was elevated in the cytosolic fraction of I/R+He15.

These results suggest that 15 min of HePoc regulates Cav-1 and Cav-3 and activates RISK pathway kinases ERK1/2 and AKT. These processes might be crucially involved in HePoc mediated cardioprotection.

1. Introduction

Coronary artery disease and successive myocardial infarction are leading causes of mortality and major medical care costs (Kramarow et al., 2013). Several experimental studies have shown that short episodes of ischaemia prior to an ischaemic event (ischaemic preconditioning) produce cardioprotection and reduce infarct size and damage (DeFily and Chilian, 1993). Conditioning cycles at the onset of reperfusion, referred to as postconditioning, are equally effective, making it a promising clinical approach to treating ischaemia/reperfusion injury (I/R) (Lupi Herrera et al., 2006). Volatile anaesthetics, e.g. sevoflurane (Toller et al., 1999) or isoflurane (Cason et al., 1997), are known to mimic cardiac protection similar to ischaemic conditioning and are mediated by identical pathways (Tsutsumi et al., 2006). However, these agents induce anaesthesia and have side effects on haemodynamic and cardiovascular parameters restricting their clinical

* Correspondence to: Academic Medical Centre (AMC), Department of Anaesthesiology University of Amsterdam, Laboratory of Experimental and Clinical Experimental Anaesthesiology (L.E.I.C.A.), Academic Medical Centre (AMC), Meibergdreef 9, 1100 DD Amsterdam, The Netherlands. .
E-mail address: N.C.Hauck@amc.uva.nl (N.C. Weber).
[1] Both authors contributed equally

http://dx.doi.org/10.1016/j.ejphar.2016.10.012
Received 30 June 2016; Received in revised form 8 October 2016; Accepted 10 October 2016
Available online 11 October 2016
0014-2999/

practicability.

The noble gas xenon, another volatile anaesthetic, has minimal cardiovascular side effects (Preckel et al., 2002) and also induces cardioprotection through conditioning protocols (Preckel et al., 2000; Weber et al., 2005). The noble gas helium, which has no anaesthetic potency or haemodynamic side effects, mimics cardioprotective conditioning similar to volatile anaesthetics (Oei et al., 2012b; Pagel et al., 2007). Helium postconditioning (HePoc) reduces infarct size and myocardial damage in rat and rabbit models after I/R injury (Huhn et al., 2009; Oei et al., 2012a, 2014, 2015).

Pathways involved in helium conditioning include G-protein-coupled receptors (GPCR), nitric oxide signaling, the reperfusion injury salvage kinase (RISK) pathway, and the survival activating factor enhancement (SAFE) pathway (Pagel et al., 2007). Many cardioprotective mechanisms have also been linked to the functionality of mitochondria during I/R (Fridolfsson et al., 2012). Consistently HePoc affects the mitochondrial permeability transition pore (mPTP) during cellular stress, preventing it from opening, and thereby reducing mitochondrial dysfunction (Pagel et al., 2008a).

Several of these HePoc effectors interact with and are possibly mediated through caveolae (Horikawa et al., 2008; Patel et al., 2007).

Caveolae are small flask-like invaginations of the cellular membrane (Palade, 1953). They are found in most cell types and regulate several physiological functions such as endocytosis, adrenergic receptor regulation and cellular signaling (Anderson, 1993). Besides sphingolipids, cholesterol and fatty acids as lipid components, caveolae are enriched in caveolins, their essential structural proteins. Caveolins exist in three isoforms, Cav-1, -2 and -3, and contain a scaffolding domain (CSD), that plays a key role in regulating and localizing signaling molecules (Patel et al., 2008). All three isoforms are found in cardiac myocytes (Patel et al., 2006) and cardiac myocyte-specific overexpression of Cav-3 in the heart induced upregulation of survival kinases and resulted in protection against I/R (Horikawa et al., 2008).

In our current study, we used cardiac tissue subjected to regional I/R, I/R and HePoc, or Sham operation to investigate HePoc induced changes of Cav-1 and Cav-3 protein localization and mRNA expression. HePoc induced cardioprotection was characterized further by examining the role of the caveolin-associated RISK pathway as possible underlying mechanism.

2. Materials and methods

2.1. Animal experiments

Animal experiments were performed in accordance with the Guide for Care and Use of Laboratory Animals (NIH Publication No. 85-23, revised 1996) and approved by the Academic Medical Centre's animal ethics committee (DAA102650). Data from these animal experiments, including haemodynamic measurements, were recently published (Oei et al., 2014).

2.2. Chemicals, solutions and culture media

Chemicals and solutions were purchased either from Merck (Millipore, Amsterdam, the Netherlands), Carl Roth (Karlsruhe, Germany), Roche (Almere, the Netherlands) or Sigma-Aldrich (Zwijndrecht, the Netherlands), unless stated otherwise.

2.3. Study design for ischaemia/reperfusion injury

Male Wistar rats (354–426 g, age range of 12–16 weeks) were acclimatized for 7 days under conditions of 12 h light and dark cycles and ad libitum access to food and water. All animals received anaesthesia and surgical procedures as described previously (Oei et al., 2012a). Rats were mechanically ventilated and the carotid artery was cannulated to measure the mean arterial pressure and draw blood

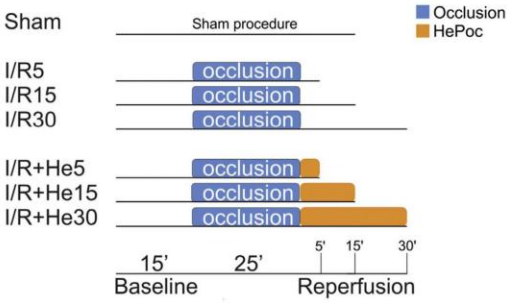

Fig. 1. : Experimental setting. After 15 min of baseline-stabilisation the left anterior descended artery (LAD) was ligated to commence ischaemia in the left ventricle. The study groups underwent 15 min of reperfusion and 15 min of reperfusion with HePoc respectively. The Sham operated group did not undergo ischaemia. The experiments were performed with 5 and 30 min periods, respectively (supplementary Fig. S3 and S4)..

samples. After 15 min of stabilisation the left anterior descending coronary artery (LAD) was encircled with a single puncture 5-0 Prolene suture (Ethicon Johnson & Johnson, Amersfoort, the Netherlands) through the myocardium. A snare was formed with the ends of the suture through a propylene tube to allow reversible ligation of the LAD, thereby inducing 25 min of ischaemia followed by reperfusion. For those animals subjected to I/R only, the ischaemic period was followed by 5, 15 or 30 min of reperfusion, respectively (I/R5, 15, 30). The treatment groups receiving HePoc commenced administration of helium gas (70% helium and 30% oxygen, Linde Gas Benelux, Dieren, the Netherlands) at 24 min of ischaemia (providing sufficient helium presence in the lungs at the onset of reperfusion). HePoc was performed for 5, 15 or 30 min of reperfusion (I/R+He5, 15, 30). The Sham group received surgical treatment without undergoing I/R or HePoc (Fig. 1).

2.4. Preparation of cytosol, membrane and mitochondrial fractions

After each protocol hearts were excised and shock frozen in liquid nitrogen. Tissue was obtained from the ischaemic area at risk (AAR) and the non-ischaemic, non area at risk, (NAAR) as described previously and ground in a pre-cooled mortar (Oei et al., 2014). Subsequently a lysis buffer (Tris base, EGTA, NaF and Na_3VO_4 (as phosphatase inhibitors), protease-inhibitor mix (aprotinin, leupetin and pepsatin), DTT and okadaic acid) was added to prevent degradation. Samples were mixed with the homogenizer (Ultra-Turrax T8, IKA) and 50 µl of sample was pipetted into new vials containing 450 µl of Tripur for RNA analysis. The rest of the homogenate was centrifuged at 1000*g*, 4 °C for 10 min, the supernatant subsequently at 10,000*g*, 4 °C for 15 min. The resulting supernatant was pipetted into new vials, while the remaining pellet was resuspended with lysis buffer (1% Triton X-100) to be used as the mitochondrial fraction. Samples were centrifuged again at 5000*g*, 4 °C for 15 min and the supernatant was used as the cytosolic fraction. The pellet was mixed with lysis buffer, vortexed and after 60 min of incubation on ice centrifuged at 5000*g*, 4 °C for 15 min. The supernatant was obtained as the membrane fraction. All fractions were stored at −80 °C.

2.5. RNA isolation and cDNA preparation

A total of 450 µl homogenate-Tripur mix was diluted 1:10 with BCP (1-Bromo-3-chloropropane) (Sigma-Aldrich, Zwijndrecht, the Netherlands), and shaken vigorously for 15 s. After 10 min of incubation at room temperature, the samples were centrifuged at 12000*g*, 4 °C for 15 min. The upper layer containing RNA was carefully pipetted into clean vials and precipitated by adding 250 µl isopropanol followed

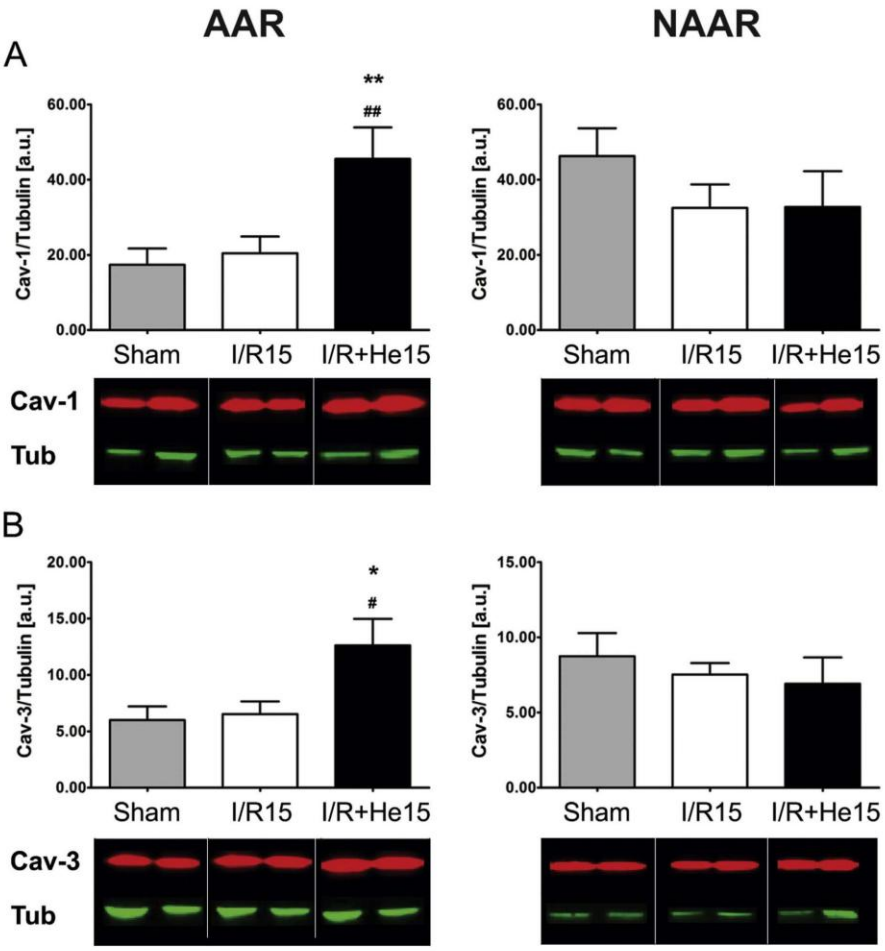

Fig. 2. : Protein levels of Cav-1 and Cav-3 in cardiac tissue of Sham, I/R15 and I/R+He15 treated animals are shown as ratios of Cav-1:tubulin and Cav-3:tubulin. Columns display the mean ± S.E.M. An asterisk indicates differences compared to Sham (*P < 0.05, **P < 0.01), whereas the pound sign indicates differences compared to I/R15 (#P < 0.05, ##P < 0.01). Bands display an example of western blot analyses. Sham: n=6, I/R15 and I/R+He15: n=7.

by another 10 min incubation period. RNA was centrifuged at 12000*g*, 4 °C for 8 min resulting in RNA pellets and supernatants, which were removed to dilute the RNA pellet in 1 ml 75% ethanol. The samples were centrifuged at 12000, 4 °C for 5 min and after this the ethanol was removed, and RNA was diluted in 20 µl of Milli-Q water. RNA was heated at 60 °C for 5 min, followed by a short spin down, mix and another heating at 60 °C for 5 min. RNA concentrations were determined by UV–vis absorbance spectroscopy (NanoDrop, Thermo Scientific, Rockford, IL, USA). RNA yields typically ranged from 0.16 to 1.08 µg/µl (data not shown). cDNA was synthesized using First Strand cDNA Synthesis Kit for RT-PCR (Roche, Almere, the Netherlands). Amplicons were diluted to 1 µg RNA/10 µl Milli-Q. 1 µl Oligo(dT) primer (50 µm) was added before samples were heated for 10 min at 65 °C. cDNA-mix was added containing 4 µl 5x RT-buffer, 2 µl dNTP-mix, 0.5 µl RNAase inhibitor (40U/µl), 0.5ul RT (20U/µl) and 2 µl Milli-Q water. The samples were heated at 55 °C for 30 min and then boiled at 85 °C for 5 min. The cDNA samples were diluted with 60 µl Mili-Q water and stored at −80 °C.

2.6. RT-qPCR

RT-qPCR samples were prepared using SybrGreen I MasterMix (Roche, Almere, the Netherlands). cDNA samples were diluted 1:5 in Milli-Q water before adding 5 µl Sybr Green and 0.5 µl of sense- and anti-sense-primer as follows: Cav-1 (forward 5′ CGT AGA CTC CGA GGG ACA TC 3′; reverse 5′ CGT ACA CTT GCT TCT CAT TCA C 3′), Cav-3 (forward 5′ CCA AGA ACA TCA ATG AGG ACA TTG TG 3′; reverse 5′ GTG GCA GAA GGA GAT ACA G 3′) and glyceraldehyde-3-phosphatedehydrogenase (GAPDH) (forward 5′ TGC CCC CAT GTT TGT GAT G 3′; reverse 5′ GCT GAC AAT CTT GAG GGA GTT GT 3′) as reference gene (all Invitrogen, Breda, the Netherlands). RT-qPCR was performed in the LightCycler480 (Roche, Almere, the Netherlands) with following conditions: Pre-incubation heating to 95 °C for 10 min, followed by 45 cycles of amplification (95 °C for 15 s, 56 °C for 10 s,

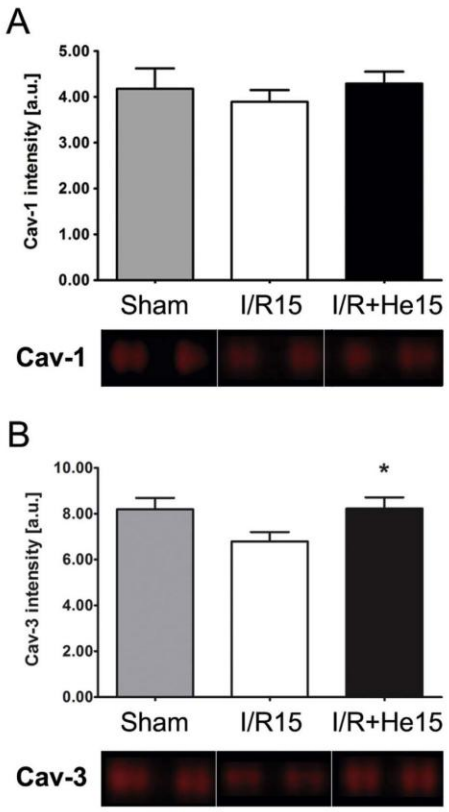

Fig. 3. Protein levels of Cav-1 and Cav-3 in serum of Sham, I/R and I/R+He treated animals. Columns display the mean ± S.E.M. An asterisk indicates differences compared to Sham (*P < 0.05 Sham vs. I/R). Bands display an example of western blot analyses. Sham: n=4, I/R15 and I/R+He15: n=7.

72 °C for 15 s) and a melting curve analysis. For each amplicon its baseline was determined and corrected using the LinRegPCR programme according to Ruijter and colleagues (Ruijter et al., 2009). Each amplicon was corrected for baseline fluorescence. Amplicons that did not reach N_q before cycle 45 were considered undetectable. The individual PCR efficiencies were calculated and amplicons with an efficiency < 1.80 or > 2.00 were excluded from further analysis. The mean efficiency of each target gene was used to calculate the starting concentration (N_0) per amplicon. All samples were normalized to the N0 of the reference gene GAPDH. Differences in expression of gene of interest in experimental groups (I/R15 vs. I/R+He15) and Sham were calculated.

2.7. Western Blot analysis

Protein concentrations were measured using Bradford Protein Assays (Bio-Rad, Hercules, CA, USA) and diluted to align concentrations. Equal amounts of protein were mixed with SDS-PAGE sample buffer (SDS, Bromophenol Blue, TrisBase, Glycerol and Mercaptoethanol), the samples were vortexed and boiled at 95 °C for 5 min. Samples were separated by SDS-PAGE using Criterion™ XT precast gels (Bio-Rad, Hercules, CA, USA) and transferred onto a Immobilin-FL Membrane (Millipore, Billericam, MA, USA). The membrane was washed in Odyssey® Blocking Buffer (LI-COR, Lincoln, NE, USA) for 60 min and incubated with caveolin-1 (1:40000), caveolin-3 (1:20,000, both from BD Biosciences, Franklin Lakes, NJ, USA), p-AKT (1:500), AKT (1:2000), p-ERK1/2 (1:2000), ERK1/2 (1:2000, all Cell Signaling Technology Camebridge, United Kingdom), p-PKCε (1:1000, upstate, Millipore, Billericam, MA, USA), PKCε (1:2000, Millipore, Billericam, MA, USA) p-PI3K (1:1000) or PI3K (1:2000, both Cell Signaling Technology, Camebridge, United Kingdom), overnight. After washing the membrane for 3×5 min in cold, fresh TBS-T, the blot was incubated for 60 min with IRDye800 CW or IRDye680 CW secondary antibody conjugated mouse- or rabbit-antibody (1:5000, LI-COR, Lincoln, NE, USA). The membranes were washed again for 3×5 min and scanned using Odyssey® Infrared Imaging System. The Odyssey® Infrared Scanning Software v2.1 was used for quantification of the blots. Results are presented as ratio of the target protein over a fraction-specific reference protein: for the cytosol fraction we used actin (1:5000, Santa Cruz, Heidelberg, Germany), for the membrane fraction tubulin (1:5000, Cell Signaling Technology, Camebridge, United Kingdom),) and for the mitochondrial fraction anti-prohibitin1 (PHB1) (1:10,000, Cell Signaling Technology, Camebridge, United Kingdom). RISK pathway proteins were analysed as ratio of phosphorylated over total protein. All western blots were performed in duplicates.

2.8. Statistical analysis

Statistical analysis was performed using in GraphPad Prism 5 (GraphPad Software, La Jolla, CA, USA). Kruskal-Wallis tests with Dunn's post hoc were used to detect differences between the groups in mRNA expression and protein levels. Statistical significance was assumed for $P < 0.05$ and indicated with an asterisk or a number sign in the figures. Variables are expressed as mean ± standard error of the mean (S.E.M.).

3. Results

3.1. Protein analyses of Caveolin-1 and Caveolin-3

Western blot analyses showed different amounts of Cav-1 and Cav-3 between 15 min of I/R, and I/R plus HePoc. HePoc significantly increased accumulation of Cav-1 and Cav-3 in the membrane fraction of ischaemic cardiac tissue, AAR, compared to Sham and I/R15 (AAR: Cav-1, I/R+He15 (45.53 ± 8.38) $P < 0.05$ vs. Sham (17.38 ± 4.31 $P < 0.05$ vs. I/R15 (20.43 ± 4.44); Cav-3, I/R+He15 (12.62 ± 2.35) $P < 0.05$ vs. Sham (5.99 ± 1.21); $P < 0.05$ vs. I/R15 (6.52 ± 1.13); Fig. 2 A and B). In the NAAR tissue caveolins did not show differences between groups (Fig. 2 A and B). In the cytosol and mitochondrial fraction no differences of Cav-1 and Cav-3 were detected in AAR or NAAR tissue (supplementary Fig. S1). The serum analysis did not present any differences in the serum for Cav-1 levels (Fig. 3 A), whereas Cav-3 showed increased amounts in I/R+He15 group (I/R+He15 (8.23 ± 0.48) $P < 0.05$ vs. I/R15 (6.79 ± 0.41); Fig. 3 B). Protocols with 5 or 30 min of I/R or I/R+HePoc did not alter amounts of Cav-1 and Cav-3 in AAR or NAAR tissue (supplementary Fig. S3 and S4).

3.2. mRNA expression

To measure mRNA expression of Cav-1 and Cav-3 RT-qPCR was performed. In the ischaemic tissue, I/R15, both Cav-1 and Cav-3 showed significantly reduced mRNA expression (AAR: Cav-1, I/R15 (4.49 ± 0.37) $P < 0.05$ vs. Sham (6.81 ± 0.91); Cav-3, I/R15 (3.82 ± 0.18) $P < 0.05$ vs. Sham (5.06 ± 0.29); Fig. 4 A and B). HePoc group presented increased expression of Cav-1 in comparison to I/R, but no difference vs. Sham. (AAR: Cav-1, I/R+He15 (5.65 ± 0.25) $P < 0.05$ vs. I/R15 (3.82 ± 0.18); Fig. 4 A). Cav-3 expression was also reduced after HePoc compared to Sham, but showed no difference vs I/R (AAR: Cav-

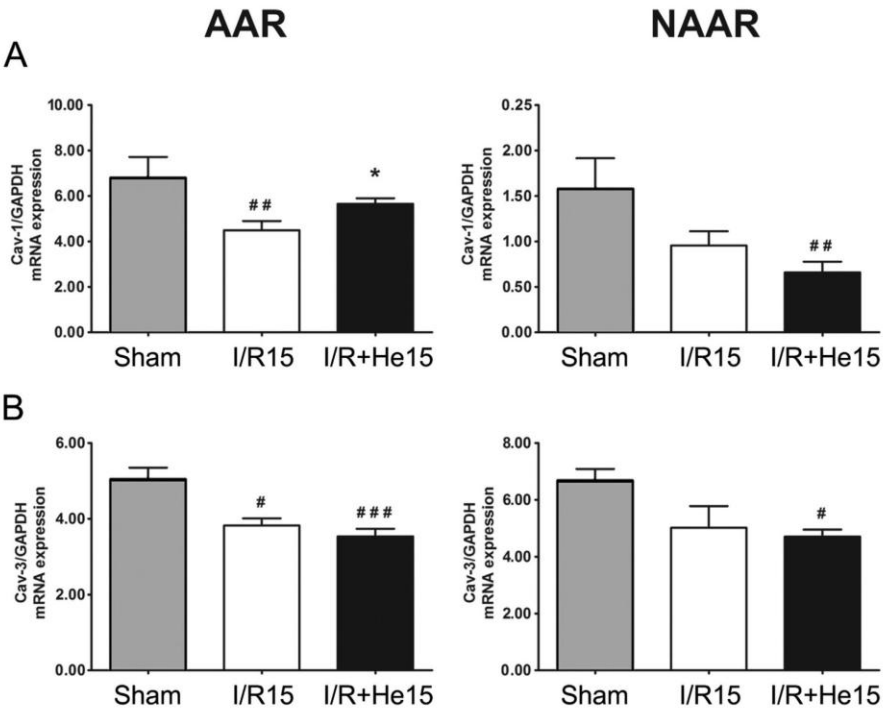

Fig. 4. : Quantification of mRNA expression of Cav-1 and Cav-3 in AAR (area at risk) and NAAR (non-area at risk) tissue with using GAPDH as reference gene. Results show the mean ± S.E.M. An asterisk differences vs. Sham (*P < 0.05, **P < 0.01, ***P < 0.001), whereas the pound sign (#) indicates differences vs. I/R15 (#P < 0.05, ##P < 0.01, ###P < 0.001). n=8 in each group.

3, I/R+He15 (3.54 ± 0.21) P < 0.05 vs. Sham (5.06 ± 0.29); Fig. 4 B). In the NAAR reduction of Cav-1 and Cav-3 mRNA expression was found after HePoc in comparison to Sham (NAAR: Cav-1, I/R+He15 (6.59 ± 1.10) P < 0.05 vs. Sham (15.77 ± 3.38); Cav-3, I/R+He15 (4.70 ± 0.31) P < 0.05 vs. Sham (6.70 ± 0.38); Fig. 4 B).

3.3. Protein levels of RISK pathway associated proteins

The reperfusion injury signaling kinase (RISK) pathway has been linked to cardioprotection. Western blot analyses of phosphorylated and total protein levels were performed to indicate RISK pathway activation in the cytosol fraction.

Increased phosphorylation levels of AKT were found in the ischaemic tissue (AAR: I/R+He15 (6.50 ± 0.68) P < 0.05 vs. Sham (4.51 ± 0.49); P < 0.05; vs. I/R15 (4.38 ± 0.33); Fig. 5 A). Increased amounts of pAKT were also detected in non-ischaemic tissue after HePoc (NAAR: I/R+He15 (6.51 ± 0.70) P < 0.05 vs. I/R15 (4.35 ± 0.30); supplementary Fig. S2). ERK1 showed increased activation after I/R compared to Sham (AAR: ERK1, I/R15 (12.37 ± 1.54) P < 0.05 vs. Sham (5.63 ± 0.62); Fig. 5 C). HePoc treated animals showed even higher phosphorylation levels of both ERK1 and 2 in the ischaemic tissue (AAR: ERK1, I/R+He15 (14.57 ± 0.93), P < 0.05 vs. I/R15 (12.37 ± 1.54); ERK2, I/R +He15 (2.68 ± 0.18) P < 0.05 vs. I/R15 (2.12 ± 0.30); Fig. 5 B-C). NAAR tissue analyses revealed, that ERK1/2 phosphorylation was reduced vs. Sham in both I/R15 and I/R+He15 (NAAR: ERK1 I/R15 (2.23 ± 0.30) P < 0.05; I/R+He15 (2.17 ± 0.21) P < 0.05 both vs. Sham; ERK2, I/R15 (4.51 ± 0.32) P < 0.05; I/R+He15 (5.03 ± 0.42) P < 0.05 both vs. Sham (12.25 ± 1.08); supplementary Fig. S2 B-C). Phosphorylation levels of PKCε and PI3K showed no differences (Fig. 5 D-E, supplementary Fig. S 2D-E).

4. Discussion

The major findings of the present study are: (1) HePoc changes accumulation of Cav-1 and Cav-3 in cardiac tissue shortly after I/R indicating change in location. (2) RISK pathway proteins AKT and ERK1/2 are activated by 15 min of HePoc. (3) Serum of HePoc animals contains increased amounts of Cav-3.

Earlier studies from our laboratory showed that HePoc reduces infarct size in cardiac tissue of several rat strains (Huhn et al., 2009; Oei et al., 2012a, 2015, 2014). The cardioprotective effect of helium has been shown in other animal models (Pagel et al., 2007, 2008c). Our earlier study reproduces results, which imply that the duration of HePoc appears to be important as cardioprotection occurs within 15 min of HePoc (Oei et al., 2014 2015). Accordingly, we now find changes in Cav-1 and Cav-3 localization only after 15 min of HePoc and no difference after 5 or 30 min, respectively. Other in vivo models have shown that longer or shorter periods of HePoc produce limited protective effect or might even impair outcome (Hale et al., 2013; Oei et al., 2015). HePoc seems to induce protective effects shortly after the onset of reperfusion. Therefore, underlying processes should commence within this time frame.

Caveolins, the structural proteins of caveolae, have been shown to be important mediators of cardioprotective pathways (Hausenloy et al., 2005; Horikawa et al., 2014). Caveolin-knockout animals present complete loss of cardioprotection (Horikawa et al., 2008; Patel et al., 2007). Several studies imply a significant role for transmembrane signaling, but involved pathways are still not completely understood

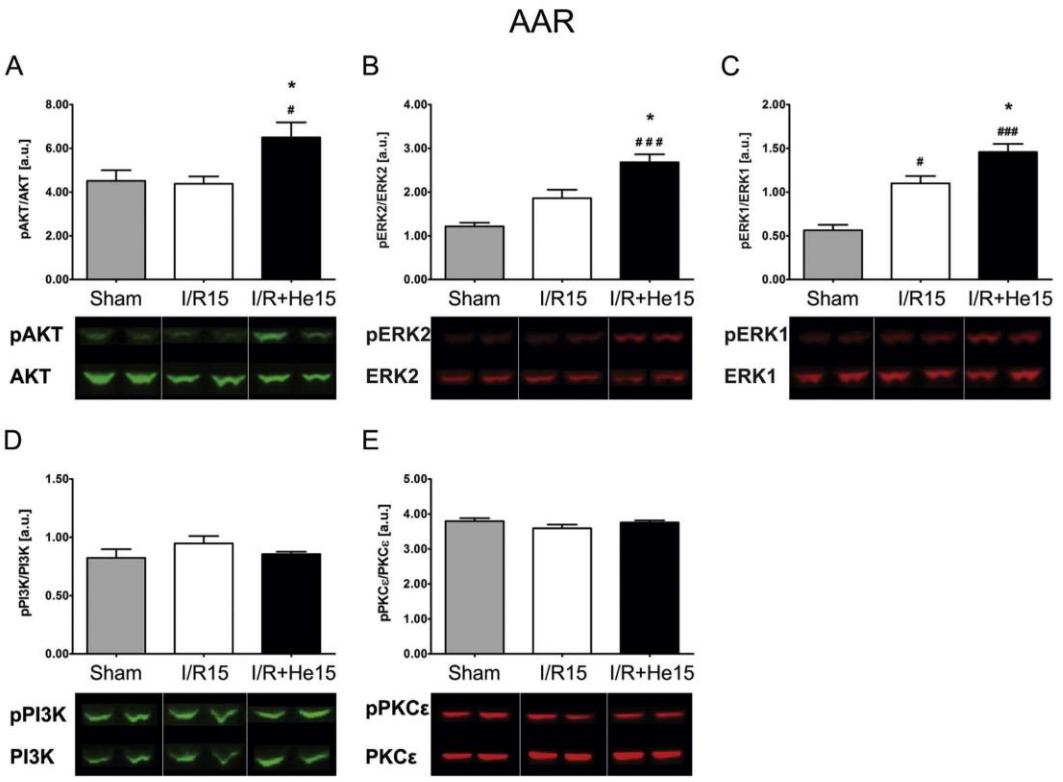

Fig. 5. : Phosphorylation levels of AKT, ERK1/2, PI3K and PKCε in cardiac tissue of Sham, I/R15 and I/R+He15 treated animals are shown as ratios of phosphorylated protein:total protein. Columns display the mean ± S.E.M. An asterisk indicates differences compared to Sham (*P < 0.05), whereas the pound sign indicates differences compared to I/R15 (*P < 0.05, **P < 0.01, ***P < 0.001). Bands display an example of western blot analyses. n=7 in each group.

(Fridolfsson et al., 2014). 15 min of HePoc restored Cav-1 mRNA expression to Sham levels in the AAR showing a significant increase versus I/R. These findings indicate that HePoc effects include mRNA changes, which our laboratory also found for several apoptotic and autophagy genes (Oei et al., 2014). These mRNA changes are unlikely to be transferred into protein expression after only 15 min of reperfusion, but indicate that HePoc induces cardioprotective pathways on different levels.

Several studies report loss of caveolae from membranes during cellular stress (Chaudhary et al., 2013; Ratajczak et al., 2003), whereas in our setting protein levels remained unchanged after I/R. The analyses of the membrane fraction of the AAR showed a significant increase of Cav-1 and Cav-3 after 15 min of HePoc. These results are in contrast to another study from our laboratory investigating He inhalation alone in a mouse model, where depletion of Cav-1 from the cardiac tissue 24 h after 30 min of helium inhalation was found (Weber et al., 2013). In the same model helium treatment induced secretion of Cav-1 and -3 into the serum (Weber et al., 2013), which is in line with increased Cav-3 levels in the serum of our in vivo model in rats. Even though the studies use different species and time periods, the results indicate that secreted caveolin might have a potentially protective effect due to its availability in the whole body.

The functions of secreted caveolins are discussed controversially. Several authors detected increased levels of caveolins in the blood of cancer patients and suggested serum caveolins as biomarkers for prostate (Sugie et al., 2013), colorectal (Erdemli et al., 2016) or lung cancer (Han et al., 2014). Interestingly, caveolins in serum from tumour patients have also been associated with pro angiogenic and pro cell survival characteristics (Tahir et al., 2001, 2008). In addition, several publications proposed specific effects of circulating caveolins on different organs. Zhang et al. showed that lower serum Cav-1 levels are associated with cerebral microbleeds, suggesting a protective role of circulating caveolins during acute cerebral ischaemia (Zhang et al., 2016). Increased serum Cav-1 has also been associated with prevention of right heart hypertrophy and pulmonary hypertension (Jasmin et al., 2006).

In summary, there is some evidence that secreted caveolins might specifically interact with tissues and organs. However, little is known about the detailed functions of the more cardiospecific Cav-3 in serum and possible cardioprotective effects of serum caveolins still need to be investigated.

Caveolae and caveolins have been shown to regulate mitochondria in different settings supporting the idea of a functional role for caveolins during cellular stress (Bosch et al., 2011; Fridolfsson et al., 2012). In highly metabolic tissue, like cardiac tissue, maintaining mitochondrial function during cellular stress is of major concern. It appears that an elevated number of caveolae, and therefore membrane localized caveolins, promotes caveolin trafficking from the plasma membrane to mitochondria and prevents mitochondrial dysfunction (Fridolfsson et al., 2012). Cellular damage is caused by opening of the

mitochondrial permeability transition pore (mPTP) during the first minute of reperfusion (Hausenloy and Yellon, 2003) causing closure of ATP-sensitive potassium channel and generation of bursts of reactive oxygen species (Pagel et al., 2008c). Helium conditioning has been shown to prevent mPTP opening, whereas administration of atractyloside, a mPTP opener, abolished helium preconditioning (Pagel et al., 2007). In our results Cav-1 and -3 protein levels showed no difference in the mitochondrial fractions. However, increased Cav-1 and -3 in the membrane fraction as well as the serum might indicate involvement of mitochondrial signaling.

Caveolins are involved in mPTP transitioning through binding of signaling molecules to the CSD (Fridolfsson et al., 2014). The CSD binds with several triggers, mediators and end-effectors of cardioprotective pathways known as RISK pathway proteins, including PI3K, AKT, PKC isoforms, and ERK1/2 (Hausenloy, 2006; Patel et al., 2008). Moreover, several of these proteins have been associated with helium conditioning (Pagel et al., 20072008b).

Anaesthetic and xenon-induced conditioning are known to depend on ERK1/2 phosphorylation (Toma et al., 2004; Weber et al., 2006). Consistently, helium has been shown to induce ERK1/2 thereby preventing mPTP opening (Pagel and Krolikowski, 2009; Pagel et al., 2007). Our findings of increased ERK1/2 phosphorylation substantiate the idea of ERK1/2 as a key mediator in helium-induced cardioprotection. Accordingly, infarct size reduction was abolished in a rabbit model, when ERK1/2 was inhibited or a mPTP opener was utilized (Pagel et al., 2007). In the same model blocking of PI3K signaling diminished cardioprotection. However, in our setting phosphorylation of PI3K was not increased after HePoc. Nevertheless we detected activation of the PI3K downstream effector AKT. Like ERK1/2, AKT has been identified to inhibit Ca^{2+}-induced opening of the mPTP in anaesthetic- and xenon-induced conditioning (Feng et al., 2005; Mio et al., 2009). In contrast to earlier studies from our laboratory investigating xenon preconditioning (Weber et al., 2005), which showed significantly higher phosphorylation of PKCε, we found no difference in HePoc compared to I/R. This is in line with another HePoc rat-model investigating pPKCε activation (Oei et al., 2012a). These results indicate that kinases and signaling cascades for different conditioning protocols and agents may vary, even though similar end-effectors play an important role.

A limitation of this study is that outcome parameters might be affected by short and transient ischaemic periods, which however are unavoidable and appear during preparation and operation on cardiac vessels resulting in intraoperative ischaemic preconditioning. Nevertheless these effects are existent in all groups and may even mimic chronic coronary artery disease in patients.

Based on the cardioprotective effects of HePoc shown in our recently published study, the current findings indicate that 15 min of HePoc result in accumulation of Cav-1 and Cav-3 in the membrane and activation of RISK pathway proteins ERK1/2 and AKT. In Conclusion our study points towards a key role of caveolins and RISK pathway in helium induced cardioprotection. As our current study is a first approach investigating cardioprotective kinases further experiments, e.g. blocking of pathways, will be necessary to confirm causality.

Funding

The present study was in part funded by a midcareer grant to NC Weber from the Society of Cardiovascular Anaesthesiologists (SCA) and the International Anaesthesia Research Society (IARS).

Declaration of interests

The authors declare that they have no conflict of interest.

Disclosures

None.

Appendix A. Supporting information

Supplementary data associated with this article can be found in the online version at doi:10.1016/j.ejphar.2016.10.012.

References

Anderson, R.G., 1993. Potocytosis of small molecules and ions by caveola. Trends Cell Biol. 3, 69–72.
Bosch, M., Mari, M., Herms, A., Fernandez, A., Fajardo, A., Kassan, A., Giralt, A., Colell, A., Balgoma, D., Barbero, E., Gonzalez-Moreno, E., Matias, N., Tebar, F., Balsinde, J., Camps, M., Enrich, C., Gross, S.P., Garcia-Ruiz, C., Perez-Navarro, E., Fernandez-Checa, J.C., Pol, A., 2011. Caveolin-1 deficiency causes cholesterol-dependent mitochondrial dysfunction and apoptotic susceptibility. Curr. Biol.: CB 21, 681–686.
Cason, B.A., Gamperl, A.K., Slocum, R.E., Hickey, R.F., 1997. Anesthetic-induced preconditioning: previous administration of isoflurane decreases myocardial infarct size in rabbits. . Hesiology 87, 1182–1190.
DeFily, D.V., Chilian, W.M., 1993. Preconditioning protects coronary arteriolar endothelium from ischemia-reperfusion injury. Am. J. Physiol. 265, H700–H706.
Erdemli, H.K., Kocabas, R., Salis, O., Sen, F., Akyol, S., Eskin, F., Akyol, O., Bedir, A., Sahin, A.F., 2016. Is serum caveolin-1 a useful biomarker for progression in patients with colorectal cancer?cancer?. Clin. Lab. 62, 401–408.
Feng, J., Lucchinetti, E., Ahuja, P., Pasch, T., Perriard, J.C., Zaugg, M., 2005. Isoflurane postconditioning prevents opening of the mitochondrial permeability transition pore through inhibition of glycogen synthase kinase 3beta. Anesthesiology 103, 987–995.
Fridolfsson, H.N., Kawaraguchi, Y., Ali, S.S., Panneerselvam, M., Niesman, I.R., Finley, J.C., Kellerhals, S.E., Migita, M.Y., Okada, H., Moreno, A.L., Jennings, M., Kidd, M.W., Bonds, J.A., Balijepalli, R.C., Ross, R.S., Patel, P.M., Miyanohara, A., Chen, Q., Lesnefsky, E.J., Head, B.P., Roth, D.M., Insel, P.A., Patel, H.H., 2012. Mitochondria-localized caveolin in adaptation to cellular stress and injury. Faseb J. 26, 4637–4649.
Fridolfsson, H.N., Roth, D.M., Insel, P.A., Patel, H.H., 2014. Regulation of intracellular signaling and function by caveolin. Faseb J. 28, 3823–3831.
Hale, S.L., Vanderipe, D.R., Kloner, R.A., 2013. Continuous heliox breathing and the extent of anatomic zone of noreflow and necrosis following ischemia/reperfusion in the rabbit heart. Open Cardiovasc. Med. J. 8, 1–5.
Han, F., Zhang, J., Shao, J., Yi, X., 2014. Caveolin-1 promotes an invasive phenotype and predicts poor prognosis in large cell lung carcinoma. Pathol., Res. Pract. 210, 514–520.
Hausenloy, D.J., Y.D.M, 2006. Survival kinases in ischemic preconditioning and postconditioning. Cardiovasc Res, 240–253.
Hausenloy, D.J., Tsang, A., Yellon, D.M., 2005. The reperfusion injury salvage kinase pathway: a common target for both ischemic preconditioning and postconditioning. Trends Cardiovasc Med 15, 69–75.
Hausenloy, D.J., Yellon, D.M., 2003. The mitochondrial permeability transition pore: its fundamental role in mediating cell death during ischaemia and reperfusion. J. Mol. Cell Cardiol. 35, 339–341.
Horikawa, Y.T., Patel, H.H., Tsutsumi, Y.M., Jennings, M.M., Kidd, M.W., Hagiwara, Y., Ishikawa, Y., Insel, P.A., Roth, D.M., 2008. Caveolin-3 expression and caveolae are required for isoflurane-induced cardiac protection from hypoxia and ischemia/reperfusion injury. J. Mol. Cell Cardiol. 44, 123–130.
Huhn, R., Heinen, A., Weber, N.C., Kerindongo, R.P., Oei, G.T., Hollmann, M.W., Schlack, W., Preckel, B., 2009. Helium-induced early preconditioning and postconditioning are abolished in obese Zucker rats in vivo. J. Pharmacol. Exp. Ther. 329, 600–607.
Horikawa, Yousuke T., Tsutsumi, Yasuo M., Patel, Hemal H., Roth, David M., 2014. Signaling epicenters: the role of caveolae and caveolins in volatile anesthetic induced cardiac protection. Curr. Pharm. Des. 20, 5681–5689.
Jasmin, J.F., Mercier, I., Dupuis, J., Tanowitz, H.B., Lisanti, M.P., 2006. Short-term administration of a cell-permeable caveolin-1 peptide prevents the development of monocrotaline-induced pulmonary hypertension and right ventricular hypertrophy. Circulation 114, 912–920.
Chaudhary, Ketul R., Cho, Woo Jung, Yang, Fenghua, Samokhvalov, Victor, El-Sikhry, Haitham E., Daniel, Edwin E., Seubert, John M., 2013. Effect of Ischemia Reperfusion Injury and Epoxyeicosatrienoic Acids on Caveolin Expression in Mouse Myocardium. J. Cardiovasc. Pharm. 61, 258–263.
Kramarow, E., Lubitz, J., Francis, R., Jr., 2013. Trends in the coronary heart disease risk profile of middle-aged adults. Ann. Epidemiol. 23, 31–34.
Lupi Herrera, E., Gaspar, J., Gonzalez Pacheco, H., Martinez Sanchez, C., Pastelin Hernandez, G., Luna Ortiz, P., Chavez Cosio, E., 2006. Reperfusion and postconditioning in acute ST segment elevation myocardial infarction. A new paradigm for the treatment of acute myocardial infarction. From bench to bedside? Arch. De. Cardiol. De. Mex. 76 (Suppl 4), S76–101.
Mio, Y., Shim, Y.H., Richards, E., Bosnjak, Z.J., Pagel, P.S., Bienengraeber, M., 2009. Xenon preconditioning: the role of prosurvival signaling, mitochondrial permeability transition and bioenergetics in rats. Anesth. Analg. 108, 858–866.
Oei, G.T., Aslami, H., Kerindongo, R.P., Steenstra, R.J., Beurskens, C.J., Tuip-de Boer, A.M., Juffermans, N.P., Hollmann, M.W., Preckel, B., Weber, N.C., 2015. Prolonged helium postconditioning protocols during early reperfusion do not induce

cardioprotection in the rat heart in vivo: role of inflammatory cytokines. J. Immunol. Res. 2015, 216798.
Oei, G.T., Heger, M., Van Golen, R.F., Alles, L.K., Flick, M., Van Der Wal, A.C., Van Gulik, T.M., Hollmann, M.W., Preckel, B., Weber, N.C., 2014. Reduction of cardiac cell death after helium postconditioning in rats: transcriptional analysis of cell death and survival pathways. Mol. Med. 20, 516–526.
Oei, G.T., Huhn, R., Heinen, A., Hollmann, M.W., Schlack, W.S., Preckel, B., Weber, N.C., 2012a. Helium-induced cardioprotection of healthy and hypertensive rat myocardium in vivo. Eur. J. Pharm. 684, 125–131.
Oei, G.T., Smit, K.F., vd Vondervoort, D., Brevoord, D., Hoogendijk, A., Wieland, C.W., Hollmann, M.W., Preckel, B., Weber, N.C., 2012b. Effects of helium and air inhalation on the innate and early adaptive immune system in healthy volunteers ex vivo. J. Transl. Med 10, 201.
Pagel, P.S., Krolikowski, J.G., 2009. Transient metabolic alkalosis during early reperfusion abolishes helium preconditioning against myocardial infarction: restoration of cardioprotection by cyclosporin A in rabbits. Anesth. Analg. 108, 1076–1082.
Pagel, P.S., Krolikowski, J.G., Pratt, P.F., Jr., Shim, Y.H., Amour, J., Warltier, D.C., Weihrauch, D., 2008a. Inhibition of glycogen synthase kinase or the apoptotic protein p53 lowers the threshold of helium cardioprotection in vivo: the role of mitochondrial permeability transition. Anesth. Analg. 107, 769–775.
Pagel, P.S., Krolikowski, J.G., Pratt, P.F., Jr., Shim, Y.H., Amour, J., Warltier, D.C., Weihrauch, D., 2008b. The mechanism of helium-induced preconditioning: a direct role for nitric oxide in rabbits. Anesth. Analg. 107, 762–768.
Pagel, P.S., Krolikowski, J.G., Pratt, P.F., Jr., Shim, Y.H., Amour, J., Warltier, D.C., Weihrauch, D., 2008c. Reactive oxygen species and mitochondrial adenosine triphosphate-regulated potassium channels mediate helium-induced preconditioning against myocardial infarction in vivo. J. Cardiothorac. Vasc. Anesth. 22, 554–559.
Pagel, P.S., Krolikowski, J.G., Shim, Y.H., Venkatapuram, S., Kersten, J.R., Weihrauch, D., Warltier, D.C., Pratt, P.F., Jr., 2007. Noble gases without anesthetic properties protect myocardium against infarction by activating prosurvival signaling kinases and inhibiting mitochondrial permeability transition in vivo. Anesth. Analg. 105, 562–569.
Palade, G.E., 1953. Fine structure of blood capillaries. J. Appl. Phys. 24, 1424–1436.
Patel, H.H., Head, B.P., Petersen, H.N., Niesman, I.R., Huang, D., Gross, G.J., Insel, P.A., Roth, D.M., 2006. Protection of adult rat cardiac myocytes from ischemic cell death: role of caveolar microdomains and delta-opioid receptors. Am. J. Physiol. Heart Circ. Physiol. 291, H344–H350.
Patel, H.H., Murray, F., Insel, P.A., 2008. Caveolae as organizers of pharmacologically relevant signal transduction molecules. Annu Rev. Pharm. Toxicol. 48, 359–391.
Patel, H.H., Tsutsumi, Y.M., Head, B.P., Niesman, I.R., Jennings, M., Horikawa, Y., Huang, D., Moreno, A.L., Patel, P.M., Insel, P.A., Roth, D.M., 2007. Mechanisms of cardiac protection from ischemia/reperfusion injury: a role for caveolae and caveolin-1. FASEB J. 21, 1565–1574.
Preckel, B., Mullenheim, J., Moloschavij, A., Thamer, V., Schlack, W., 2000. Xenon administration during early reperfusion reduces infarct size after regional ischemia in the rabbit heart in vivo. Anesth. Analg. 91, 1327–1332.
Preckel, B., Schlack, W., Heibel, T., Rutten, H., 2002. Xenon produces minimal haemodynamic effects in rabbits with chronically compromised left ventricular function. Br. J. Anaesth. 88, 264–269.
Ratajczak, P., Damy, T., Heymes, C., Oliviero, P., Marotte, F., Robidel, E., Sercombe, R., Boczkowski, J., Rappaport, L., Samuel, J.L., 2003. Caveolin-1 and -3 dissociations from caveolae to cytosol in the heart during aging and after myocardial infarction in rat. Cardiovasc Res 57, 358–369.
Ruijter, J.M., Ramakers, C., Hoogaars, W.M., Karlen, Y., Bakker, O., van den Hoff, M.J., Moorman, A.F., 2009. Amplification efficiency: linking baseline and bias in the analysis of quantitative PCR data. Nucleic Acids Res. 37, e45.
Sugie, S., Mukai, S., Tsukino, H., Toda, Y., Yamauchi, T., Nishikata, I., Kuroda, Y., Morishita, K., Kamoto, T., 2013. Increased plasma caveolin-1 levels are associated with progression of prostate cancer among Japanese men. Anticancer Res. 33, 1893–1897.
Tahir, S.A., Yang, G., Ebara, S., Timme, T.L., Satoh, T., Li, L., Goltsov, A., Ittmann, M., Morrisett, J.D., Thompson, T.C., 2001. Secreted caveolin-1 stimulates cell survival/clonal growth and contributes to metastasis in androgen-insensitive prostate cancer. Cancer Res. 61, 3882–3885.
Tahir, S.A., Yang, G., Goltsov, A.A., Watanabe, M., Tabata, K., Addai, J., Fattah el, M.A., Kadmon, D., Thompson, T.C., 2008. Tumor cell-secreted caveolin-1 has proangiogenic activities in prostate cancerCancer research 68, 731–739.
Toller, W.G., Kersten, J.R., Pagel, P.S., Hettrick, D.A., Warltier, D.C., 1999. Sevoflurane reduces myocardial infarct size and decreases the time threshold for ischemic preconditioning in dogs. Anesthesiology 91, 1437–1446.
Toma, O., Weber, N.C., Wolter, J.I., Obal, D., Preckel, B., Schlack, W., 2004. Desflurane preconditioning induces time-dependent activation of protein kinase C epsilon and extracellular signal-regulated kinase 1 and 2 in the rat heart in vivo. Anesthesiology 101, 1372–1380.
Tsutsumi, Y.M., Patel, H.H., Lai, N.C., Takahashi, T., Head, B.P., Roth, D.M., 2006. Isoflurane produces sustained cardiac protection after ischemia-reperfusion injury in mice. Anesthesiology 104, 495–502.
Weber, N.C., Schilling, J.M., Finley, J.C., Irvine, M., Kellerhals, S.E., Niesman, I.R., Roth, D.M., Preckel, B., Hollmann, M.W., Patel, H.H., 2013. Helium inhalation induces caveolin secretion to blood. FASEB J. 27 (1089), 1083.
Weber, N.C., Stursberg, J., Wirthle, N.M., Toma, O., Schlack, W., Preckel, B., 2006. Xenon preconditioning differently regulates p44/42 MAPK (ERK 1/2) and p46/54 MAPK (JNK 1/2 and 3) in vivo. Br. J. Anaesth. 97, 298–306.
Weber, N.C., Toma, O., Wolter, J.I., Obal, D., Mullenheim, J., Preckel, B., Schlack, W., 2005. The noble gas xenon induces pharmacological preconditioning in the rat heart in vivo via induction of PKC-epsilon and p38 MAPK. Br. J. Pharm. 144, 123–132.
Zhang, J., Zhu, W., Xiao, L., Cao, Q., Zhang, H., Wang, H., Ye, Z., Hao, Y., Dai, Q., Sun, W., Xiong, Y., 2016. Lower serum caveolin-1 is associated with cerebral microbleeds in patients with acute ischemic stroke. Oxidative Medicine and Cellular Longevity 2016, 9026787.

7.5 Gezina T.M.L. Oei, Michal Heger, Rowan F. van Golen, Lindy K. Alles, **Moritz Flick**, Allard C. van der Wal, Thomas M. van Gulik, Markus W. Hollmann, Benedikt Preckel, Nina C. Weber; Reduction of cardiac cell death after helium postconditioning in rats: transcriptional analysis of cell death and survival pathways. Mol Med. 2015 Jan 20; 20:516-26. doi:10.2119/molmed.2014.00057.

MolecularMedicine

Reduction of Cardiac Cell Death after Helium Postconditioning in Rats: Transcriptional Analysis of Cell Death and Survival Pathways

Gezina TML Oei,[1] Michal Heger,[2] Rowan F van Golen,[2] Lindy K Alles,[2] Moritz Flick,[1] Allard C van der Wal,[3] Thomas M van Gulik,[2] Markus W Hollmann,[1] Benedikt Preckel,[1] and Nina C Weber[1]

[1]Department of Anesthesiology, Laboratory of Experimental Intensive Care and Anesthesiology (L.E.I.C.A.), [2]Department of Experimental Surgery, and [3]Department of Pathology, Academic Medical Center, University of Amsterdam, Amsterdam, The Netherlands

Helium, a noble gas, has been used safely in humans. In animal models of regional myocardial ischemia/reperfusion (I/R) it was shown that helium conditioning reduces infarct size. Currently, it is not known how helium exerts its cytoprotective effects and which cell death/survival pathways are affected. The objective of this study, therefore, was to investigate the cell protective effects of helium postconditioning by PCR array analysis of genes involved in necrosis, apoptosis and autophagy. Male rats were subjected to 25 min of ischemia and 5, 15 or 30 min of reperfusion. Semiquantitative histological analysis revealed that 15 min of helium postconditioning reduced the extent of I/R-induced cell damage. This effect was not observed after 5 and 30 min of helium postconditioning. Analysis of the differential expression of genes showed that 15 min of helium postconditioning mainly caused upregulation of genes involved in autophagy and inhibition of apoptosis versus I/R alone. The results suggest that the cytoprotective effects of helium inhalation may be caused by a switch from pro-cell-death signaling to activation of cell survival mechanisms, which appears to affect a wide range of pathways.

Online address: http://www.molmed.org
doi: 10.2119/molmed.2014.00057

INTRODUCTION

Coronary artery disease and subsequent myocardial infarction is a common cause of death (1). In the acute phase of myocardial infarction, occlusion of a cardiac vessel by a thrombus or stationary embolus leads to myocardial hypoxia, which is followed by cessation of aerobic respiration and ATP production in the affected cardiomyocytes. The rapid energy depletion gradually suppresses metabolic activity and leads to the induction of cell death pathways and eventually the demise of cardiomyocytes. Reperfusion and reoxygenation of the infarcted tissue, as a result of, for example, pharmacological dissolution or dislodgement of the clot, ameliorate the extent of hypoxia-induced cell death, but in turn inflict lethal reperfusion injury (2). The type of cell death that is manifested depends on how fast reoxygenation occurs as a result of reperfusion (2) and may proceed via necrosis, apoptosis or autophagy. Cell survival is mediated mainly by activation of antiapoptotic proteins and stimulation of prosurvival autophagy (3–5).

The use of the colorless, odorless, nonanesthetic noble gas helium in patients with respiratory disease was first described in 1934 (6). The benefits of helium mixed with oxygen (heliox) were attributed to its reduced density and consequently reduced work of breathing in respiratory conditions. In the last few years, the use of heliox has been tested in acute respiratory diseases in both children and adults (7,8) and for decompression illness (9). In addition, helium has been shown to reduce the extent of cell death in myocardial, neuronal and epithelial tissue subjected to ischemia/reperfusion (I/R), as reviewed in (10). In the heart, helium preconditioning considerably reduces infarct size in rat and rabbit models of cardiac I/R by coronary artery ligation (data of these studies are summarized in Supplementary Figure S1). On average, the infarct size reduction was 18% to 25% after exposure to helium preconditioning

Address correspondence to *Markus W Hollmann, Department of Anesthesiology, Academic Medical Center, University of Amsterdam, Meibergdreef 9, 1105 AZ Amsterdam, The Netherlands. Phone: +31-(0)20-566-3630 or +31-(0)20-566-3633 (secretary); Fax: +31-(0)20-6979441; E-mail: m.w.hollmann@amc.uva.nl.*
Submitted March 25, 2014; Accepted for publication August 26, 2014; Epub (www.molmed.org) ahead of print August 26, 2014.

(11–20). Helium postconditioning (HePOC), the clinically more relevant form of conditioning, also protects the myocardium, as has been demonstrated in several rat strains (15,21). Some mechanistic insight into the damage-ameliorating effects of helium gas during I/R has been provided in the last few years (22). Apoptotic pathways have been shown to be involved in helium conditioning (17–19).

Given the fact that helium preconditioning and HePOC reduce the extent of I/R-induced cell death, helium may affect the transcriptional regulation of cell death and survival pathways and thereby promote prosurvival signaling. Here we used a regional cardiac I/R model in rats to determine the differential expression patterns of genes related to apoptosis, necrosis and autophagy following ischemia, I/R or I/R with different regimes of HePOC. Transcriptional analysis of these pathways not only allowed us to test the hypothesis that HePOC reduces the magnitude of death signaling and stimulates survival pathways, but also provided insight into the significance of each mode of cell death and cell survival in every phase of I/R under native conditions and following HePOC.

MATERIALS AND METHODS

Animal Model of Ischemia/Reperfusion

Animal experiments were approved by the Academic Medical Center's animal ethics committee (DAA102650). Animals were treated in accordance with the *Guide for the Care and Use of Laboratory Animals* (1996) (24). Male Wistar rats (354 to 426 g, age range of 12 to 16 wks) were acclimatized for 7 d under conditions of 12-h light and dark cycles and ad libitum access to food and water.

Rats were anesthetized and surgically prepared as described previously (21). In short, rats were mechanically ventilated and cannulation of the carotid artery was done for measurement of the mean arterial pressure and heart rate and for blood sampling. The left anterior descending coronary artery (LAD) was ligated with a single puncture 5-0 Prolene suture (Ethicon [Johnson&Johnson], Amersfoort, the Netherlands) through the myocardium. The ends of the suture were threaded through propylene tubing to enable tightening and loosening of the snare for the induction of I/R. The helium postconditioning groups received helium gas (Linde Gas Benelux, Dieren, the Netherlands) at the onset of reperfusion (Figure 1). To make sure that sufficient helium was present in the lungs and normal air washed out at the onset of reperfusion, helium administration was started at 24 min of ischemia.

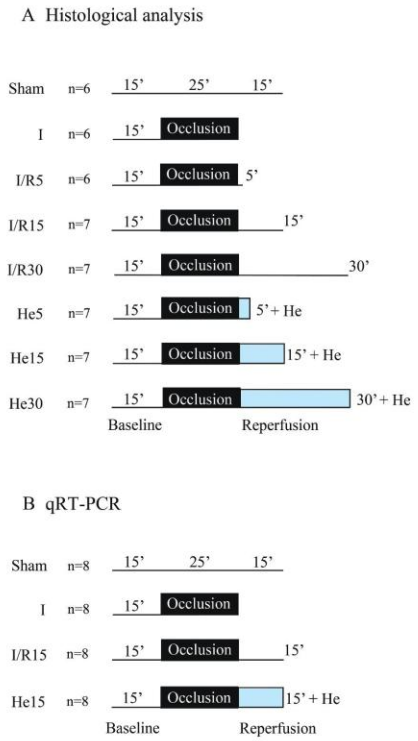

Figure 1. Schematic overview of the experimental protocols. (A) Experimental setup for histological analysis. Rats were euthanized after 25 min (25') of ischemia and 5, 15, or 30 min (5', 10', or 30') of reperfusion (groups I/R5, I/R15, I/R30; the group I had ischemia alone; the sham group had no I/R. The number behind the reperfusion block indicates the duration (in minutes) of the reperfusion phase. Helium postconditioning (He) encompassed the entire reperfusion phase (groups He5, He15, He30). (B) Experimental setup for gene analysis by qRT-PCR. Rats were euthanized after 25 min of ischemia or after 15 min of reperfusion.

Study Design (Figure 1)

The study was divided into two test arms for the determination of (1) histological damage, and (2) quantitative reverse transcriptase polymerase chain reaction (qRT-PCR) experiments. Additionally, Western blot experiments were performed to investigate levels of proteins involved in autophagy in the I/R15 and He15 groups (I/R15 received 15 min of reperfu-

sion; He15 received 15 min of helium postconditioning; for additional information on the groups, see Figure 1 legend).

Histological Staining and Analysis

For histological processing of the hearts, the organs were mounted on a modified Langendorff setup and perfused retrograde with isotonic saline solution to wash out blood from the coronary circulation. Next, the coronary circulation was flushed with 10 mL of ice-cold fixative (96% ethanol, acetic acid, 10% buffered formalin and Milli-Q water [Millipore, Amsterdam, the Netherlands] in a 50:5:10:35 volume ratio). Adequate retrograde perfusion was confirmed visually by uniform changes in size and color of the myocardium. The heart was then removed from the Langendorff setup and stored in ice-cold fixative. Fixed rat hearts were dehydrated in graded steps of ethanol and xylene and cut in half, longitudinally at the center of the ligation of the LAD (Supplementary Figure S2). The left half of the heart was embedded in paraffin and sectioned with a microtome along the cutting plane (4-µm thick sections). The sections were deparaffinized, stained with hematoxylin and eosin (H&E) and mounted using VectaMount (Vector Laboratories, Burlingame, CA, USA).

A histological scoring system was developed to semiquantitatively analyze the extent of myocardial damage in I/R-subjected rat hearts and to determine the extent of cardiomyocyte protection by HePOC. The scoring parameters are listed in Table 1. H&E-stained sections were viewed under a light microscope (confocal microscope SP8 X; Leica, Rijswijk, the Netherlands). The area at risk was delineated on the basis of the pathological demarcation zone at low power view (10× magnification), whereby the puncture wound from the suture was used as an anchor point. The area at risk always extended from the periphery of the puncture wound to the apical end. Semiquantitative scoring of histopathological parameters of myocardial damage (contraction band necrosis, interstitial edema, granulocyte adherence/extravasation, extravasation of erythrocytes) was performed at higher power magnification (400×) in the full thickness of the myocardium. The endocardial segment and an epidcardial segment of myocardium were scored separately. All parameters were scored in four fields of view (FOVs) per segment in the area at risk (400×).

Table 1. Histological scoring parameters used to semi-quantify myocardial slices.

Parameter	Score	Quantitative value
1. Contraction bands/coagulation necrosis	0	Absent
	1	1%-10% of cardiomyocytes
	2	11%-50% of cardiomyocytes
	3	51%-100% of cardiomyocytes
2. Interstitial edema	0	Absent
	1	Present
3. Granulocyte infiltration	0	Absent
	1	Present
4. Platelet aggregates/thrombi	0	Absent
	1	Present
5. Extravasation of red blood cells	0	Absent
	1	Present

qRT-PCR

At the end of the experiment (Figure 1B), the heart was excised under deep anesthesia. The area at risk (AAR) was cut from the rest of the myocardium (area not at risk [NAAR]) and sliced in two pieces on ice, which was snap frozen in liquid nitrogen and stored at –80°C until further analysis. All analyses were performed in myocardial tissue at risk. For a detailed description of RNA extraction, cDNA synthesis and run parameters, see Supplementary Table S1.

Melting curve analysis was performed at the end of the PCR run. Amplicons that showed amplification of nonspecific products were excluded from analysis. The data was further processed according to Ruijter and colleagues (24). Each amplicon was corrected for baseline fluorescence and a common fluorescence threshold (Nq) for all arrays was set in the upper half of the log-linear phase of the amplification plot. Amplicons that did not reach Nq before cycle 40 were considered undetectable. Next, the individual PCR efficiencies were calculated and amplicons with an efficiency <1.80 or >2.00 were excluded from further analysis. The individual efficiencies were subsequently used to calculate the starting concentration (N_0) per amplicon. All samples were normalized to the mean N_0 of the housekeeping genes that showed the most stable expression over all arrays (that is, *Ldha* and *Rplp1*).

Two comparisons were made. First, the differences between experimental groups (ischemia, I/R15 and He15) and the sham group was calculated according to

$$\frac{\frac{N_0\text{GOI}}{N_0\text{Housekeeping}}\text{I/R}}{\frac{N_0\text{GOI}}{N_0\text{Housekeeping}}\text{sham}}$$

and expressed as fold difference versus the sham group. The GOI (gene of interest) within one group is thus first normalized against the housekeeping gene, afterward a comparison between each experimental group and the sham group was made. Heat maps of these expression profiles were generated using Mayday Microarray Data Analysis software (25). A total of 84 genes involved in cell death and survival pathways were investigated and divided in four categories: necrosis, proapoptosis, antiapoptosis and autophagy. For a description of each gene also see Supplementary Table S2. Due to multiple roles for some genes, the total number of genes in each category was 27 (necrosis), 23 (proapoptosis), 14 (antiapoptosis) and 33 (autophagy). After exclusion of genes with insufficient n-numbers in either group due to melting curve, efficiency or undetectable levels of mRNA, a total of

20 (necrosis), 21 (proapoptosis), 14 (antiapoptosis) and 29 (autophagy) genes were included in the heat maps.

Secondly, a comparison between the I/R and He15 group was made. For this, the means of the He15 group were divided by the means of the I/R group and presented as fold increase. Gene selection was performed according to the criteria as described above. A total of 20 (necrosis), 20 (proapoptosis), 14 (antiapoptosis) and 30 genes (autophagy) were included in the analysis.

Western Blot Analysis

Western blot analysis was performed in AAR and NAAR tissue to allow for investigation of the two distinct types of tissue within one sample. For preparation of cytosol, membrane and mitochondrial fractions as well as for Western blot analysis, see "Methods: Western Blot Analysis" in the Supplement Data. In short, samples were loaded on a Criterion Gel. Proteins were separated by electrophoresis and transferred onto an Immobilin-FL membrane. The membrane was incubated overnight at 4°C with beclin1 (Cell Signaling Technology, Leiden, the Netherlands, 1:1000) or sequestosome1 (Abcam, Cambridge, MA, USA, 1:2000) antibody. After washing in fresh, cold TBS-T, the blot was subjected to the appropriate horseradish peroxidase conjugated secondary antibody for 1 h at room temperature. Subsequently, immunoreactive bands were visualized on an Odyssey Infrared Imaging System. Densitometric analysis of the blots was performed in Odyssey Infrared Scanning Software. Results are presented as the ratio of the target protein over the fraction-specific control protein: for the cytosol fraction this was actin (1:5000), for the membrane fraction NaKATPase (Cell Signaling Technology, 1:5000), for the mitochondrial fraction PHB1 (Cell Signaling Technology, 1:10000).

Statistical Analysis

Statistical analysis was performed in GraphPad Prism (GraphPad Software, La Jolla, CA, USA). Baseline hemodynamics were analyzed using one way analysis of variance (ANOVA) with a Tukey *post hoc* test for multiple comparisons. Differences in mRNA expression and protein levels between the I/R and He15 group were tested using a Mann-Whitney test. A P value of < 0.05, indicated with an asterisk in the figures, was considered significant.

All supplementary materials are available online at www.molmed.org.

Table 2. Hemodynamics (mean arterial pressure and heart rate) sampled after 15 min of baseline, 24 min of ischemia and 15 min of reperfusion.[a]

Group[b]	Baseline	After 24 min of ischemia	After 5 min of reperfusion	After 15 min of reperfusion	After 30 min of reperfusion
			Mean AP[c] (mmHg)		
Sham	111 ± 13	113 ± 22	113 ± 21	98 ± 20	
I	95 ± 16	110 ± 15			
I/R5	90 ± 33	95 ± 19	73 ± 20		
I/R15	95 ± 24	93 ± 20	83 ± 21	62 ± 8	
I/R30	96 ± 29	91 ± 28	80 ± 24	79 ± 21	60 ± 15
He5	102 ± 20	108 ± 23	78 ± 21		
He15	102 ± 20	108 ± 17	96 ± 14	75 ± 11	
He30	97 ± 25	100 ± 24	95 ± 18	91 ± 23	69 ± 15
			Mean HR[d] (BPM)		
Sham	372 ± 20	373 ± 20	363 ± 24	352 ± 32	
I	341 ± 40	367 ± 32			
I/R5	338 ± 29	354 ± 29	330 ± 18		
I/R15	320 ± 60	340 ± 50	326 ± 46	306 ± 44	320 ± 39
I/R30	329 ± 62	359 ± 39	342 ± 38	346 ± 41	
He5	360 ± 36	366 ± 16	344 ± 35		
He15	338 ± 35	365 ± 36	350 ± 37	324 ± 34	
He30	343 ± 57	366 ± 36	347 ± 47	359 ± 40	328 ± 51

[a]Data are shown as mean ± SD. At each time point there were no significant differences between different experimental groups.
[b]On group infomation, see Materials and Methods and Figure 1.
[c]Mean AP, mean arterial pressure in mmHg.
[d]Mean HR, mean heart rate in beats/minute.

RESULTS

Hemodynamic Parameters

Aortic pressure and heart rate (mean ± SD) during the experiments are shown in Table 2. Baseline hemodynamics did not vary between groups.

Histological Damage Profiles

Histological analysis was performed to assess cell damage at a microscopic level (n = 4-6 per group). The morphology of cardiomyocytes clearly differed among the experimental groups. Hearts in the sham group contained normal unaltered cardiomyocytes; myofibrils were ordered in a structured manner and exhibited similar morphology. The absence of cardiomyocyte damage, inflammatory cell infiltrates, red blood cell extravasation, thrombosis and edema resulted in a mean total histology scores of 0. Representative micrographs of sham-operated animals are shown in Figure 2B and Supplementary Figure S3.

After 25 min of ischemia, hypercontraction of myofibers was observed in some slices (Supplementary Figure S4), without loss of the native structure and morphology of cardiomyocytes similar to the sham-operated group. In the 5-min reperfusion group, waviness of myofibers and contraction bands could be observed and were accompanied by other signs of tissue damage (Supplementary Figure S5). At 15 or 30 min of reperfusion, the cardiac tissue exhibited clear signs of damage that entailed necrosis, interstitial edema, granulocyte

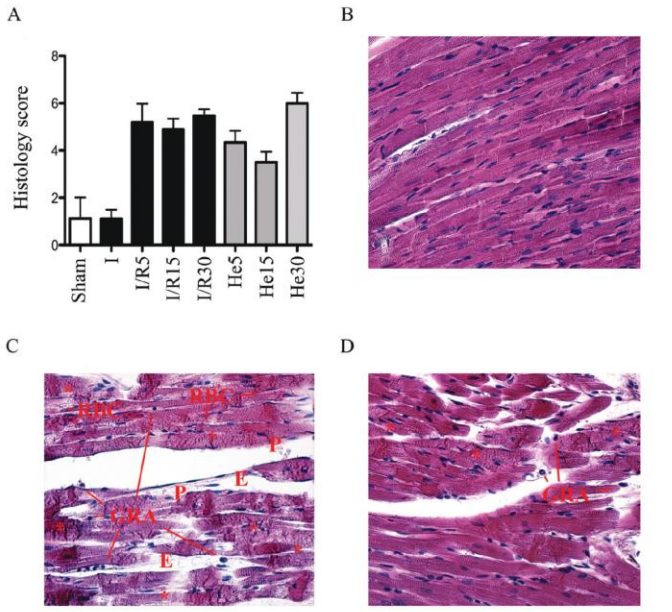

Figure 2. (A) Total histology score plotted per group. Representative histological sections of (B) hearts in the sham, (C) I/R15, and (D) He15 group. E indicates tissue edema; P, presence of platelets and thrombi; RBC, extravasation of red blood cells; GRA, extravasation of granulocytes; asterisks (*), contraction band or coagulation necrosis. Original magnification 400×.

infiltration, platelet aggregates/thrombi and extravasation of red blood cells (Figure 2C). This was observed in all histological specimens (Supplementary Figures S6, S7) and was reflected in the total histology score (Figure 2A).

Fifteen min of HePOC reduced the extent of cell damage, which was reflected in the trend of an overall lower total histology score in this group compared with all other intervention groups (Figure 2A). Interestingly, 15 min of HePOC (Supplementary Figure S9) resulted in less cell damage compared with 30 min of helium (Supplementary Figure S10), indicating that prolonged helium inhalation is not beneficial for cardiac I/R. The morphological features of cardiomyocytes that had been exposed to 30 min of HePOC were similar to those of cardiomyocytes in the I/R15, I/R30 and He5 group (Supplementary Figures S6, S7, S8). A representative micrograph of myocardium exposed to I/R15 and He15 is shown in Figures 2C and D, respectively. The extent of necrosis, edema, extravasation of red blood cells, granulocyte infiltration and platelet aggregation is much lower after He15 (see Figure 2D) compared with I/R15 (see Figure 2C). This is also reflected in the total histology score (see Figure 2A).

mRNA Expression Profiles in Hearts Subjected to Ischemia, Ischemia/Reperfusion and HePOC

Exposure of cardiomyocytes to ischemia, I/R15 and He15 caused differential gene expression in all cell death pathways compared with cardiomyocytes in the sham-operated group (Figure 3). Many genes of the cell death pathways in the ischemia and I/R15 groups are regulated in a similar manner, that is, the expression patterns of genes involved in the execution of necrosis, apoptosis and autophagy are affected similarly under both conditions of ischemia and I/R. To specify this: most genes are similarly up- or downregulated after ischemia and I/R15. This can be seen from the actual number of genes that are up- or downregulated in each group of genes. Fifteen of 20 genes involved in necrosis pathways were downregulated after ischemia and 14 of 20 after I/R15. Simultaneously, genes involved in proapoptosis were upregulated (I, 11 of 21; I/R15, 12 of 21) and antiapoptotic genes were downregulated (10 of 14 in both groups). Ischemia and I/R15 also downregulated most genes involved in autophagy: 21 of 29 and 23 of 29, respectively.

The addition of 15 min of helium postconditioning changed the expression profiles of whole sets of genes. This can be seen easily when one compares the last column to the third column. Helium particularly upregulated genes involved in antiapoptotic pathways (10 of 14) and autophagy (16 of 29). By contrast, ischemia and I/R15 downregulated the majority of antiapoptotic genes and genes involved in autophagy. This suggests that the protective effect of 15 min of helium postconditioning is linked to expression of genes involved in autophagy and antiapoptotic signaling.

Figure 3 first of all shows that gene expression patterns that are visible during reperfusion already emerge during ischemia. Additionally, it shows that exposure to a short 15-min episode of HePOC is powerful enough to exert changes on expression patterns of genes involved in cell death pathways, which occurs already during early reperfusion. Taken together, the data suggests that the effects of helium postconditioning are immediate and undo some of the detrimental changes in gene expression that have been initiated during ischemia and are extended during reperfusion.

Effects of HePOC on Cell Death, Cell Survival and Autophagy

Beside the general changes in gene expression profiles during ischemia, reperfusion and POC in comparison to sham

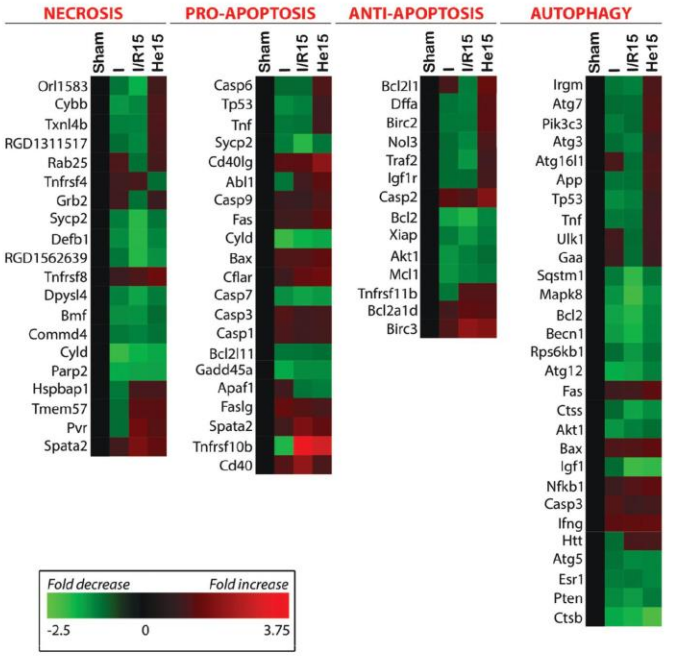

Figure 3. Heat maps indicating the differential expression of genes in the ischemia (I), I/R, and I/R + He (He15) relative to the sham group, classified per cell death/survival pathway and autophagy. The significance of the color-coding, indicating the extent of fold decrease (green) and fold increase (red), is provided in the inserted legend. The function(s) of the genes is (are) summarized in Supplementary Table S2.

animals, a direct comparison between the I/R15 and He15 group has been made. In Figure 4, the fold increase and decrease of each gene within one of four categories of cell damage/survival after He15 in comparison to I/R15 is depicted. This figure shows which genes are upregulated and downregulated (most strong upregulation to downregulation from left to right in the figure) after HePOC and could therefore play a key role in helium's underlying cardioprotective mechanism.

In line with results shown in Figure 3, in comparison to I/R15, He15 particularly upregulates genes involved in autophagy and antiapoptosis: 27 of 30 genes involved in autophagy were upregulated, and 12 of 14 antiapoptotic genes. This underlines the general finding that the cardioprotective mechanism of HePOC is related to an increase in the expression of genes employed in autophagy and against apoptosis.

Apart from general trends, individual genes were found to be significantly upregulated after He15 as compared to I/R15. Within the necrosis group of genes, *Olr1583*, *Sycp2*, *Cybb*, *Txnl4b* and *Dpysl4* all were significantly upregulated after He15 as compared to I/R15 only. Their function *in vivo* is described in Supplementary Table S2 and the relation of these genes to HePOC will be addressed in the discussion.

Protein Levels of Beclin-1 and Sequestosome

Differences in protein levels of beclin-1 and sequestosome between the I/R15 and He15 groups were consistent in AAR and NAAR tissue, indicating a tissue-independent effect of helium inhalation. In the mitochondrial fraction, 15 min of helium postconditioning significantly increased the amount of beclin-1, which was found in both the AAR and NAAR tissue (see also Figure 5). No differences in sequestosome protein levels could be found between the I/R15 and He15 groups. For an overview of sequestosome Western blot results, see Supplementary Figure S11.

DISCUSSION

In this study, helium-induced postconditioning was investigated by microscopic assessment of cell damage and analysis of its transcriptional effects on cell death and survival pathways (necrosis, apoptosis and autophagy). We showed that signs of cell damage in H&E-stained histological slices were reduced after 15 min of helium. Additionally we showed that in comparison to I/R15 only, He15 upregulated genes in all categories; necrosis, pro- and antiapoptosis and autophagy. However, He15 predominantly upregulated genes involved in autophagy and inhibition of apoptosis. Taken together, these data suggested that the HePOC-induced reduction of I/R-induced cell damage is mediated by an instantaneous upregulation of genes employed in autophagy and the inhibition of apoptosis during early reperfusion. We therefore suggest that the upregulation of these genes at least counterbalances or even overrules the upregulation of the pro-cell-death genes, resulting in cardioprotection after HePOC.

In earlier studies from our laboratory, infarct size reduction (analyzed by triphenyl tetrazolium chloride [TTC]–Evans blue staining) after HePOC was found in several rat strains (15,21,26). Fifteen minutes of 70% helium during early reperfusion reduced infarct size as a percentage of area at risk from 47% ± 2% (mean ± SEM) in control to 30% ± 2% in the HePOC group (Supplementary Figure S12), while the area at risk as percentage of total ventricular tissue was similar in both groups; 21% ± 2% in CON and 22% ± 2% (data not shown). This is in line with the results of

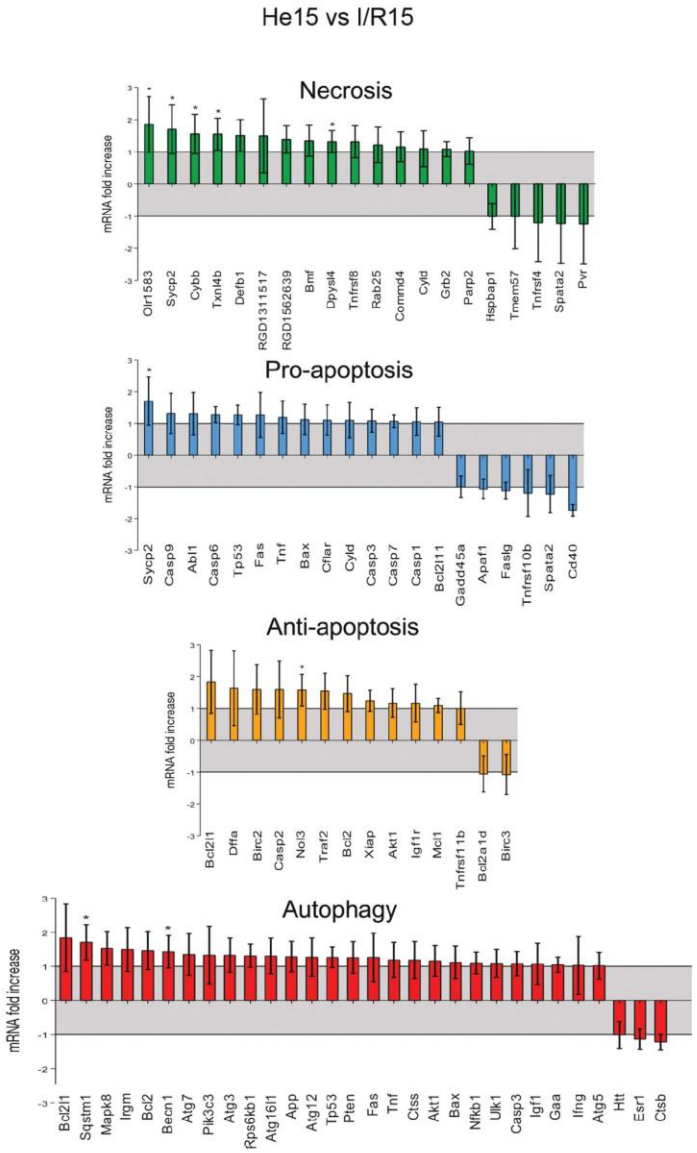

Figure 4. Regulation of genes after 15 min of helium postconditioning shown as fold increase or decrease in comparison to I/R15 per category. *$p < 0.05$

the current study, in which histological analysis showed less cellular damage after He15 in comparison to I/R15. He15 slices exhibited less contraction band necrosis, edema, extravasation of red blood cells and granulocytes and fewer platelets/thrombi than I/R15 slices. Interestingly, histological slices of 30 min of helium showed excessive cellular damage in comparison to 15 min of helium. Again, this is in line with results from infarct size experiments analyzed by TTC staining, in which 30 min of helium during early reperfusion abrogated the protection that was seen after 15 min of HePOC (26). Prolonged episodes of helium inhalation did not protect the rabbit heart against I/R (27), neither did prolonged helium inhalation protect forearm endothelium in a study with male human volunteers (28).

From enzymatic and histologic assessment of cell damage after HePOC, we therefore drew the conclusion that (1) helium reduces cardiomyocyte damage which results in smaller infarct size, and (2) it does so only after 15 min of HePOC. This led to the investigation of transcriptional profiles of genes employed in cell death and survival pathways after 15 min of HePOC. Although mRNA expression profiles after 25 min of ischemia also were analyzed in this study, we focused on reperfusion because that seems to be the time window in which HePOC exerts its effects. Histological analysis showed a reduction of cell damage after HePOC at 15 min of reperfusion. From TTC staining, we know that the protective effect of 15 min of HePOC also can be found after 2 h of reperfusion (15,21,26); 1 h and 45 min after the postconditioning stimulus is discontinued. It is very likely that within this time window both necrotic and apoptotic cell death are reduced by helium postconditioning, and that prosurvival mechanisms such as autophagy contribute substantially. We aimed to investigate whether signs of cellular survival on an mRNA expression level could be found as early as the 15 min reperfusion episode.

Separate studies investigating the effects of helium conditioning on specific proteins and their concomitant posttrans-

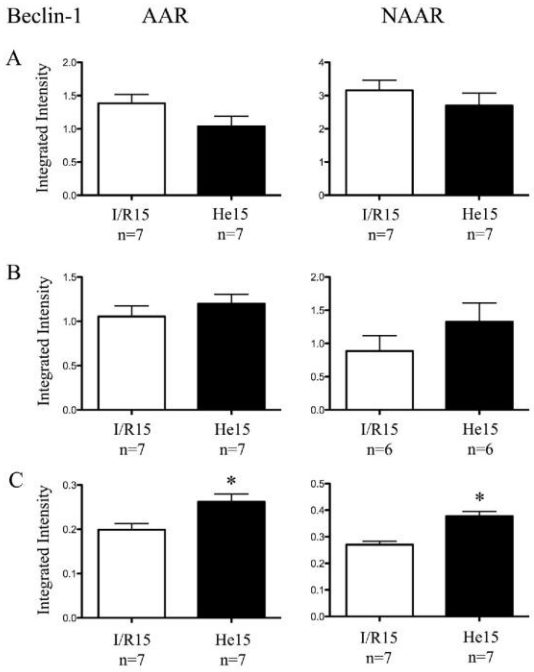

Figure 5. Protein levels of beclin-1. Data are shown as mean ± SEM, *$p < 0.05$. Ratios: (A) beclin-1:actin (cytosol fraction); (B) beclin-1:NaKATPase; (C) beclin-1:PHB1.

lational modifications in the cell death and survival pathways have been conducted (22). However, cell death and survival pathways interact, and various ways of cellular stress might trigger necrotic, apoptotic and autophagic pathways simultaneously, leading to activation of common downstream cell death elements or might offset each other (4). We therefore used PCR arrays to investigate four categories of cell death/survival simultaneously. Generally it is thought that necrosis occurs quickly and centrally, whereas apoptotic cell death takes a bit longer owing to the slowly orchestrated execution of the apoptotic cell death program and mainly occurs in the border zone of the area at risk (3). In this study, we investigated gene expression in the area at risk to find out which type of cell death is particularly affected by HePOC. The trend of the current study suggests that orchestration of genes against apoptosis and proautophagy leads to the reduced cellular damage that is found in histological analyses at 15 min of reperfusion. This could make sense, as programmed cell death might play a far more important role than anticipated: in rats, chronic (7 d) ligation of a coronary artery resulted in a peak-mycocyte death within the first 4.5 h after ligation in which apoptosis predominated (29).

Autophagy is originally categorized as a survival mechanism in which cells consume their own proteins, lipids and organelles to maintain protein and organelle quality and to provide amino acids, energy and free fatty acids in case of nutrient deficiency. Cell constituents and parts of the cytoplasm are first engulfed in autophagosomes, after which fusion with lysosomes take place. Hereafter, degradation and recycling occurs. It is suggested that once this process becomes overactive, it becomes detrimental to cells and might end in autophagic cell death or in another type of cell death, such as apoptosis (5,30,31). Yet, inhibition of autophagy might lead to cellular damage, for example due to an increased sensitivity to apoptotic signs, stressing the potential prosurvival role of autophagy (32). In vivo, sevoflurane late preconditioning (33) and ischemic POC (34) increased autophagic vacuoles and reduced infarct size.

In the current study, we found a simultaneous upregulation of genes employed in pathways against apoptosis and proautophagy; this could relate to the infarct size reduction that was observed after HePOC (15,21, 26) as well as the results from histological analysis in this study. Three significantly regulated genes - *Becn1* and *Sqstm1* (autophagy) and *Nol3* (antiapoptosis) in this analysis were of particular interest. *Nol3* (nucleolar protein 3), which is also known as an apoptosis repressor with caspase recruitment domain (ARC), inhibits apoptosis on a level further down the apoptotic cascade as it directly binds to and inhibits caspase-8 activity. Phosphorylation of ARC by protein kinase CK2 activates this protein, while calcineurin dephosphorylates and inactivates ARC (35). Not only did ARC overexpression decrease infarct size after I/R (5), anesthetic-induced preconditioning was associated with an increase of phosphorylation of ARC, a reduction in activity of calcineurin and a reduction in caspase-8 activity and cytochrome c release (35). This is in line with our results; I/R decreases *Nol3* expression while He15 increases it.

Our results show a general change in mRNA levels of genes involved in autophagy, including upregulation of the autophagy enhancer protein Becn1 after HePOC in comparison to I/R15. The inactivation of beclin-1 *(Becn1)*, a protein involved in autophagosome formation, reduced infarct sizes (36) thereby suggesting a detrimental effect of au-

tophagosome formation on infarct size. *Becn1* loses its proautophagic function after interaction with *Bcl-2* (5), which is logical according to the hypothesis that an increased rate of autophagy in apoptotic cells probably leads to cell death (37). Thus, a combined downregulation of the antiapoptotic *Bcl-2* with an upregulation of *Becn1* during reperfusion facilitates cell death, presumably necrosis. In our study, I/R caused a downregulation of both *Becn1* and *Bcl-2* in comparison to sham, which was diminished by helium postconditioning. Additionally, *Becn1* protein levels were significantly higher after HePOC. These findings are comparable to results from a study in rats, in which ischemic postconditioning increased protein- and mRNA-levels of beclin-1 (34).

Protein analysis of Becn1 in cytosol, membrane and mitochondrial fractions of AAR and NAAR showed an identical pattern: after HePOC, there was a tendency toward a decrease in cytosol fractions, a tendency toward increase in the membrane fraction and a significant increase in the mitochondrial fraction. A possible reason for these findings is the translocation of the protein when autophagy is induced. The first step in autophagy is the formation of the phagophore; a membrane composed of different parts of organelles such as the Golgi complex, the ER and mitochondria. Subsequently, the autophagosome is formed and fuses with lysosomes, after which degradation of the cargo takes place (38,39). *Becn1* is actively involved in the first step; it stimulates the formation of the phagophore and the autophagosome at the contact site of the ER and mitochondria (40). Hence, the increased *Becn1* levels in the mitochondrial and membrane fractions. *Becn1* also is needed for autophagosome-lysosome fusion, a crucial step for an effective autophagy flux. Not only ischemic preconditioning, but also nonclassical preconditioning agents are known to induce autophagy and enhance the autophagic flux (41).

Albeit complex, autophagy flux can be measured in several ways. *Sqstm1* (sequestosome 1) is generally considered a read out for autophagic activity; protein levels of Sqstm1 are regulated by autophagy as they are degraded in its machinery, due to its role in the delivery of ubiquitinated cargo to autophagosomes (39,42,43). It is especially linked to mitophagy: the process in which depolarized or damaged mitochondria are directed toward degradation in the autophagosome. Discarding damaged constituents of mitochondria is essential in I/R injury and plays a role in aging and cardiovascular disease (44,45). In mice, infarct size reduction after ischemic postconditioning was accompanied by translocation of Sqstm1 to mitochondria and presence of Parkin, an E3 ubiquitin ligase. In Parkin$^{-/-}$ mice the translocation of Sqstm1 to mitochondria was absent and infarct size reduction was blunted (46). These findings are in line with our results, as the I/R-induced downregulation of *Sqstm1* was attenuated after helium postconditioning. However, the mRNA upregulation after HePOC did not seem to translate to changes at a protein level. This could be explained by the fact that a true measurement of autophagic flux has not been done. From literature, it is known that upregulation of *Sqstm* mRNA does not always translate to an increase in protein levels (39). Sqstm1 protein levels are not only influenced by processing through the autophagosome machinery, they also are influenced by proteosomal degradation (39), a different pathway of protein degradation within a cell (43).

Although Figure 5 is particularly useful to observe trends, it also shows that some genes categorized in the necrotic pathway were upregulated significantly after He15: *Olr1583*, *Sycp2*, *Cybb*, *Txnl4b* and *Dpysl4*. Their function *in vivo* is described in Supplementary Table S2. After a quick glance at these genes, it looks as if some unexpected genes play a role in cardioprotective mechanisms. *Olr1583* and *Dpysl4* are not directly known to be expressed in the heart, but do play a role in HePOC. *Olr1583* (Olfactory receptor 1583), a member of the olfactory gene family, is found predominantly in the olfactory epithelium of the nose and is involved in the recognition of specific odorants (47). However, evidence exists that at least one specific member of the olfactory receptor family also exists in the heart. Olfactory receptor 1 transcripts were detected in the developing heart, suggesting that the olfactory receptor might play a role in cardiac development (48). In the current study, we show that *Olr1583* is expressed in the heart and that this expression is downregulated by I/R, but upregulated after He15. *Dpysl4* (dihydropyrimidinase-like 4), also known as *CRMP3*, is expressed in the developing brain, but its function is unclear (49,50). An inhibitory effect on brain development (50) as well as a crucial role in neurite outgrowth and axonal differentiation (49) has been described. We showed a downregulation of *CRPM3* in heart tissue after I/R in comparison to sham-operated animals and an attenuation of downregulation after He15.

Two other genes, *Sycp2* and *Txnl4b*, are involved in the cell cycle and biological diversity. *Sycp2* (synaptonemal complex protein 2) is part of the so-called synaptonemal complex, a meiosis-specific nuclear structure that is involved in recombination of chromosomes during the prophase, resulting in chromosomal crossover (51). *Sycp2* therefore plays a role in genetic variation. Txnl4b (thioredoxin-like 4B) or DIM-2 is a gene required in cell cycle progression as it transits cells from the synthesis (S)-phase to the growth 2 (G2) phase, and it is involved in pre-mRNA splicing (52). Pre-mRNA leads to different types of mRNA, which in turn results in different proteins. In a way, pre-mRNA plays a role in the establishment of the vast diversity of proteins that exists in eukaryotes. I/R downregulated both *Sycp2* and *Txnl4b*, while He15 attenuated the downregulation of *Sycp2* and even upregulated *Txnl4b*.

Cybb (Cytochrome b-245, β polypeptide), also known as *Gp91-phox* or *Nox2*, encodes for a protein called cytochrome b-245, which is a constituent of the NADPH-oxidase. The NADPH-oxidase produces superoxide and hydrogen peroxide in phagocytes that are used for the

killing of pathogens (53) in vascular smooth muscle cells, endothelial cells (54,55) and cardiomyocytes (56). Nox2 is upregulated in infarcted areas after myocardial infarction in the rat (54) and after hypoxia-reoxygenation in porcine coronary artery endothelial cells (PCAEC) (55). Pharmacological or genetic blockade of the NAPDH oxidase in PCAECs reduced the hypoxia/reoxygenation-induced reactive oxygen species levels. Interestingly, this was accompanied by a reduction in vessel outgrowth (55), suggesting a role for NADPH oxidase in angiogenesis and neovascularization.

Nox2 and NADPH oxidase upregulation might be associated with cell death due to increased levels of oxidative stress, however, under certain circumstances, upregulation could signal prosurvival (57). It is not unlikely that the outcome depends on the intensity and extent of the ROS signal, the present kinases and caspases in the tissue, the stress signal that induced it and the type of tissue (57). Nox-induced ROS was shown to be involved in the differentiation of cardiomyocytes from embryonic stem cells and neonatal cardiomyocytes. Nox2 expression peaked at embryonic d 12, suggesting a critical role for Nox2 in early cardiomyogenesis. As Nox2 is also upregulated after myocardial infarction, it is not unlikely that it plays a role in differentiation of cardiac progenitor cells (56). In our study, I/R downregulated the *Cybb/Nox2* gene, while He15 upregulated it. Taken together, the relative upregulation of *Cybb/Nox2*, *Sycp2* and *Txnl4b* suggest that HePOC is possibly related to organ development and cell reproduction. This idea is underlined by the finding that *Olr1583* and *Dpysl4* are expressed in the heart and affected by HePOC.

A limitation of this study is the lack of subsequent experiments investigating protein levels of all the corresponding genes in the mRNA expression profile. Furthermore, posttranslational modifications often determine net function and the effect of a protein. Additionally, autophagy and mitophagy are complex processes, and their investigation requires sophisticated research techniques. However, the goal of this study was to obtain an insight in the cell death and survival pathways that are involved in HePOC.

Because of the aforementioned goal of this study, no experiments were conducted to obtain specific hemodynamic measurements such as pressure–volume loops. As no studies have been done to investigate the contractile properties of the myocardium after helium postconditioning, it would be interesting to use a conductance catheter in future experiments. However, calibrating the volume component is a complex procedure, as it can be done by ultrasound, blood conductivity or stroke volume measurements. This might limit its feasibility (58,59). ECG recordings during I/R could point out another interesting problem often occurring in human coronary artery disease: (lethal) arrhythmia. In 1969, it was shown in dogs that heliox inhalation reduced the occurrence of ventricular fibrillation during the acute phase of coronary occlusion (60). It is questionable though, how relevant the problem of arrhythmia is in the small rodent model of regional I/R, as the dog and human heart differs in the presence of collateral arteries. Additionally, in humans, the presence of multiple atherosclerotic plaques (that is, multiple vessel disease) often poses the most significant threat. The likelihood of reducing I/R-induced arrhythmias by an intervention in a small rodent model is small when significant arrhythmia is not a dominant problem in the first place.

Our study does indicate that HePOC exhibits a wide array of effects on cell death and survival, and that it does so in an acute manner. A clue as to the underlying mechanism of HePOC could be found within the complex interplay of the abovementioned cellular processes. Beside the cell death and survival pathways, it is likely that oxidative stress pathways also are involved in helium postconditioning. Future research could focus on this direction, but should, in any case, comprise antiapoptotic and autophagic pathways as well as the long-term effect of HePOC on gene transcription and translation.

CONCLUSION

In conclusion, helium-induced cardioprotection by 15 min of POC seems to be associated with activation of prosurvival cell mechanisms. Helium influences the balance between pro- and antiapoptosis, in favor of genes directed *against* apoptosis. Simultaneously, it stimulates genes involved in autophagy and possibly cell reproduction and tissue development. This suggests that helium exerts its protective effects through a cell-surviving mechanism that comprises a whole set of pathways.

DISCLOSURES

The authors declare they have no competing interests as defined by *Molecular Medicine*, or other interests that might be perceived to influence the results and discussion reported in this paper.

REFERENCES

1. Kramarow E, Lubitz J, Francis R. (2013) Trends in the coronary heart disease risk profile of middle-aged adults. *Ann. Epidemiol.* 23:31–4.
2. Ovize M, *et al.* (2010) Postconditioning and protection from reperfusion injury: where do we stand? Position paper from the Working Group of *Cellular* Biology of the Heart of the European Society of Cardiology. *Cardiovasc. Res.* 87:406–23.
3. Hamacher-Brady A, Brady NR, Gottlieb RA. (2006) The interplay between pro-death and pro-survival signaling pathways in myocardial ischemia/reperfusion injury: apoptosis meets autophagy. *Cardiovasc. Drugs Ther.* 20:445–62.
4. Jain MV, *et al.* (2013) Interconnections between apoptotic, autophagic and necrotic pathways: implications for cancer therapy development. *J. Cell. Mol. Med.* 17:12–29.
5. Konstantinidis K, Whelan RS, Kitsis RN. (2012) Mechanisms of cell death in heart disease. *Arterioscler. Thromb. Vasc. Biol.* 32:1552–62.
6. Barach A. (1934) Use of helium as a new therapeutic gas. *Proc. Soc. Exp. Bio. Med.* 32:462–4.
7. Moraa I, Sturman N, McGuire T, van Driel ML. (2013) Heliox for croup in children. *Cochrane Database Syst. Rev.* 12:CD006822.
8. Rodrigo G, Pollack C, Rodrigo C, Rowe BH. (2006) Heliox for nonintubated acute asthma patients. *Cochrane Database Syst. Rev.* 18:CD002884.
9. Bennett MH, Lehm JP, Mitchell SJ, Wasiak J. (2012) Recompression and adjunctive therapy for decompression illness. *Cochrane Database Syst Rev.* 5:CD005277.
10. Oei GT, Weber NC, Hollmann MW, Preckel B. (2010) Cellular effects of helium in different organs. *Anesthesiology.* 112:1503–10.

8. Cooperation

In Cooperation With:

The Laboratory of Experimental Intensive Care and Anesthesiology (L.E.I.C.A.)
Department of Anesthesiology
(Chair: Prof. Dr. med. Dr. rer. nat. Markus W. Hollmann, D.E.A.A.)
Academic Medical Center
University of Amsterdam
Amsterdam, the Netherlands

Supervisor: Dr. Nina C. Hauck-Weber

9. Acknowledgement

The presented work was completed in the period from February 2014 to October 2016, in a collaboration between the Department of Anesthesiology and Intensive Care Medicine of the University Hospital Schleswig-Holstein, Kiel, and the Department of Anesthesiology of the Amsterdam Medical Center, Amsterdam.

I sincerely thank Prof. Dr. med. Markus Steinfath and Prof. Dr. med. Norbert Weiler for the possibility to perform my medical thesis in the Department of Anesthesiology and Intensive Care Medicine of the University Hospital Schleswig-Holstein, Kiel.

A very special thank you is given to my supervisors, Prof. Dr. Martin Albrecht, head of the Kiel laboratory, and Dr. Nina C. Hauck-Weber, head of the Amsterdam laboratory, who have supported me on this long journey and taught me so much. I am very grateful for their many hours and countless advices to help me during the work on this thesis.

For their support in the laboratory I would also like to thank Raphaela Kerindongo, Anita Tuip-de Boer, Dr. Gezina Oei, Renske Strenska and Dr. Karina Zitta. A big thank you is also given to Rianne Nederlof, Anna-Linda Peters and Matt Harmond for their enthusiastic support and friendship inside and outside the laboratory.

Finally, I would like to thank my parents and my sister, who have helped me so much during my studies and the work on this thesis.